

**UNIVERSIDADE FEDERAL DE SANTA MARIA  
CENTRO DE CIÊNCIAS RURAIS  
PROGRAMA DE PÓS-GRADUAÇÃO EM ENGENHARIA FLORESTAL**

**QUANTIFYING SEDIMENT FLUXES AND SOURCES  
IN EUCALYPTUS AND GRASSLAND CATCHMENTS  
IN THE BRAZILIAN PAMPA BIOME**

**TESE DE DOUTORADO**

**Mirian Lago Valente**

**Santa Maria, RS, Brasil**

**2018**



**QUANTIFYING SEDIMENT FLUXES AND SOURCES IN  
EUCALYPTUS AND GRASSLAND CATCHMENTS IN THE  
BRAZILIAN PAMPA BIOME**

**Mirian Lago Valente**

Tese apresentada ao Curso de Doutorado do Programa de Pós-Graduação em Engenharia Florestal, Área de Concentração em Silvicultura, da Universidade Federal de Santa Maria (UFSM, RS), como requisito parcial para obtenção do grau de **Doutor em Engenharia Florestal**.

**Orientador: Prof. PhD José Miguel Reichert**

**Santa Maria, RS, Brasil**

**2018**

Valente, Mirian Lago  
Quantifying sediment fluxes and sources in eucalyptus  
and grassland catchments in the brazilian pampa biome /  
Mirian Lago Valente.- 2018.  
142 p.; 30 cm

Orientador: José Miguel Reichert  
Coorientadora: Jussara Cabral Cruz  
Tese (doutorado) - Universidade Federal de Santa  
Maria, Centro de Ciências Rurais, Programa de Pós  
Graduação em Engenharia Florestal, RS, 2018

1. Forest hydrology 2. Erosion and sedimentology 3.  
Catchments paired 4. Fingerprinting approaching 5.  
Eucalyptus commercial forest I. Reichert, José Miguel  
II. Cabral Cruz, Jussara III. Título.

Sistema de geração automática de ficha catalográfica da UFSM. Dados fornecidos pelo autor(a). Sob supervisão da Direção da Divisão de Processos Técnicos da Biblioteca Central. Bibliotecária responsável Paula Schoenfeldt Patta CRB 10/1728.

---

© 2018

Todos os direitos autorais reservados a Mirian Lago Valente. A reprodução de partes ou do todo deste trabalho só poderá ser feita mediante a citação da fonte.

E-mail: mirian\_sm@yahoo.com.br

**Universidade Federal de Santa Maria  
Centro de Ciências Rurais  
Programa de Pós-Graduação em Engenharia Florestal**

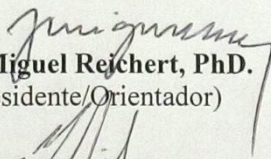
A Comissão Examinadora, abaixo assinada,  
aprova a Tese de Doutorado

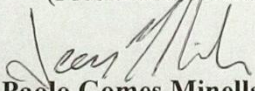
**QUANTIFYING SEDIMENT FLUXES AND SOURCES IN  
EUCALYPTUS AND GRASSLAND CATCHMENTS IN THE  
BRAZILIAN PAMPA BIOME**

elaborada por  
**Mirian Lago Valente**

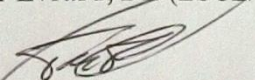
como requisito parcial para obtenção do grau de  
**Doutor em Engenharia Florestal**

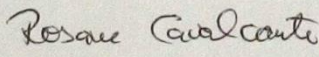
**COMISSÃO EXAMINADORA:**

  
**José Miguel Reichert, PhD.**  
(Presidente/Orientador)

  
**Jean Paolo Gomes Minella, Dr. (UFSM)**

  
**Olivier Evrard, Dr. (LSCE/CNRS)**

  
**Tales Tiecher, Dr. (UFRGS)**

  
**Rosane Barbosa Lopes Cavalcante, Dr. (CMPC)**

Santa Maria, 01 de março de 2018.



*Dedico aos meus queridos pais e irmão,  
por serem meus exemplos de carácter, amor e compreensão..*

*..e a minha “Rosa de todas as cores”, avó Anna (sempre presente), meu maior exemplo  
de amor, fé e perseverança!*





## **AGRADECIMENTOS**

A Deus, pelo dom da vida e por todas as coisas.

À CAPES, pelas bolsas de estudo no Brasil e na França.

Aos professores que tive, pelos ensinamentos.

Aos amigos do LAFIS, UFSM, LSCE e CEA por tornarem os dias de trabalho mais divertidos.

Ao meu orientador, José Miguel Reichert, pela confiança desde o início do trabalho.

Ao meu orientador na França, Olivier Evrard, que não mediu esforços para agregar qualidade ao meu trabalho de tese.

À professora Jussara Cabral Cruz pela amizade, apoio e coorientação.

Aos professores e pesquisadores Jean Paolo Gomes Minella, Tales Tiecher, Rosane Barbosa Lopes Cavalcante e Elemar Antonino Cassol pelas contribuições nas bancas de qualificação e de defesa do doutorado.

Aos meus pais e irmão, pelo apoio nas minhas escolhas e fazerem com que eu queira melhorar sempre.

A todos que medem, analisam e compartilham dados para a ciência, por iluminarem o meu caminho.

*“Today we are faced with the pre-eminent fact that, if civilization is to survive, we must cultivate the science of human relationships”*

*(Franklin Delano Roosevelt)*

*“A nation that destroys its soils destroys itself”*

*(Franklin Delano Roosevelt)*



## RESUMO

Tese de doutorado  
Programa de Pós-Graduação em Engenharia Florestal  
Universidade Federal de Santa Maria

### **QUANTIFICAÇÃO DE FLUXOS E FONTES DE SEDIMENTO EM BACIAS HIDROGRÁFICAS COM EUCALIPTO E CAMPO NO BIOMA PAMPA BRASILEIRO**

AUTORA: MIRIAN LAGO VALENTE  
ORIENTADOR: JOSÉ MIGUEL REICHERT

Data e Local da Defesa: Santa Maria, 01 de março de 2018.

O Brasil é um dos maiores produtores de florestas plantadas com eucalipto no mundo. Na região Sul do país, os efeitos da silvicultura com esse gênero nos processos hidrossedimentológicos ainda não são bem conhecidos na escala de bacia hidrográfica. O conhecimento das fontes de sedimento e suas variações espaciais e temporais constituem um pré-requisito para a concepção de medidas de gestão eficazes para uso e manejo do solo. Objetivou-se com o presente trabalho avaliar as respostas hidrossedimentológicas em duas bacias hidrográficas pareadas localizadas na região da Campanha no estado do Rio Grande do Sul, e avaliar a contribuição relativa das fontes de sedimentos e do processo de erosão dominante. As áreas de estudo estão localizadas no município de São Gabriel, RS e, tem como uso predominante do solo, plantação de *Eucalyptus saligna* (EC-0,83 km<sup>2</sup>) e pastagem com pecuária extensiva (GC-1,10 km<sup>2</sup>), respectivamente. A fim de quantificar os impactos dos diferentes usos do solo, as variáveis vazão, turbidez e precipitação pluvial foram monitoradas, sendo registradas a cada 10 minutos de intervalo durante o período entre setembro de 2013 a março de 2017. Além da automatização dos dados, amostras de água e sedimento foram coletadas durante os eventos de chuva no vertedor de cada bacia. A fim de identificar a origem do sedimento em função do uso do solo, traçadores oriundos da abordagem convencional (radionuclídeos, isótopos estáveis e geoquímicos) e espectroscopia (visível) foram combinados para obter a melhor discriminação das fontes para a fração fina de sedimentos (em suspensão, < 0,063 mm). Para a fração grossa (sedimento de fundo, 0,063-2 mm) apenas os elementos geoquímicos foram avaliados. Os resultados evidenciam maior perda de água por escoamento superficial e, conseqüentemente, maior produção de sedimento em suspensão e em arraste para a GC em relação à EC, sendo os valores maiores em até 12 vezes. Em relação à contribuição do uso do solo na origem da produção de sedimento fino, observou-se, para a GC, a seguinte magnitude média: pastagem com aveia (49%) > canal (26%) ≥ campo natural degradado (25%) com erro < 15 %, sendo o método espectroscópico melhor para a sua discriminação. Para a EC, a magnitude média correspondeu a: canal (81%) > eucalipto (16%) > estradas florestais (3%) sendo a combinação dos diferentes traçadores similar para a discriminação. Considerando a fração fina de sedimentos, a maior contribuição dessa fração ocorreu por meio dos processos erosivos subsuperficiais nas duas bacias hidrográficas de estudo, sendo caracterizada, no presente estudo, pelas áreas de canal e estradas. Para a fração grossa de sedimento, a discriminação dos processos erosivos não foi possível apenas com a análise dos elementos geoquímicos. O uso de diferentes traçadores de sedimento demonstra a divergência da seleção de traçadores para a discriminação da contribuição de cada uso do solo na produção de sedimento, mesmo que as áreas apresentem classes de solos iguais. Os resultados do monitoramento e a identificação das

fontes de sedimentos contribuem para uma melhor compreensão do efeito do uso do solo sobre a produção de sedimentos na escala de bacia hidrográfica, que são úteis para o planejamento da gestão dos recursos naturais. Além disso, evidencia-se que, tanto pelo monitoramento hidrossedimentológico quanto pela traçagem de sedimentos, a atividade de silvicultura com eucalipto nesta região apresenta menor contribuição de sedimento comparada com o uso de campo com pecuária extensiva que é uso representativo da região.

**Palavras-chave:** Erosão do solo; *Eucalyptus* spp.; Bioma Pampa; Processos hidrossedimentares; Abordagens *fingerprinting*; Espectroscopia.

## ABSTRACT

Doctoral Thesis  
Graduate Program in Forest Engineering  
Federal University of Santa Maria

### **QUANTIFYING SEDIMENT FLUXES AND SOURCES IN EUCALYPTUS AND GRASSLAND CATCHMENTS IN THE BRAZILIAN PAMPA BIOME**

AUTHOR: MIRIAN LAGO VALENTE

ADVISOR: JOSÉ MIGUEL REICHERT

Place and Date of the Defense: Santa Maria, March 1<sup>st</sup>, 2018.

Brazil is one of the largest producers of forests planted with eucalyptus in the world. In the southern region of the country, the effects of silviculture with this genus in hydro-sedimentological processes are still not well known in the basin scale. Knowledge of sediment sources and their spatial and temporal variations is a prerequisite for designing effective management measures for land use and management. The objective of this study was to evaluate the hydro-sedimentological responses in two paired river basins located in the “Campanha” region in the state of Rio Grande do Sul, and to evaluate the relative contribution of sediment sources and the dominant erosion process. The study areas are located in the municipality of São Gabriel, RS, Brazil, with predominant soil use, *Eucalyptus saligna* (EC-0.83 km<sup>2</sup>) and pasture with extensive livestock (GC-1.10 km<sup>2</sup>), respectively. In order to quantify the impacts of different land uses, the variables flow, turbidity and precipitation were monitored and recorded every 10 minutes of interval during the period between September 2013 and March 2017. In addition to the automation of the data, water and sediment were collected during rainfall events in the outlet of each catchment. In order to identify the origin of the sediment as a function of soil use, tracers from the conventional approach (radionuclides, stable and geochemical isotopes) and (visible) spectroscopy were combined to obtain the best source discrimination for the fine fraction of sediments suspension, <0.063 mm). For the coarse fraction (bottom sediment, 0.063-2 mm) only the geochemical elements were evaluated. The results evidenced a higher water loss due to surface runoff and, consequently, higher sediment yield and bed load to GC in relation to EC, with values higher up to 12 times. In relation to the contribution of soil use to the origin of fine sediment production, the following average magnitude was observed for GC: pasture with oats (49%) > channel (26%) ≥ degraded natural field (25%) with error <15%, the spectroscopic method being the best for its discrimination. For EC, the mean magnitude corresponded to: channel (81%) > eucalyptus (16%) > forest roads (3%) being the combination of different tracers similar for discrimination. Considering the fine fraction of sediments, the largest contribution of this fraction occurred through subsurface erosive processes in the two studied catchments, being characterized in the present study by the canal and road areas. For the coarse fraction of sediment, the discrimination of the erosive processes was not possible only with the analysis of the geochemical elements. The use of different sediment tracers demonstrates the divergence of tracer selection for discriminating the contribution of each soil use to sediment production, even though the areas present equal soil classes. The results of monitoring and identification of sediment sources contribute to a better understanding of the effect of land use on sediment production at the basin scale, which are useful for guiding the management of natural resources. In addition, it shows that, due to hydro-

sedimentological monitoring and sediment tracing, the silviculture activity with eucalyptus in this region presents less contribution of sediment compared to field use with extensive livestock that is a representative use of the region.

**Key words:** Soil erosion; *Eucalyptus* spp.; Pampa biome. Hydro-sedimentary process; Fingerprinting approaches. Spectroscopy.

# CONTENTS

RESUMO.....	12
ABSTRACT.....	14
1 INTRODUCTION .....	19
1.1 Hypotheses.....	23
1.2 Aim and objectives.....	23
1.3 Outline.....	23
2 ARTICLE I: HYDRO-SEDIMENTOLOGICAL RESPONSE IN THE CATCHMENT FORESTED WITH EUCALYPTUS AND WITH LIVESTOCK ON GRASSLAND, IN THE PAMPA BIOME.....	25
Abstract.....	25
2.1 Introduction.....	26
2.2 Materials and methods.....	29
2.2.1 Study site and general setup .....	29
2.2.1.1 Eucalyptus catchment (EC) .....	30
2.2.1.2 Grassland catchment (GC).....	31
2.2.2 Hydro-sedimentological monitoring .....	33
2.2.3 Quantification of sediment load (suspended and bed load) .....	33
2.2.4 Hysteresis between streamflow and suspended sediment concentration .....	35
2.3 Results.....	36
2.3.1 Hydro-sedimentological events.....	36
2.3.2 Land use effect on hydro-sedimentometric dynamics.....	41
2.3.3 Hysteresis analysis .....	45
2.4 Discussion.....	48
2.4.1 Effect of soil use on the hydro-sedimentological variables .....	48
2.4.2 Sediment yield and transfer for the paired catchments .....	49
2.5 Conclusions.....	52
2.6 References.....	53
3 ARTICLE II: COMBINATION OF SPECTROCOLORIMETRY AND CONVENTIONAL METHODS FOR IDENTIFYING SEDIMENT SOURCES IN TWO CATCHMENTS IN THE PAMPA BIOME.....	58
Abstract.....	58
3.1 Introduction.....	59
3.2 Materials and methods.....	62
3.2.1 Source material sampling .....	62
3.2.2 Laboratory analysis .....	63
3.2.3 Sediment source discrimination and apportionment .....	64
3.3 Results.....	67
3.3.1 Sediment source discrimination .....	67
3.3.1.1 Grassland catchment.....	67



3.3.1.2 Eucalyptus catchment.....	69
3.3.2 Discriminant function analysis in the paired catchments .....	71
3.3.3 Source apportionment .....	78
UV-VIS Partial least squares regression .....	81
3.3.4 UV–VIS Reflectance spectra and characterization.....	82
3.4 <i>Discussion</i> .....	84
3.4.1 Sediment source apportionment.....	84
3.4.2 Sediment tracing methods.....	87
3.5 <i>Conclusions</i> .....	88
3.6 <i>References</i> .....	89
4 ARTICLE III: QUANTIFYING SURFACE AND SUBSURFACE EROSION PROCESSES USING SEDIMENT TRACING IN PAIRED RURAL CATCHMENTS IN THE PAMPA BIOME .....	95
<i>Abstract</i> .....	95
4.1 <i>Introduction</i> .....	95
4.2 <i>Materials and methods</i> .....	98
4.2.1 Source material and sediment sampling .....	98
4.2.2 Laboratory analysis.....	99
4.2.3 Sediment fingerprinting using a mixing model .....	101
4.3 <i>Results</i> .....	101
4.3.1 Fine sediment in the paired catchments .....	101
4.3.1.1 Discrimination of sediment sources .....	101
4.3.1.2 Discriminant function analysis.....	104
4.3.1.3 Source apportionment.....	107
4.3.2 Coarse sediment in the paired catchments .....	108
4.3.2.1 Discrimination of sediment sources .....	108
4.3.2.2 Discriminant function analysis.....	110
4.3.2.3 Source apportionment.....	111
4.4 <i>Discussion</i> .....	112
4.4.1 General discussion about the dominant erosion processes .....	112
4.5 <i>Conclusions</i> .....	113
4.6 <i>References</i> .....	113
5 DISCUSSION.....	118
6 CONCLUSIONS .....	121
6.1 <i>Recommendations and perspectives for further investigations</i> .....	121
REFERENCES .....	123
APPENDIX A - CHARACTERIZATION OF STUDY AREAS .....	128
APPENDIX B – MONITORING SECTIONS.....	129
APPENDIX C – DATA SERIES DURING STUDY PERIOD.....	131

APPENDIX D - HYDRO-SEDIMENTOLOGICAL VARIABLES DURING RAINFALL  
EVENTS ..... 133

APPENDIX E - MONTHLY HYDRO-SEDIMENTOLOGICAL VALUES ..... 139

# 1 INTRODUCTION

In South America, the grasslands, or Pampa biome, extend over an area of approximately 750,000 km<sup>2</sup>, shared by Brazil, Uruguay and Argentina. In Brazil, the Pampa biome is restricted to the state of Rio Grande do Sul and corresponds to 63% of the state territory and 2.07% of the national territory (MMA, 2018). The "Campanha" region, corresponding to a significant portion of this biome, is located in the southern half of RS and has the vegetation cover characterized by herbaceous, besides some trees sparse.

Grasslands are still determinant in the economy, culture and way of life of the "gaúcho" society (BOLDRINI et al., 2010). According MMA (2012), livestock farming on native grassland has been the main economic activity in this region since the Iberian Colonization, with the introduction of cattle by the Jesuits around 1634, and thus this activity characterizes formation of the State and its regional identity. According to Nabinger et al. (2000) and Pillar et al. (2009), continuous and extensive grazing on natural fields is the basis of livestock production, but low pasture productivity results from unsustainable management. As a result, in the last 30 years there has been a 25% decrease in the total area of natural grasslands due to strong expansion of agricultural activities.

Additionally, forestry activity has the lesser extent (2.7%) and corresponded to 780,900 ha of the State territory, where 55% corresponds to eucalyptus plantations, 33.9% to pinus, and 11.5%, to acacia (AGEFLOR, 2017). This expansion is a response to the increased demand for forest-based raw-materials, and consequently resurfaced previous concerns on environmental sustainability when introducing exotic, fast-growing forest species (MATEUS, PADILHA, 2017). In 2000, the RS already had 253 thousand hectares with pine and eucalyptus (SBS, 2012). However, in 2004, new plantations were installed in the Pampa biome in areas previously without significant forest activity.

Since then, forestry with eucalyptus in the southern half has raised many questions regarding the possible impacts on water and soil resources, especially in relation to water demand and quality. Forestry activity in Brazil requires a large legal apparatus, which requires short- and long-term studies and protection of local flora and fauna, with a view to environmental sustainability. In April 2008, CONSEMA n° 187/2008 (RIO GRANDE DO SUL, 2008), which regulates that new plantations comply with the Zoning for Silviculture Activity, through studies that contemplate climatic water balance, considering the precipitation, evapotranspiration and water storage capacity in the soil, in order to evaluate water availability

for the development of forest species, as well as the establishment of environmental quality standards and impact assessment, having as planning unit the river catchment.

In the catchment scale, hydrological variables can be monitored to evaluate the impacts of land use change on hydrological processes. Two methods are usually applied to understand these changes: paired catchments or long time series from single catchments (BIRKINSHAW et al., 2014). Some studies in this biome purpose to compare the effects between grasslands and forest plantations approach on water resources. In general, afforestation of grasslands reduced streamflows due to increased evaporation of rainfall intercepted by the forest canopy, but during the dry season the forested catchment have a higher value of streamflow (BAUMHARDT, 2010, 2014; LANZA, 2015; PELÁEZ, 2014; REICHERT et al., 2017; SILVEIRA et al., 2016).

In addition to the hydrological, the sedimentary processes generated by the former have greater complexity when considering the catchment scale. There are uncertainties regarding the sources delivering sediment and the quantity of material that reaches the river channel, where the quantity of sediment supplied to the channel also depends on catchment connectivity (BROSINSKY et al., 2014; SEAR et al., 2003).

Total sediment load in rivers generally consists of suspended sediment and bed load. When analyzing the granulometric distribution of these sediments transported in the channel, the fraction transferred in suspension consists of fine material (silt and clay, <0.063 mm), mainly due to the erosion of drained areas across the catchment. Precisely because they are fine material, they can be transported for long distances inside the channel. A small amount of coarse material (sand) is also present in this suspended load, and in the case of a regime characterized by high velocity and turbulence, this amount of suspended sand can increase significantly. By contrast, the sediments moving through saltation on the bottom of the channel are characterized by the presence of large amounts of coarse material, such as sand and boulders (0.063-60 mm), mostly due to erosion in the channel itself (SARI et al., 2013).

Usually, suspended sediment is predominantly greater than bed sediment (65 to 90%), while the bed load discharge represents only the smallest part of the total solid discharge, averaging 5 to 10 %, although in some cases it may reach 30% (CARVALHO, 2008). Nonetheless, these proportions vary with the granulometry of the sediment transported, which depends on the material that makes up the river bed and the turbulence of the water (YANG, 2006).

Data obtained by Peláez (2014) in the municipality of São Gabriel showed that the mean total sediment yield per event corresponded to 0.31 Mg km<sup>-2</sup> for the catchment with

eucalyptus, in which suspended sediment ( $<0.063$  mm) varied between 4.8 - 99.7 % of the total and the bed load (0.063-2 mm) varied between 0.2-95.1% of total sediment. In the catchment with grassland, the mean sediment yield was  $3.1 \text{ Mg km}^2$ , and the variation for the sediment in suspension was 44.5-50% and 50-55.4% for bed load. The author also verified by means of small-plot experiment (3 x 1 m with 9% slope) water losses of up to  $2 \text{ L m}^{-2}$  had a soil loss of  $7 \text{ kg ha}^{-1}$ , whereas at flow rates greater than  $2 \text{ L m}^{-2}$  loss corresponded to  $17 \text{ kg ha}^{-1}$  for planting with eucalyptus, while for field use up to  $3.5 \text{ L m}^{-2}$  the soil loss was up to  $10 \text{ kg ha}^{-1}$  and for values higher than  $3.5 \text{ L m}^{-2}$  erosion increased to  $50 \text{ kg ha}^{-1}$ .

Understanding the hydro-sedimentological dynamics, with respect to the contribution of the sources for sediment yield at the catchment scale, is essential for environmental management, since it allows ameliorating areas affected by water erosion, allocating of financial resources in conservation projects, and contributing to improve our understanding of mechanisms related to sediment transport dynamics, which are also associated with contaminant transport towards drainage channels (MINELLA et al., 2009; TIECHER et al., 2015).

Considering the complexity of the processes of disaggregation, mobilization, transport and deposition of sediments by water erosion, the sediment fingerprinting approach has been developed and applied in several countries (e.g. France, Japan, Mexican, Chile) for different catchment/basin scales and land uses, in order to identify areas that actively contribute to sediment production. This approach refers to the tracking of sediments moving from upper catchment areas to the drainage channel, constituting a valuable supplement to traditional monitoring techniques of hydro-sedimentary processes.

The main tracers are fallout radionuclides, carbon and nitrogen parameters, stable isotopes, elemental geochemistry, mineral magnetic, color parameters and DNA (LACEBY et al., 2017). Although many studies have been successful with the application of fingerprinting approaches in the world (EVRARD et al., 2011; MIZUGAKI et al., 2008; NAVRATIL et al., 2012; OWENS et al., 2012; SCHULLER et al., 2013; SMITH et al., 2011; 2012; WILKINSON et al., 2009). In Brazil, most of them were carried out in agricultural catchments in RS (e.g. FRANZ et al., 2014; LE GALL et al., 2016; MIGUEL et al., 2014a, b; MINELLA et al., 2008, 2009, 2014; TIECHER et al., 2014, 2015, 2016; 2017a,b, 2018). In Brazil, Rodrigues et al. (2018) found drainage network had the highest relative contribution fine ( $<0.063$  mm) and coarse sediment (0.063-2 mm), but such studies are still incipient in Brazil.

Challenges and opportunities to be studied were presented by Lacey et al. (2017). They concluded that sediment source fingerprinting studies have recently tended to avoid in depth examinations of fundamental topics such as the impact of organic matter on biogeochemical properties, which tracer properties are non-conservative (e.g. soluble, reactive), and what is the impact of particle size on tracer property predictability. On using sediment color, Erskine (2013) concluded that changes in soil color with sediment transport are poorly known, and further work is clearly required to better understand the limitations of soil color as a tracer. Although sediment source tracing techniques based on geochemical and radiometric fingerprinting approaches, Blake et al. (2012) mentioned that there are still important limitations in terms of the potential for source discrimination, because these approaches cannot provide crucial crop-specific information on sediment source. Besides that, they comment that compound specific stable isotope analyses have the potential to elucidate processes in hydro-geomorphological studies, but it has remained largely unexplored. Lastly, Koiter et al. (2013) suggest that the application of statistical approaches without consideration of how unique sediment fingerprints have developed and how robust they are within the environment is a major limitation of many recent studies. Nonetheless, it is recommended to use a large number of tracer elements when there are many sources of sediment for analysis aiming to reduce the mathematical uncertainties in the determination (COLLINS, WALLING, 2002; YU, OLDFIELD, 1989).

Thus, the studies of sediment tracing techniques with hydro-sedimentological monitoring are important to be applied in the “Campanha” region. From the scientific point of view, since most of the studies carried out in Brazil still concentrate on the fine fraction of sediment, with geochemical and color tracers and in agricultural areas and this reliable information on sediment sources is critical if mitigation measures are to be targeted effectively. From a more applied point of view, obtaining information on forest hydrology and the dynamics of erosion processes and sediment production in areas occupied by forest stands is essential for the good management of plantations by companies in the sector. Thus, the results will guide the evaluation of the magnitude of the erosive process, the impacts of the use and management on water resources, propose measures of soil conservation and maintenance of productivity and water, information that is essential to adjust the required certifications in the sector.

Thereby, this research evaluated the production and sources of sediment during the hydro-sedimentological events, especially at the rainfall-flood event scale for different land uses of the Campanha region (livestock and forestry with eucalyptus).

## 1.1 Hypotheses

Catchment with eucalyptus commercial plantations has improved soil physical structure, thus increasing water infiltration in the soil, reducing surface runoff and peak flow and, consequently, decreasing sediment yield and source sediment.

The application of traditional sediment fingerprinting method, based on geochemical variables only, is insufficient to identify erosive processes for fine and coarse sediments in the study areas, and their respective land use sources soil.

## 1.2 Aim and objectives

### Aim

To compare the dominant hydro-sedimentological process of two paired catchments characterized by different land uses, one covered with eucalyptus plantations and other with grassland and livestock farming, located in the Pampa (Southern Grasslands) biome.

### Objectives

Identify the water and sediment transfer patterns during rainfall events in two paired catchments with different land uses;

Provide guidelines about sediment tracers for sediment sources delivering fine-sediment (<0.063 mm) considering their different land uses sources soil in each catchment.

Identify the dominant sediment processes in the paired catchments for two sediment fractions (<0.063 mm and 0.063-2 mm).

## 1.3 Outline

The present thesis is organized in six chapters. Chapter 1 provides a general introduction describing the motivation of the research and giving an overview of the thesis, together with the objectives and hypotheses of this research. Chapters 2, 3 and 4 describe the methodology, the results and the references, which are presented in the form of three scientific

articles as follows: Article I - Hydro-sedimentological response in the catchment forested with eucalyptus and with livestock on grassland, in the Pampa biome; Article II - Combination of spectrophotometry and conventional methods for identifying sediment sources in two catchments in the Pampa biome; and Article III - Quantifying surface and subsurface erosion processes using sediment tracing in paired rural catchments in the Pampa biome. Chapter 5 and 6 consists of discussion and conclusions of thesis.



## 2 ARTICLE I: HYDRO-SEDIMENTOLOGICAL RESPONSE IN THE CATCHMENT FORESTED WITH EUCALYPTUS AND WITH LIVESTOCK ON GRASSLAND, IN THE PAMPA BIOME

### Abstract

Water erosion is a natural process of soil erosion. However, it can generate deleterious impacts on soil erosion and water quality due to the inappropriate use and management of soil. To quantify these impacts, water discharge, suspended sediment concentration and rainfall were monitored continuously in two paired catchments. The catchments are located in the southernmost State of Brazil: one forested catchment with *Eucalyptus saligna* (EC -0.83 km<sup>2</sup>) and other covered with the traditional land use of Pampa biome, grassland with livestock farming (GC-1.10 km<sup>2</sup>). Sediment transport dynamics were characterized using statistical methods and hysteresis patterns, flood duration and effective discharge. The results show that discharge patterns were dominated by peak runoff events resulting from intensive rainfall, especially for GC (4-fold higher peak flows than in EC). Also, suspended (<0.063 mm) and bed load sediment (0.063-2 mm) were quantified. Variations in suspended sediment concentrations were associated with discharge fluctuations and influenced by land use soil. The data show that sediment transport processes were influenced by the land use soil, where the GC have the high water loss and sediment yield compared to EC. The events with the greatest maximum rainfall intensity showed rapid responses in sediment flow and concentration, especially in GC, with mean of suspended sediment yield annual of 22.4 (EC) and 67.9 Mg km<sup>-2</sup> (GC). The coarse sediment yield mean, during sampling, was 0.053 Mg km<sup>-2</sup> (GC) and 0.006 Mg km<sup>-2</sup> (EC). Besides that, the hysteresis pattern revealed closer sediment sources in GC and further distances in EC. The results show that catchment with eucalyptus plantation

**Keywords:** Biome Pampa; Land use; *Eucalyptus* spp.; Hydro-sedimentological process; Hysteresis.

## 2.1 Introduction

Sediment yield is a natural part of river systems and sedimentation plays an essential role in structuring the landscape, creating ecological habitats and transporting nutrients, with sediment loads significantly varying throughout the year (VERCRUYSSSE et al., 2017). For most streams, sediment particles carried in suspension are fine sand and silt sized and clay sized particles, that is, they have diameters less than about 0.2 mm (GOMI et al., 2005).

Erosion processes are size-selective during the supply, transport and storage steps of sediment movement (KOITER et al., 2013). Thus, particles that are too large to be carried in suspension are rolled, pushed or saltate along the bed and typically comprise material greater than 2 mm in diameter. However, during the rainfall events, about 70 to 90% of the sediments are transported by the rivers (CARVALHO, 2008), and this quantity depends of edaphic, physiographic, climatic and soil use and management characteristics. The total sediment load in rivers consists of suspended sediment and bed load. In general, the suspended sediment is predominantly greater than the bed load (about 60 to 95% of the total load), according to Morgan (2005) and Carvalho (2008). By contrast, the bed load discharge represent an average of 5 to 10%, and in some cases can be 30% (CANTALICE et al., 2014; CARVALHO, 2008; LENZI et al., 2003).

Soil disturbance can increase fine sediment supply to channels, while changes in hydrologic regimes can alter storm flow response and thus increase sediment transport (GOMI et al., 2005). Thus, the monitoring hydro-sedimentary processes is essential for a better understanding of the erosive processes acting on a catchment scale for different land uses, while for the rainfall event scale the processes are verified in greater detail (MINELLA, 2007).

The relationship between streamflow and sediments concentration during rainfall events can be characterized by hysteresis analyses, contributing to the understanding of sediment and water transfer in the catchment during rainfall events. Hysteresis patterns express the temporal variability in suspended sediment concentration and emphasize the context specificity of the observed processes (VERCRUYSSSE et al., 2017). The analysis of hysteresis patterns can provide useful insights into the presence of feedback mechanisms and thresholds determining suspended sediment transport (EDER et al., 2010; KRUEGER et al., 2009; MARTTILA, KLØVE, 2010).

In the Pampa biome of southern Brazil, the introduction of commercial plantations with eucalyptus in the last years has generated discussions about the impacts on water and soil,

although the forestry activity in the State corresponds to only 2.7% (AGEFLOR, 2017). This biome, located in the southern half of State has its vegetation cover characterized by herbaceous, where the fields constitute the predominant landscape, where livestock farming on native grassland has been the main economic activity in this region since the Iberian Colonization, with the introduction of cattle by the Jesuits around 1634 (BOLDRINI et al., 2010; MMA, 2018).

The continuous increase in forest-products demand and the consequent increase in forested lands raise concerns regarding the environmental impacts and sustainability of forestry. Thereby, the State of Rio Grande do Sul published Resolution CONSEMA n°. 187/2008 (RIO GRANDE DO SUL, 2008) which regulates the use of plantations in accordance with the Zoning for Forestry Activity, through studies that consider the climatological water balance, where consider rainfall, evapotranspiration and soil water storage capacity in order to evaluate the water availability for the development of forest species, as well as the establishment of environmental quality standards and impact assessment, having as its planning unit the river catchment.

The establishment of forests, therefore, modifies the hydrological cycle and consequently the hydro-sedimentological processes. Forest canopies cause rainfall partitioning into interception, throughfall and stemflow, and thus affect soil moisture patterns, infiltration, groundwater recharge and water yield (CHANG, 2006; SILVEIRA, ALONSO, 2009). However, after one year of implementation these systems form understorey vegetation cover, with a tendency to water use by plantation be similar to the amounts observed for native forests (LIMA, 1996; PIRES et al., 2006).

Changes in the rainfall–runoff relationship has been investigated in paired experimental small catchments showing a decreasing streamflow due to the afforestation of grasslands (ANDRÉASSIAN, 2004; BAUMHARDT, 2010; 2014; GERMER et al., 2009; GUSH et al., 2002; REICHERT et al., 2017; SILVEIRA et al., 2016). However, the forest vegetation significantly favors soil water infiltration capacity, especially when there is a rapid increase in soil organic matter, as in homogeneous eucalyptus plantations (GUIMARÃES, 2015). Previous studies, mentioned by Valente and Calil (2016), also showed that forests are essential ecosystems for conservation and maintenance of the water resources of a catchment, especially with regard to quantitative-qualitative aspects.

In extensive livestock conditions, the continuous and extensive grazing on natural grasslands in the State is the basis of livestock production, but low pasture productivity results

from unsustainable management (NABINGER et al., 2000; PILLAR et al., 2009), which reflects on environmental (soil erosion) and social issues (productivity decrease). Holt et al. (1996) and Müller et al. (2001) observed physical degradation of soil with pasture due to continuous cattle trampling, promoting soil compaction, and increasing bulk density, microporosity and soil resistance to penetration. High animal stocking rates on grasslands and subsequent overgrazing resulted in soil erosion with loss of soil carbon and in grassland species diversity (OVERBECK et al., 2007). Thus, livestock acts as a bioerosive agent since it changes as relief forms and accelerates the surface geomorphological processes (THOMAZ, DIAS, 2009).

In a literature review on land use change and ecosystem service provision in Pampas and Campos grasslands of southern South America, Modernel et al. (2016) found scarce information on changes in the ecosystem services water provision, nutrient cycling and erosion control.

In Brazil, there are few studies in the forested catchment have been done covering the different sediment fractions, e.g. fine (<0.063 mm) and coarse sediment (0.063-2 mm) (PELÁEZ, 2014; RODRIGUES et al., 2018). Furthermore, much of the research on the size characteristics of eroded sediment has been done in agricultural soils and most studies involved field or laboratory-based rainfall simulation experiments (MAHMOODABADI, SAJJADI, 2016; MARTINEZ-MENA et al., 1999).

There are some information on sediment yield during rainfall events in the catchment scale, e.g. Peláez (2014) observed a total sediment yield of 9.3 and 101.8 Mg km<sup>-2</sup> in the eucalyptus and grassland catchments, respectively. Rodrigues et al. (2014) in a study with two forested catchments with eucalyptus, observed in one year the sediment yield was 41.6 and 38.5 Mg km<sup>-2</sup> for them. The authors also observed during an extreme event provided greater sediment yield in these areas, where was observed 99.8 and 51.7 Mg km<sup>-2</sup>. Nonetheless, there are more studies with suspended sediment monitoring in the forested catchments - but the samples were not collected during event - (CÂMARA et al., 2006; CRUZ et al., 2016; VALENTE et al., 2015; VITAL et al., 1999), and in the plot scale (CARDOSO et al., 2004; OLIVEIRA, 2008; 2011; OLIVEIRA et al., 2014; PINESE JÚNIOR et al., 2008).

Thus, there still is a gap in understanding of hydrological and sedimentological dynamics in areas of eucalyptus forests, because consolidated knowledge is an important aspect when making decisions regarding appropriate land use and management of natural resources, which aim to increase environmental productivity and sustainability.

The objective of this chapter is to compare the effects of hydro-sedimentological parameters to quantify sediment yield of two fractions sizes of sediments (<0.063 mm and 0.063-2 mm) and characterize the eroded sediment on different land use in the paired catchments (eucalyptus and grassland) in the Brazilian Pampa Biome.

## 2.2 Materials and methods

### 2.2.1 Study site and general setup

The study was conducted in two paired catchments, one covered with eucalyptus plantation (*Eucalyptus saligna*) belonging to the CMPC Riograndense Cellulose company and the other occupied by grassland and livestock farming located at Farm Alvorada, a private property (see Figure 1 and Appendix A).

These catchments are located in the municipality of São Gabriel, in the physiographic region named *Campanha* in Rio Grande do Sul State, southern Brazil. Both catchments drain into the Vacacaí and Vacacaí-Mirim rivers, covering an area of 11,077.34 km<sup>2</sup> and are located in the center-west portion of the State, between the geomorphological provinces *Depressão Central* and *Escudo Sul Rio-Grandense* (SEMA, 2017), which in turn drain into the Guaíba River Basin, part of the National Hydrographic Region South Atlantic, and finally to the Atlantic Ocean.

Climate is Cfa, humid subtropical, with no drought, according to Köppen climate classification, with average annual temperature of 18.6 °C and average annual rainfall is 1356 mm (ALVARES et al., 2013; MORENO, 1961). Soils in both catchments are derived from weathering of metamorphic rocks and granite-gneiss (amphibolite metamorphism; orthogneiss lithologies, metadiorite, and metaperidotite), according Ramgrab et al. (2004), with soils physically fragile and with low natural fertility and agricultural potential (MORALES, 2013).

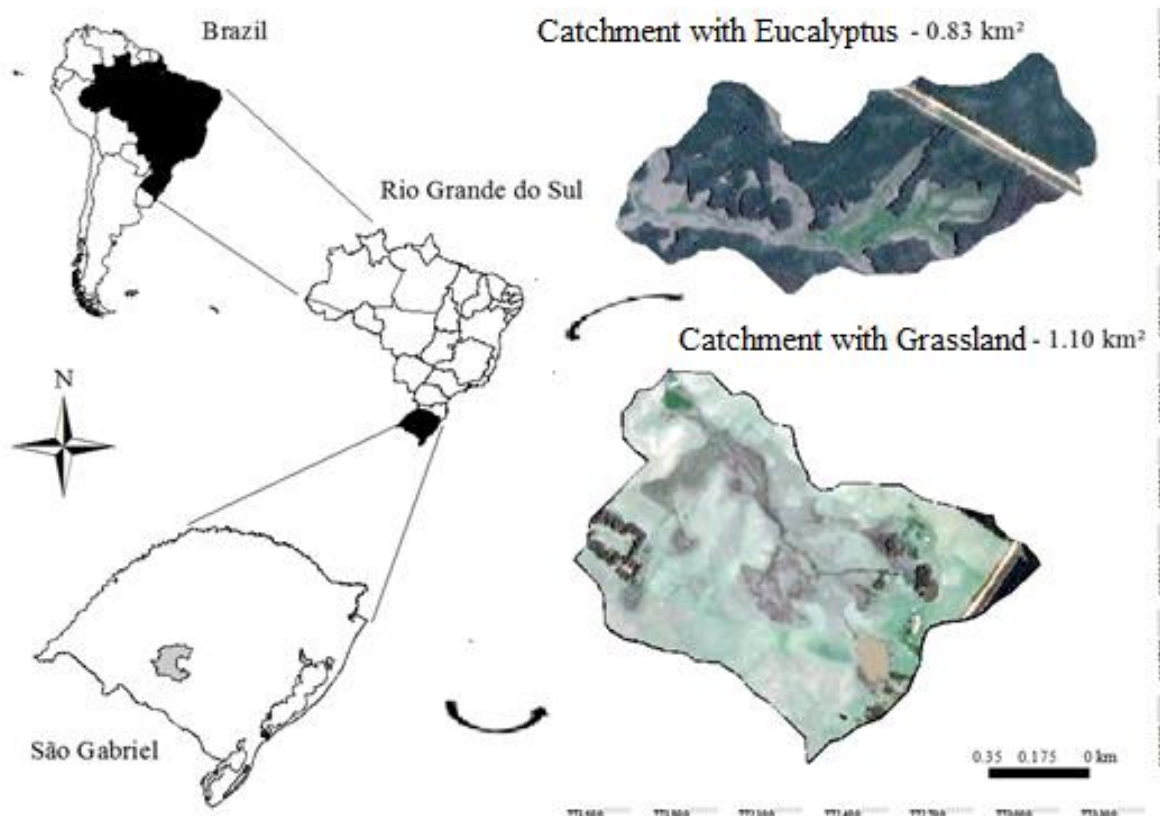


Figure 1 – Location of the municipality of São Gabriel and the limits of the catchments with eucalyptus and with grassland.

#### 2.2.1.1 Eucalyptus catchment (EC)

The EC has a drainage area of 0.83 km<sup>2</sup> and a perimeter of 4.17 km, with a 1.51 compactness coefficient and average time of concentration of 2:52 h calculated based on average of rainfall events (REICHERT et al., 2017). The river hierarchy is of second order, in which channels originate from the junction of two channels of first order (STRAHLER, 1957). The EC landscape is characterized by elevations between 230 and 315 m asl, with an average elevation of 272 m and mean slope of 7.7% (Figure 2a, c).

The soils are classified (Figure 2e) as *Argissolo Vermelho Distrófico* (Ultisols), *Argissolo Vermelho-Amarelo Distrófico* (Ultisols), *Cambissolo Háplico Alumínico* (Inceptisols), *Neossolo Regolítico Eutrófico* (Entisols) and *Neossolo Litólico Eutrófico* (Entisols), in the Brazilian Soil Classification System (EMBRAPA, 2006) and, in parentheses, by Soil Taxonomy (USDA, 1999).

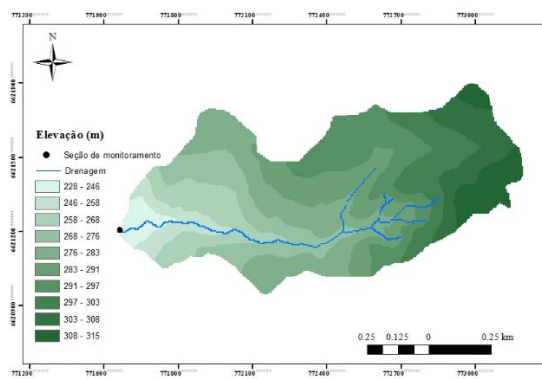
Land use is mainly *Eucalyptus saligna* (40% of total area with stand were planted in 2006 and 21% stand planted in 2014 after cutting), grassland with brush weeds (22.1%),

riparian vegetation (7.9%), unpaved roads (5.8%), and outcrops (2.6%), see Figure 2g. Eucalyptus stands had 3.0 m × 3.3 m spacing and the stand planted in 2006 had average diameter at breast height of 0.17 m and average height of 25 m. The grassland with *Baccharis* spp. consisted of grasses and shrubs, in which *Aloysia gratissima* (Verbenaceae) and *Heterothalamus alienus* (Asteraceae) were the most abundant species. The riparian vegetation consisted of arboreal stratum of native species, with individuals of 6–8 m in height, namely *Sebastiania commersoniana*, *Rollinia salicifolia*, *Styrax leprosus*, *Eugenia uniflora*, *Luehea divaricata*, *Casearia decandra*, *Diospyros inconstans*, *Myrcianthes pungens* and *Ocotea* ssp (PELÁEZ, 2014).

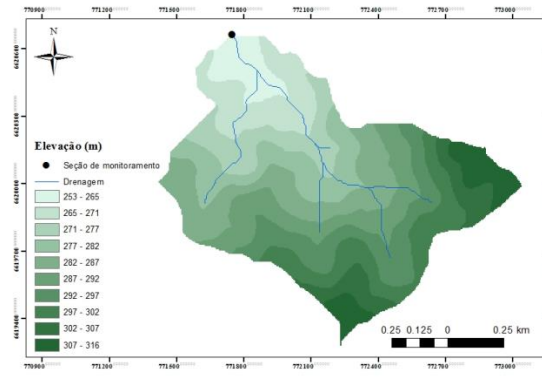
#### 2.2.1.2 Grassland catchment (GC)

The GC has a drainage area of 1.10 km<sup>2</sup> and a perimeter of 4.32 km, with a 1.22 compactness ratio, average time of concentration of 1:47 h calculated based on average of rainfall events (REICHERT et al., 2017), and fluvial hierarchy of second order. The GC landscape is characterized by elevations between 255 and 310 m asl with an average elevation of 273 m and mean slope of 3.1% (Figure 2b, d). The soils are classified as *Argissolo Vermelho* (Ultisols), *Cambissolo* (Inceptisols), and *Neossolo* (Entisols), respectively, in the Brazilian Soil Classification System (EMBRAPA, 2006) and, in parentheses, by Soil Taxonomy (USDA, 1999) (Figure 2f).

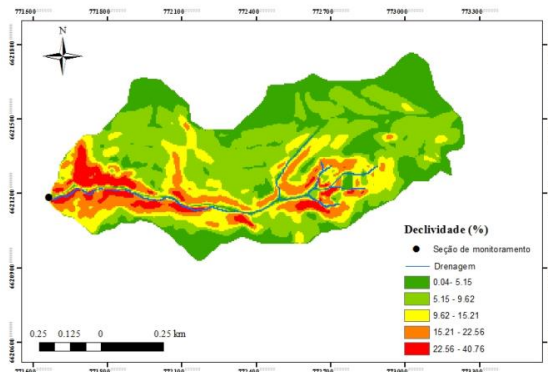
Land use was degraded native-grassland (61.7% of the total area of the GC), pasture composed of oats (*Avena strigosa*) (31.1%), eucalyptus patches and isolated individuals (3.3%), riparian vegetation (2.1%), reservoir (1.7%), and buildings (0.1%), according Figure 2h. The GC upper vegetation stratum in degraded native-grassland was composed of *Saccharum angustifolium*, *Aristida laevis*, *Baccharis riograndensis*, *Andropogon lateralis* and *Eryngium pandanifolium*, whereas the lower stratum consisted of *Paspalum* ssp., *Axonopus affinis* and *Fimbristylis autumnalis* (PELÁEZ, 2014). The degraded native-grassland has low vegetation cover, partially due intensive grazing and due absence of liming and fertilizer application to improve soil fertility for pasture growth. Grazing by beef cattle reduced species diversity and soil quality due animal trampling, where biomass is reduced and soil is exposed to erosion processes. One head of cattle per hectare, on average, is maintained in the area. The cultivated pasture is renewed annually with black oats, where soil tillage was accomplished by disking once a year, generally in April or May, and lime (but no fertilization) was applied before.



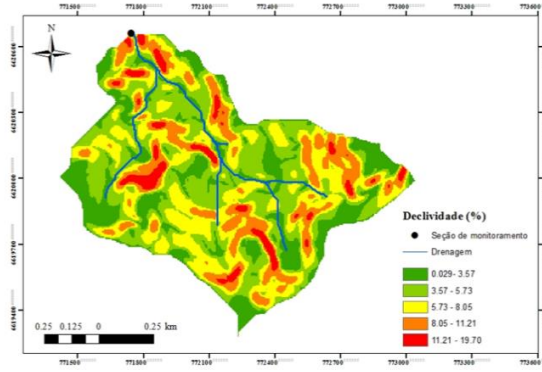
(a)



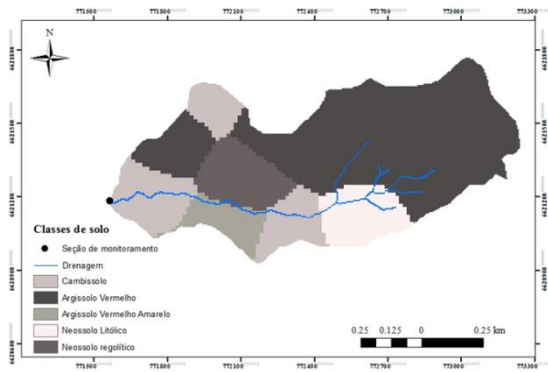
(b)



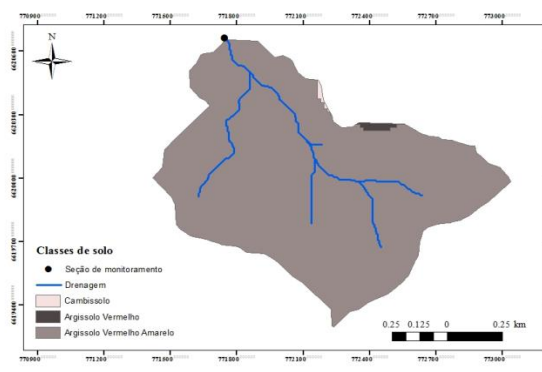
(c)



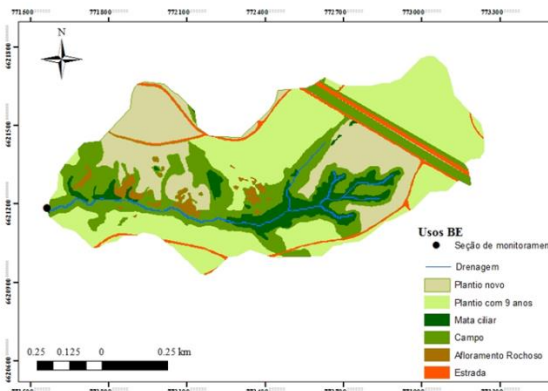
(d)



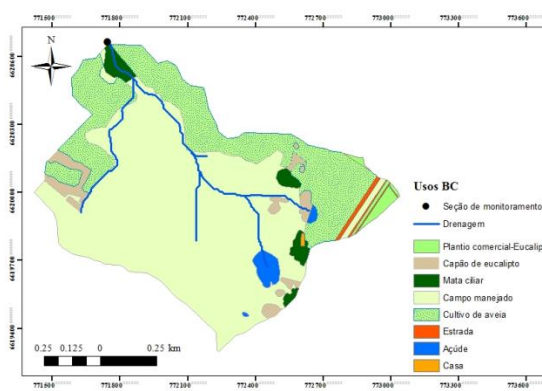
(e)



(f)



(g)



(h)

Figure 2 – Elevation maps for EC (a) and GC (b), slope maps for EC (c) and GC (d), soil classes for EC (e) and GC (f) and land uses soil for EC (g) and GC (h) in São Gabriel-RS.



### 2.2.2 Hydro-sedimentological monitoring

The monitoring was conducted from September 2013 to March 2017 using automated monitoring sections, equipped with instruments measuring water level (limnigraphs), turbidity (turbidimeters) and rainfall (pluviograph), see Appendix B. The sensors were installed near the triangular weirs located at the catchment outlets and the data loggers recorded data at 10-minute intervals (see Appendix B). From the set of equations of the different flow stages, the flow ( $\text{m}^3 \text{s}^{-1}$ ) in each catchment was obtained by means of the general equation (Appendix B). The general equations were calculated and validated at the maximum vertical height of 1 and 0.8 m, respectively for GC and EC, which correspond to the flow limits of 8,131 and 2,711  $\text{L s}^{-1}$ .

The turbidimeter records the values in energy pulses (millivolts, mV) which were later converted into Turbidity Nephelometric Unit (NTU). Sensor calibration and turbidity estimation was performed using polymer bead calibration solutions. The concentrations used for the calibration curve were: 0 (distilled water), 20, 50, 100, 400, 1000 and 3000 NTU. Calibrations were performed at monthly intervals, where 20 readings (repetitions) were performed for each concentration.

### 2.2.3 Quantification of sediment load (suspended and bed load)

Sampling of suspended sediment was conducted manually during rainfall events with a USDH-48 sampler (Appendix B), to obtain time series of sediment concentration data. Due to the need of continuous data acquisition, turbidity measurements were used for estimating suspended sediment concentrations. This device provides data for estimating the concentration of suspended sediments based on the relationship between suspended sediment concentration and turbidity established by a rating curve (Figure 3). Bed load was monitored using a BLH-84 sampler, according to the method proposed by Edward and Glysson (1999). Sediment concentration was quantified by drying and weighing this material at the *Laboratório de Física do Solo* at UFSM, by the evaporation method (SHREVE, DOWNS, 2005). Total sediment yield was determined from the integration of the solid discharge throughout the entire monitoring period (for both suspended and bed load). Also, grain size distribution was analyzed with a laser granulometer for catchments sediments samples, after oxidation of organic matter with  $\text{H}_2\text{O}_2$  and dispersion with NaOH (MUGGLER et al., 1997).

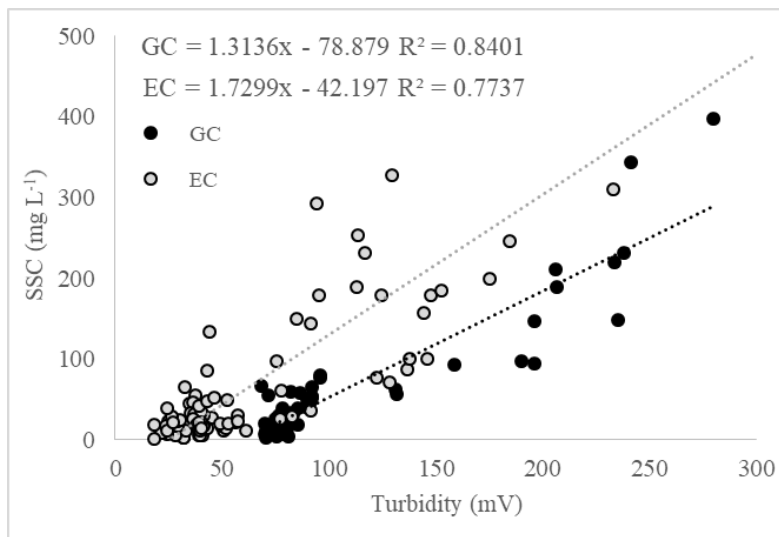


Figure 3 – Relation between turbidity and suspended sediment concentration for the estimation of SSC based on the events sampled in the catchments, São Gabriel, RS.

Table 1 shows the sampling frequency of the water plus sediment mixture for distinct discharge ranges during the monitored period.

Table 1 – Control of sampling frequency of the mixture of water and sediments based on the flow rate sampled for the grassland (GC) and eucalyptus catchments (EC), São Gabriel, RS.

Discharge (L s <sup>-1</sup> )	Frequency of sampling (%)			
	Fine sediment		Coarse sediment	
	GC	EC	GC	EC
0-100	39	91	4	54
101-200	25	15	4	21
201-300	4	18	13	8
301-400	3	5	4	13
401-500	9	4	13	0
501-600	2	0	4	4
601-700	2	0	4	0
701-800	2	0	0	0
801-900	0	0	9	0
901-1000	3	0	17	0
1001-2501	6	0	13	0
2501-4501	3	-	13	0
4501-6500	1	-	0	0
6501-8500	1	-	0	0

Note: -, validated flow limits for each area: 8,131 L s<sup>-1</sup> (GC) and 2,711 L s<sup>-1</sup> (EC).

During the study period, 15 rainfall-flow-sediment events were sampled simultaneously in the both areas (see Appendix C). There were errors and failures in the data records during the sampling of some events. Most failures occurred in the turbidimeter data

records. Thus, some quantified suspended sediment concentration (SSC) values could not be compared with the turbidity values of the sensor (mV).

Sediment yield was calculated using Equation 1. Total sediment yield corresponds to the sum of solid discharge obtained during a given rainfall and the entire period of automatic monitoring.

$$SY = \sum_{i=1}^n k(SSC * Q_i) \quad (1)$$

With: SY is the sediment yield (t); SSC is the sediment concentration (mg L<sup>-1</sup>); Q<sub>i</sub> is the instantaneous water discharge (L s<sup>-1</sup>); k is a unit conversion factor; n is the number of instantaneous SSC and Q measurements taken at a given time.

The values of the bed sediment discharge were determined by using Equation 2, established by Gray (2005):

$$Q_{bl} = \sum_i^n \left( \frac{m}{(w*t)} \right) * b * 0.0864 \quad (2)$$

With: Q<sub>bl</sub> is the bed load discharge (Mg day<sup>-1</sup>); m is the sediment mass (g); w is the nozzle section (m); t is the sampling time (s); b is the bed width (m); 0.0864 is a unit conversion factor for Mg day<sup>-1</sup>.

#### 2.2.4 Hysteresis between streamflow and suspended sediment concentration

Hydro-sedimentary sediment pattern in the catchments was evaluated by analyzing the shape of the hydrographs and sedigraphs and the relationship between streamflow and suspended sediment concentration. More specifically, the events were classified according to the hysteresis loop index (HI), which is obtained from the analysis of streamflow (Q) and suspended sediment concentration (SSC) data and the construction of the associated Q versus SSC graph, (Q<sub>max</sub>) and the minimum initial flow rate (Q<sub>min</sub>) of the event. The central value between the maximum and minimum flow of the rising limb (Q<sub>cen</sub>) of the event is calculated according to (Equation 3).

$$Q_{cen} = 0.5 * (Q_{max} - Q_{min}) + Q_{min} \quad (3)$$

For the central value (Q<sub>cen</sub>), the values of sediment suspension concentration in the rising limb (SSC RL) and in the falling limb (SSC FL) are shown in the relationship between suspended sediment concentrations and streamflow (hysteresis graph). The values of SSC RL and SSC FL can be obtained from the interpolation between the points for which SSC and Q

measurements are available. If the hysteresis curve has a clockwise direction, the hysteresis index (HI) will be positive and calculated using (Equation 4); and if the hysteresis curve has an anti-clockwise direction, the hysteresis index (HI) will be negative and calculated following Equation 5.

$$HI = \left( \frac{SSC_{RL}}{SSC_{FL}} \right) - 1 \quad (4)$$

$$HI = \left( \frac{-1}{\left( \frac{SSC_{RL}}{SSC_{FL}} \right)} \right) + 1 \quad (5)$$

## 2.3 Results

### 2.3.1 Hydro-sedimentological events

The dynamics of flow and concentration of suspended sediments during the events results in hydrograms and sedigraphs rarely synchronized in time. The sedigraphs occurring in the monitored period demonstrate that the maximum concentration of suspended sediments occurred before the maximum flow in GC, and after the peak in EC (Figure 4).

When the maximum concentration of sediment in suspension occurs before the maximum flow, the sediments originate from nearby sources. Thus, these sediments were mobilized, transported and deposited quickly. Further, it demonstrates dissipation of rainfall energy is higher in GC, possibly due to low vegetation cover, and the soils with physical fragility and little depth favor surface runoff and conditions e more favorable for erosion and sediment yield, especially during extreme rainfall events.

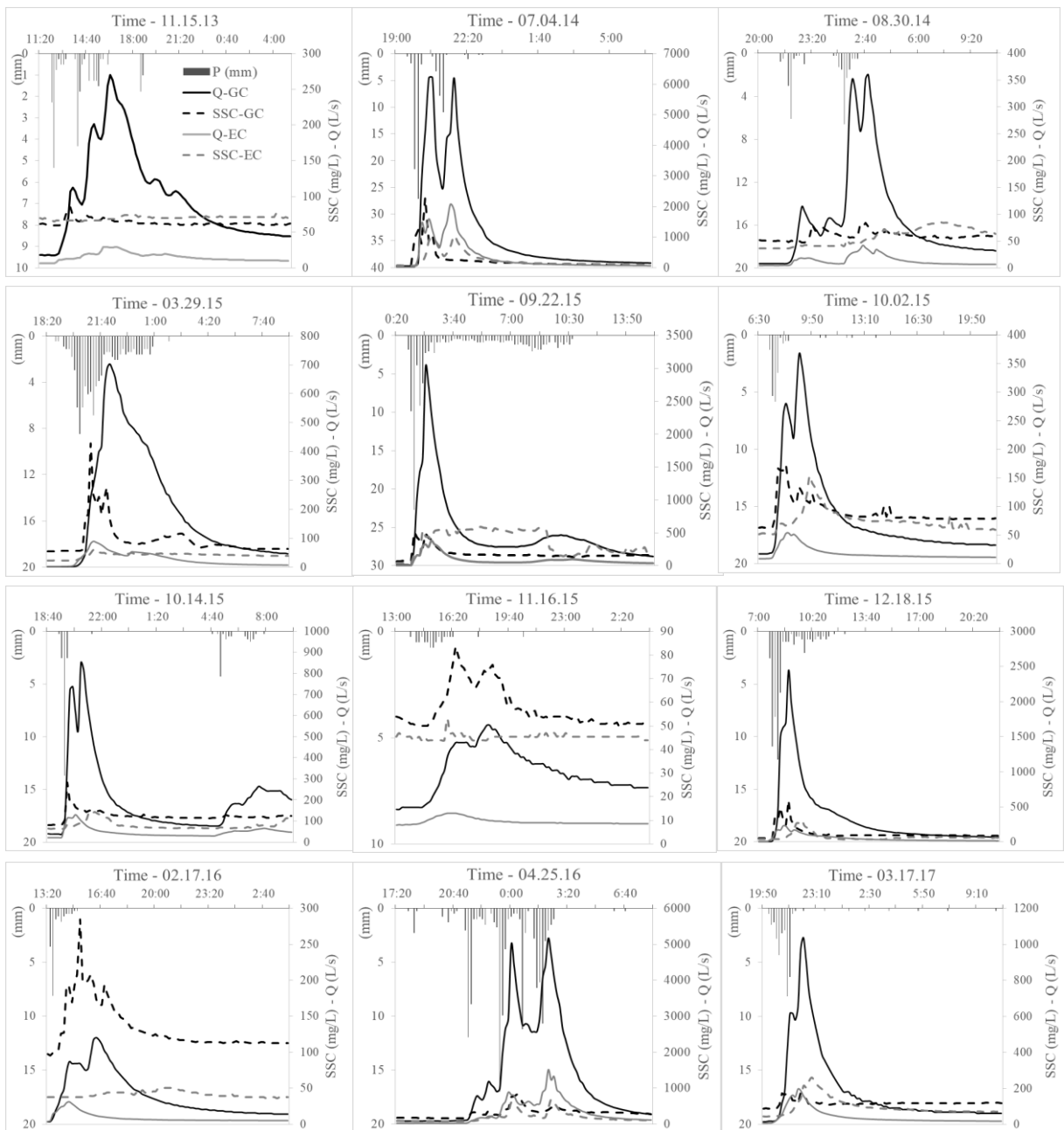


Figure 4–Time series for events with different flow (Q), suspended sediment concentration (SSC) and magnitude and rainfall were selected to represent the typical peak events in the Eucalyptus and Grassland catchments.

Evidence of rapid hydro-sedimentary response by rainfall event in GC was observed for all events (Figure 4), e.g., for the different magnitudes of rainfall intensity (varying from 3.3 until 54.1 mm h<sup>-1</sup>). For these events, the flow peak in GC was 3.3 to 10.6 times higher than in EC, depending on rainfall volume and intensity. Consequently, suspended sediment concentration was higher and sediment yield was 12 times higher in GC compared to EC, as verified during events occurring on 03.29.2015 and 04.25.2016, with very-steep rising and falling hydrograph limbs, which shows the quick response of flow and sediments after the rainfall.

The rising and falling limb of the events were more pronounced in GC compared to EC. Some hydrographs in GC (Figure 4, events 11.16.15; 02.17.16) with lower rainfall volume had smaller rising and falling limbs due to the slow response to rainfall events, but still the sedigraphs response was more pronounced for these events. For the events on 07.04.14, 10.14.15 and 04.25.16, after the high rainfall intensity, the flow increase did not provide increased suspended sediment concentration. This behavior, observed in some events, is due to the transport capacity and sediment exhaustion with subsequent event peak flows associated with less suspended sediment being transported in the GC. By contrast, for the same events in EC, each flow peak was accompanied by higher suspended sediment concentration, which possibly indicates greater sediment transfer during the consecutive events with high volume.

In EC, flow had less steep rise and falling and lower magnitude of maximum streamflow. The rainfall interception process by canopy, litter and stemflow reduces the volume and impact of rainfall on soil and favors water infiltration, which results in lower runoff, streamflow and suspended sediment concentration. The effect of land use on suspended sediment concentration and yield in the catchments showed a different pattern depending on the magnitude of the events.

Total rainfall ranged between 4.6 and 154.5 mm, with a mean of 31.2 mm (see Appendix D). Maximum rainfall intensity was 54.1 mm h<sup>-1</sup>. In general, runoff was higher in GC with maximum and mean runoff coefficients, respectively, of 45.5 and 10.2%, and 12.4 and 2.2% in EC (Figure 5b). These values demonstrate how much more water is lost in the catchment with grassland, in which the maximum and mean values of peak flow also were observed; consequently, suspended sediment concentrations and bed load were higher in the GC (Figure 5f).

Figure 5 summarizes the main characteristics of rainfall, streamflow and suspended sediment concentrations associated with 51 of the 150 monitored events, because the direct comparison of data in both catchments (EC and GC) was possible only for these events. Data obtained during all events were provided in Appendix D.

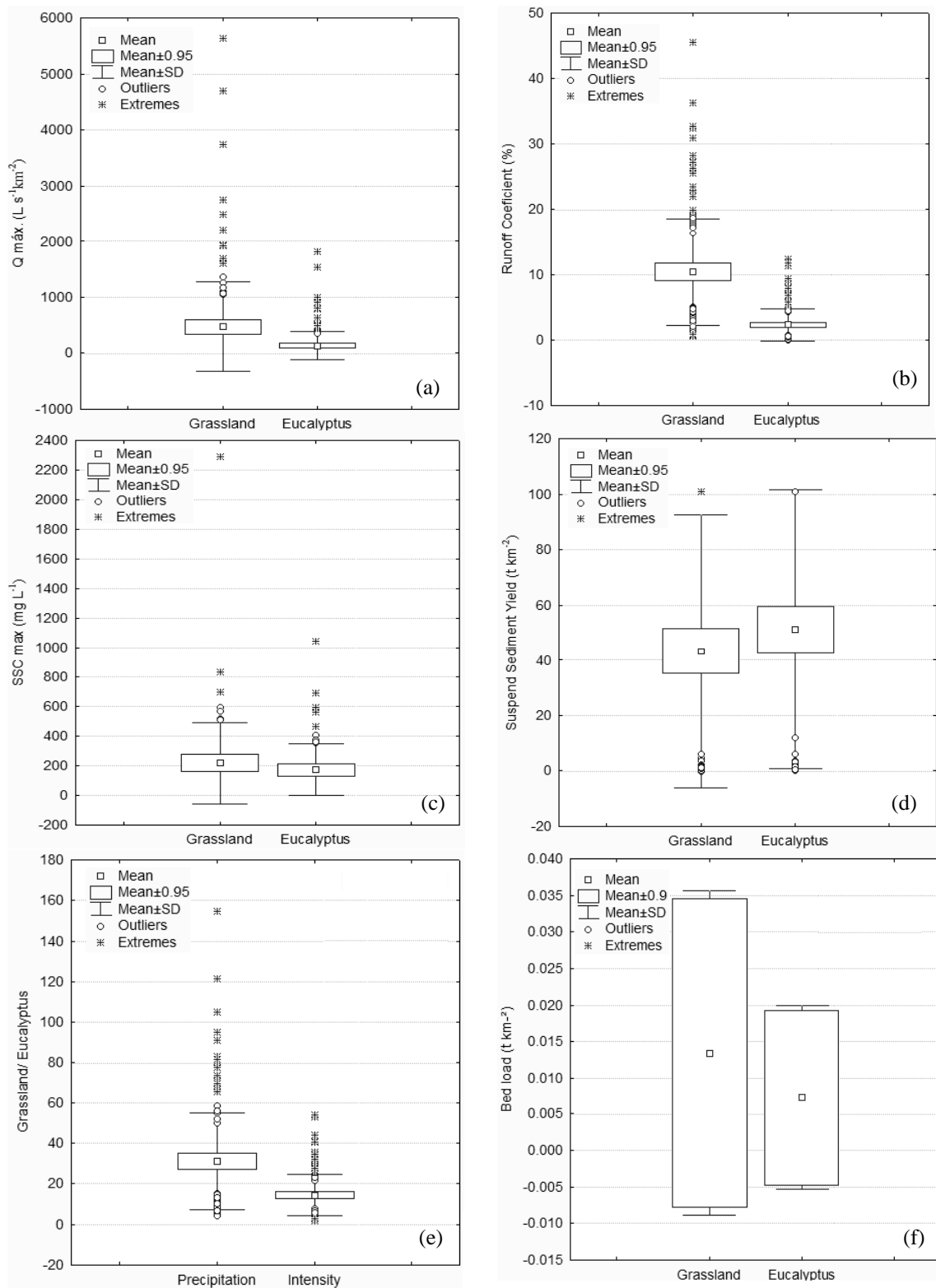


Figure 5 – Box-plot of hydro-sedimentary variables: maximum streamflow (a); runoff (b); suspended sediment concentration maximum (c); suspended sediment yield (d); rainfall and maximum intensity in 1 hour (e) and bed load (f) of events monitored in the grassland and eucalyptus catchments.

Five events were considered as extreme magnitude, more than  $40 mm h^{-1}$  of intensity (13/Jan; 03/Mar and 04/Jul/2014; 22/Sep and 18/Dic/2015, see Appendix D). As the study

period was affected by the *El Niño* phenomenon, the analysis of high volume events is importante, since the frequency of their occurrence has been increasing in the last years, being more damaging to the environment. Extreme climatic events can occur under different forms, such as floods, prolonged droughts, strong winds, landslides and others (see Appendix A with “strong winds” episode recorded in the experimental area).

The events with the highest sediment yield occurred on 04/Jul/2014, after 77 mm (53.1 mm h<sup>-1</sup>) of cumulative rainfall, which resulted in higher values of flow peak (6,206.0 and 1,513.6 L s<sup>-1</sup>, respectively, in GC and EC), suspended sediment concentrations (2,290.2 (GC) and 1,046.8 mg L<sup>-1</sup> (EC) and total sediment yields (26.8 (GC) and 11.8 Mg km<sup>-2</sup> (EC)), see more information in the Figure 5a,c and Appendix D. This event occurred few weeks after eucalyptus harvesting in 20% of the plantation (between March and May of 2014), followed by on-line planting and even with the soil exposed the sediment yield was lower than GW. This condition of forest harvest, done in the staggered way, shows that the sediment yield remained similar to the period before forest harvest, thus continuing to be lower than the sediment yield in the grassland catchment. For this event, sediment yield corresponded to 65 and 83% of the total yield recorded in the monitoring year from Sep. 2013 to Aug. 2014 in GC and EC catchments, respectively.

For bed load, the highest yield observed was for events with higher rainfall intensity and volume, especially in GC (Figure 5f). Higher bed load transfers were also found in the GC site (0.053 Mg km<sup>-2</sup>) compared to EC site (0.006 Mg km<sup>-2</sup>), and they amounted less than 1% of the total sediment yield. For this event, higher sediment yield also was accompanied by greater loss of water in the form of surface runoff (45% in GC and 11% in EC).

Similar sediment yield behavior was observed on 25/Apr/2016, where the maximum discharge in the EC was five times less compared to the GC (1,513.6 and 5,169.0 L s<sup>-1</sup>, respectively). Consequently, the suspended sediment concentration peak was lower in the EC (692.6 mg L<sup>-1</sup>) compared to GC (829.6 mg L<sup>-1</sup>) and similar results were obtained for sediment yield (6.2 Mg km<sup>-1</sup> for -EC and 26.7 Mg km<sup>-1</sup> in the GC).

Thirty-seven events presented flow exceeding 500 L s<sup>-1</sup> during the monitoring period in GC (value mean was 508.2 L s<sup>-1</sup>), compared to only seven events in EC (value mean was 111.3 L s<sup>-1</sup>), see Appendix D. For events with rainfall lower or equal than 30 mm, higher peak flows were observed in GC with mean of runoff coefficient of 6.62% compared to 1.33% in EC, although higher water loss occurred in this catchment. The maximum suspended sediment concentration was, in general, higher in GC with average of three times more than in EC. A



similar response was observed for the events on 15/Sep, 26/Nov, 18/Dic/2013; 10/Aug/2014 and 06/Jan/2017.

Figure 6 shows linear regressions between studied variables: discharge and suspended sediment concentration during events ( $r^2=0.58$  for GC and  $r^2=0.43$  for EC), sediment yield with the product of runoff and peak discharge ( $r^2=0.68$  for GC and  $r^2=0.90$  for EC), and between bed load and discharge ( $r^2=0.24$  for GC and  $r^2=0.13$  for EC).

In general, observed the coefficients of determination was less than 0.5, it means a not good relationship between the variables and that need more observations for that the prediction between them will be more reliable.

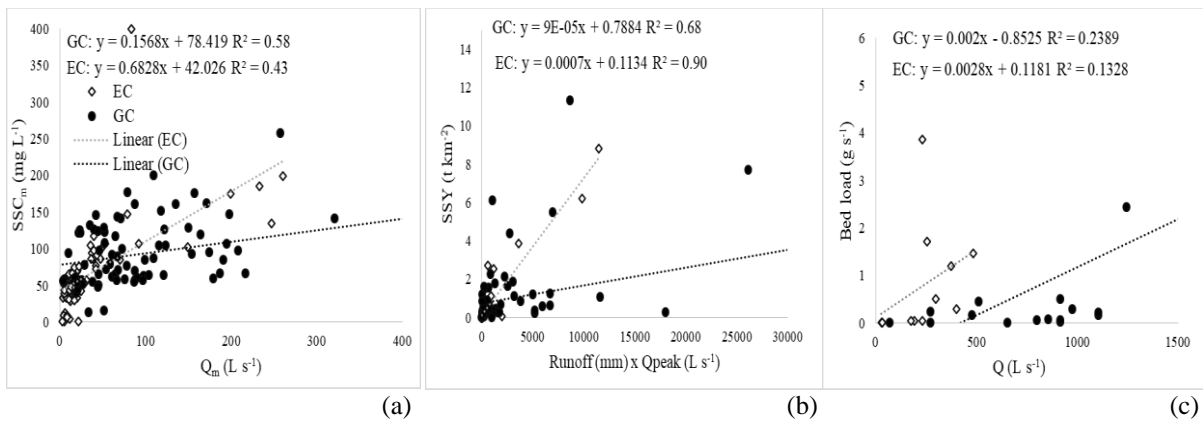


Figure 6 – Relationship between the mean of suspended sediment concentration ( $SSC_m$ ) and the mean discharge ( $Q_m$ ) (a); the suspended sediment yield (SSY) with the product of runoff and peak discharge (b) and the bed load and discharge (c) per event. For the eucalyptus and grassland catchments.

### 2.3.2 Land use effect on hydro-sedimentometric dynamics

A summary of hydro-sedimentometric annual results obtained during the monitoring period is provided in Table 2. In general, the maximum flow and the highest runoff and sediment yield were observed in the GC catchment, as well as maximum suspended sediment concentrations.

The highest annual precipitation (1823 mm) was recorded in 2015-2016. As commented before, during the study period (2014-2016), the Rio Grande do Sul State was strongly affected by the *El Niño* phenomenon, which contributed to an increase of 25% compared to historical annual rainfall average.

Table 2 – Annual mean, minimum, maximum and standard deviation of variables streamflow (Q), suspended sediment concentration (SSC), suspended sediment yield (SSY) and rainfall (P) during the study period (Sep/2013–Mar/2017).

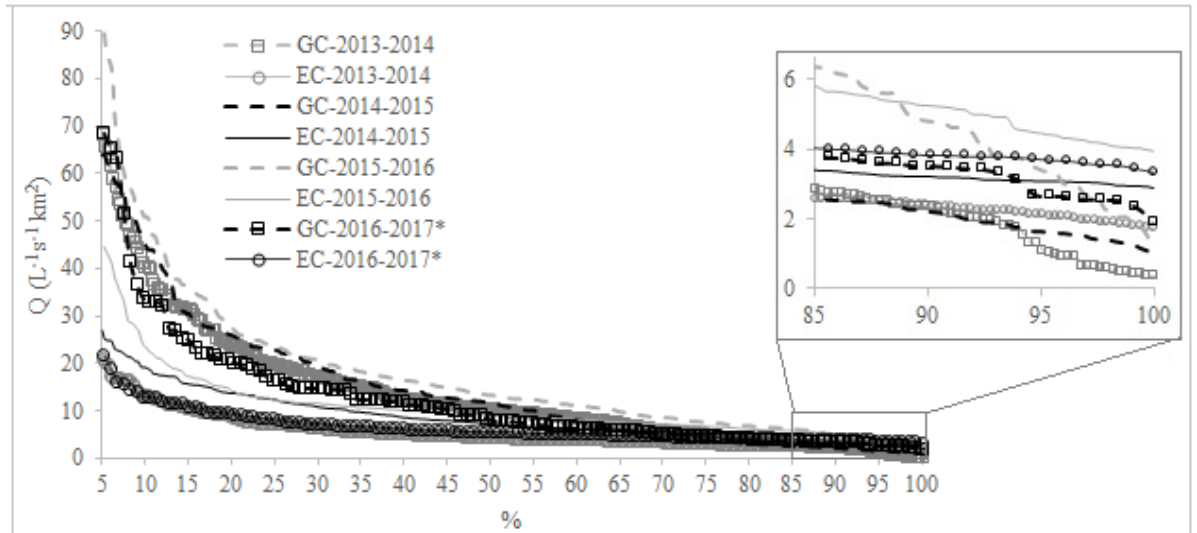
Variable	Eucalyptus catchment				Grassland catchment			
	Mean	Min	Max	SD <sup>a</sup>	Mean	Min	Max	SD <sup>a</sup>
<b>Q (L s<sup>-1</sup> km<sup>-2</sup>)</b>								
Sept./2013- Aug./2014	8.4	1.0	2493.1	32.3	22.5	0.2	5641.8	96.1
Sept./2014- Aug./2015	10.6	2.0	462.7	16.1	19.7	0.7	1175.0	47.2
Sept./2015- Aug./2016	16.1	2.5	1823.6	39.3	35.5	0.5	4699.1	115.8
Sept./2016- Mar./2017	7.2	3.0	236.7	14.3	14.8	1.2	1064.7	40.3
<b>SSC (mg L<sup>-1</sup>)</b>								
Sept./2013- Aug./2014	50.6	28.8	1046.8	20.4	53.4	45.0	2290.2	8.8
Sept./2014- Aug./2015	41.0	15.1	357.5	12.4	61.4	46.8	427.6	16.7
Sept./2015- Aug./2016	48.8	32.0	695.3	26.6	73.5	35.6	809.6	30.1
Sept./2016- Mar./2017	42.9	32.5	260.1	14.4	60.0	38.4	364.6	17.9
<b>SSY (Mg km<sup>-2</sup>)</b>				<i>Total</i>				<i>Total</i>
Sept./2013- Aug./2014	0.07	0.03	0.09	11.74	0.07	0.02	0.20	32.29
Sept./2014- Aug./2015	0.08	0.03	0.17	15.49	0.11	0.02	0.43	45.04
Sept./2015- Aug./2016	0.11	0.06	0.36	39.98	0.33	0.02	4.13	126.55
Sept./2016- Mar./2017	0.11	0.06	0.60	4.01	0.16	0.05	2.91	14.01
<b>P (mm)</b>	<i>Cum<sup>b</sup></i>			<i>Total</i>	-	-	-	-
Sept./2013- Aug./2014	146.3	35.6	249.1	1755.6	-	-	-	-
Sept./2014- Aug./2015	145.7	36.2	275.7	1748.2	-	-	-	-
Sept./2015- Aug./2016	159.6	80.8	321.8	1822.9	-	-	-	-
Sept./2016- Mar./2017	176.9	90.1	323.2	977.0	-	-	-	-

Note: a – SD standard deviation; b - total rainfall cumulative.

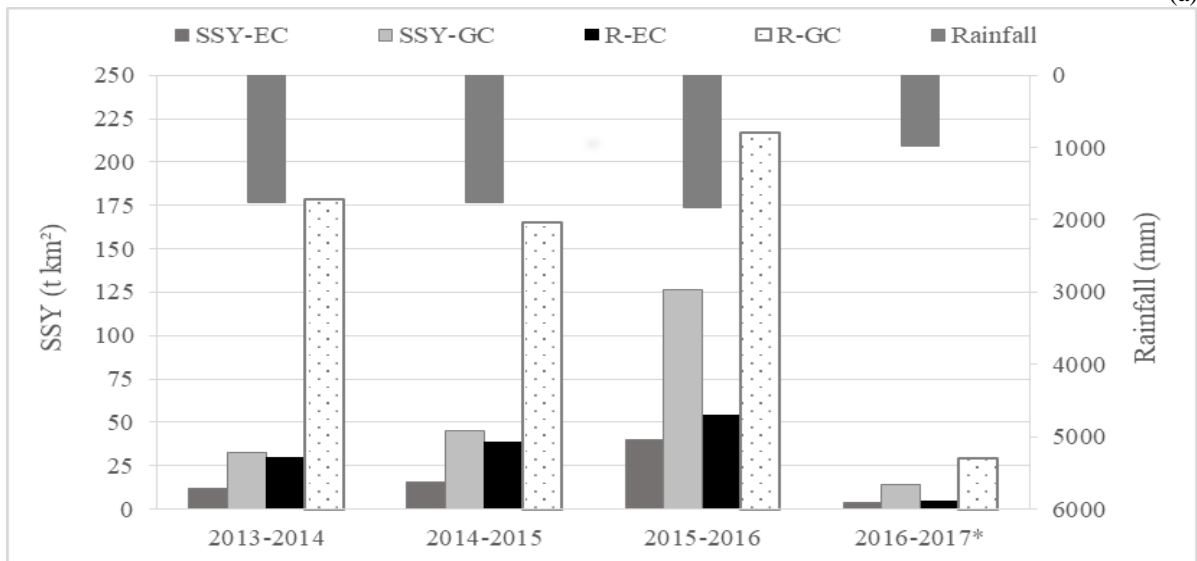
Table 2 and Figure 7 show high streamflow peak in GC and, consequently, high runoff and suspended sediment yield. During the year of Sep/2015-Aug/2016, the highest annual suspended sediment yield and runoff were observed in both catchments (39.9 Mg km<sup>-2</sup> for EC, and 167.7 Mg km<sup>-2</sup> for GC). However, when the maximum values of flow and SS concentrations was compared among years, the highest values were verified on 2013-2014, due the higher intense event occurred on 07.04.14.

For each year monitored, the streamflow exceedance was represented in Figure 7a. The 5% time streamflow (Q<sub>5</sub>) varied from 65 to 90 L s<sup>-1</sup> km<sup>-2</sup> in the GC and from 20 to 45 L s<sup>-1</sup> km<sup>-2</sup> in the EC for all period (2013–2017; Figure 7a). The 5% time streamflow (Q<sub>5</sub>) during wetter year (year 3 – 2015-2016) was approximately double (90 L s<sup>-1</sup> km<sup>-2</sup>) in GC (45 L s<sup>-1</sup> km<sup>-2</sup> in the EC) and approximately 40% greater in the EC and 26 % in GC compared to other years. The 50% time streamflow (Q<sub>50</sub>) was approximately 60% greater in GC (10 L s<sup>-1</sup> km<sup>-2</sup>) than in EC (4 L s<sup>-1</sup> km<sup>-2</sup>) during 2013-2014; also was greater in GC for 2014-2015 (33%); in 2015-2016 (36%) and during 2016-2017 (25%). The 75% time streamflow (Q<sub>75</sub>) was approximately similar between GC and EC (value around 3 and 8 L s<sup>-1</sup> km<sup>-2</sup>). The 95% time

streamflow ( $Q_{95}$ ) was approximately greater in the EC than in the GC (value around 1 and 4  $L s^{-1} km^{-2}$ ). Thus, the results in Figure 7a show a higher water availability in EC in the minimum streamflow compared to GC.



(a)



(b)

Figure 7 – Exceedance probability curves for streamflow in the grassland catchment (GC) and eucalyptus catchment (EC) during all study time period (2013–2017: where \* is incomplete year) and the respective suspended sediment yield, runoff and rainfall.

Figure 7b and the data of Appendix E shows that even after the harvesting operation of 21% eucalyptus stand and the new planting in the sequence, between Mar-May/2014, higher runoff and sediment yield were in GC, as mentioned before. Thus, although the soil was exposed to erosive processes during the rainfall, this condition was not sufficient to exceed those values observed in the GC site, and adds to the hypothesis that areas with managed pasture, together with extensive livestock, contribute more runoff and consequently more sediment yield than forest plantations in the Pampa biome. The period between September 2015

and August 2016 (Figure 7b) had the highest water losses (runoff) and sediment yield, and during this period there was many consecutive rainfall events with a high volume of precipitation (see Appendix C).

Table 3 shows the granulometric characteristics (sand, silt and clay percentages) for some sediments collected in the respective study areas. In general for both catchments, there is higher percentage of sediments samples, followed by sand for the lag deposits, and by clay for events and traps. The granulometric characteristics were similar for both main land uses, both with similar soil types.

Table 3 – Percentage of sand, silt and clay for each sediment sampling strategy in the eucalyptus and grassland catchments.

Sediment (yy.mm.dd)	Eucalyptus catchment			Grassland catchment		
	Sand	Silt %	Clay	Sand	Silt %	Clay
Event - 14.07.04	8.2	73.6	18.2	7.5	76	16.5
Event - 14.10.30	0	91.5	8.5	5.6	81.4	13
Event - 14.12.21	0.8	81.6	17.6	5.9	81.5	12.7
Event - 15.10.08	7.9	75.7	16.4	6.3	81.2	12.5
Event - 16.10.07	5.8	74.5	19.7	5.6	77.3	17.1
Event - 16.10.19	12.7	71.7	15.7	7	80.5	12.5
Lag deposit - 14.07.05	24.6	70	5.4	17.7	75.6	6.7
Lag deposit - 14.08.20	17.2	75.1	7.6	13.5	78.9	7.6
Lag deposit - 14.09.20	26	69.2	4.9	-	-	-
Lag deposit - 14.12.20	23.2	71.5	5.3	-	-	-
Lag deposit - 15.03.12	22.4	72.1	5.5	-	-	-
Lag deposit - 15.06.18	22	72.1	5.9	18.4	73.9	7.7
Lag deposit - 15.10.15	23.5	71.1	5.3	-	-	-
Lag deposit - 15.12.03	25.6	69.3	5.1	18.7	73.1	8.1
Lag deposit - 16.02.03	15.3	76.5	8.2	10.2	78.8	11
Lag deposit - 16.06.23	25.3	69.5	5.2	-	-	-
Lag deposit - 16.09.03	9.8	82	8.2	-	-	-
Lag deposit - 16.10.16	22.7	71.6	5.7	-	-	-
Lag deposit - 16.11.15	24.3	70.3	5.4	-	-	-
Trap - 14.02.12	7.7	76.2	16.2	-	-	-
Trap - 15.07.17	2.6	89.6	7.8	6.5	83.3	10.2
Trap - 16.03.31	5.1	83.8	11.1	6.9	79.8	13.3
Trap - 16.10.12	7.6	81.6	10.8	8.2	77.1	14.8
Mean Event	5.9	78.1	16	6.3	79.7	14
Mean Lag deposit	21.7	72.3	6	15.7	76.1	8.2
Mean Trap	5.7	82.8	11.5	7.2	80.1	12.7

### 2.3.3 Hysteresis analysis

Table 4 summarizes the main characteristics of the events selected for hysteresis analyses (see Appendix D). In general, the hysteresis with direction Clockwise (CC) had higher values for all variables (discharge, suspended sediment concentration, rainfall and intensity) for both catchments.

Table 4 – Summary of SSC-Q hysteresis patterns monitored in the outlet of research area during the study period, 2013–2017.

Hysteresis pattern	Number of flow peaks	Mean peak discharge ( $L^{-1} s^{-1} km^{-2}$ )	Mean peak suspended sediment ( $mg L^{-1}$ )	Mean event rainfall (mm)	Mean rainfall intensity ( $mm h^{-1}$ )
Grassland catchment					
Anti-clockwise	23	265.9	153.6	23.3	13.0
Clockwise	61	558.4	246.2	31.7	15.4
Eucalyptus catchment					
Anti-clockwise	67	175.7	169.2	38.7	18.3
Clockwise	7	185.6	185.9	44.6	23.1

Most of hysteresis patterns had CC for GC (Table 4), which means that the maximum suspended sediment concentrations are advanced in relation to the maximum flow which can be related to geomorphological characteristics and spatial configuration of the landscape and of the fluvial channel, considered the main potential source of sediments. Bank collapses were observed in both areas during the study period, which was more frequent in GC near the outlet. In this situation the sediments are mobilized, transported and deposited in the channel bank and can be the main source of sediments.

Figure 8 shows the hysteresis loops plotted for events selected for each catchment, for the same events commented before. Anti-clockwise (AC) hysteresis was observed for EC, meaning sediment comes from more distant sources. However, large amounts of lag deposit were observed in the stream channel (see Appendix A). Even with a similar pattern in the direction of the hysteresis loop, the HI ranged from -2.5 to 9.2 and -1.4 to 1.2, with an average value of 0.6 and -0.5 for GC and EC, respectively (more information in Appendix D).

The Figures 4 and 8, some inferences about the behavior of hysteresis for the study areas can be made. The total rainfall of the events occurred in 07.04.14 and 09.22.14 (intensities of 53 and 54  $mm h^{-1}$ ), resulting in higher HI for GC with CC direction and for the EC with AC direction. Although the discharge peak continues (as observed in 10.14.15 and 04.25.16), in GC, when the previous peaks was higher than the last, the last discharge peak produced smaller

suspended sediment concentration peak, indicating that sediment availability controls suspended sediment transport. The hysteresis loop and simple line were anticlockwise for both areas (see second peak in GC, Figure 4). As the first peak had already transported and eroded the available sediment for transport, this second peak suffered from low sediment availability for transport and this mainly controlled the flushed suspended sediment.

In EC, the high suspended sediment concentration was evidenced in the sedigraphs falling limb, which may be due to the presence of suspended organic carbon or solid colloidal particles, which also contribute to the increase of water turbidity. Although the peak concentrations occurred at almost the same time as discharge peaks (as verified for almost all events, Figure 4), the hysteresis graph still showed anticlockwise loops. Figure 4 shows just two events with CC in EC (see more in the Appendix D), but it was an event with low rainfall and this behavior could not be verified just with the graphical. Further, as the local geology is mainly formed by granites, the sand fraction predominates in the soil, and thus coarser sediments deposited mainly in the channel bed in EC. Therefore, such characteristics may result in lower amounts of sediment transported in suspension, besides being indicative that the predominant erosive process occurs in the channel.

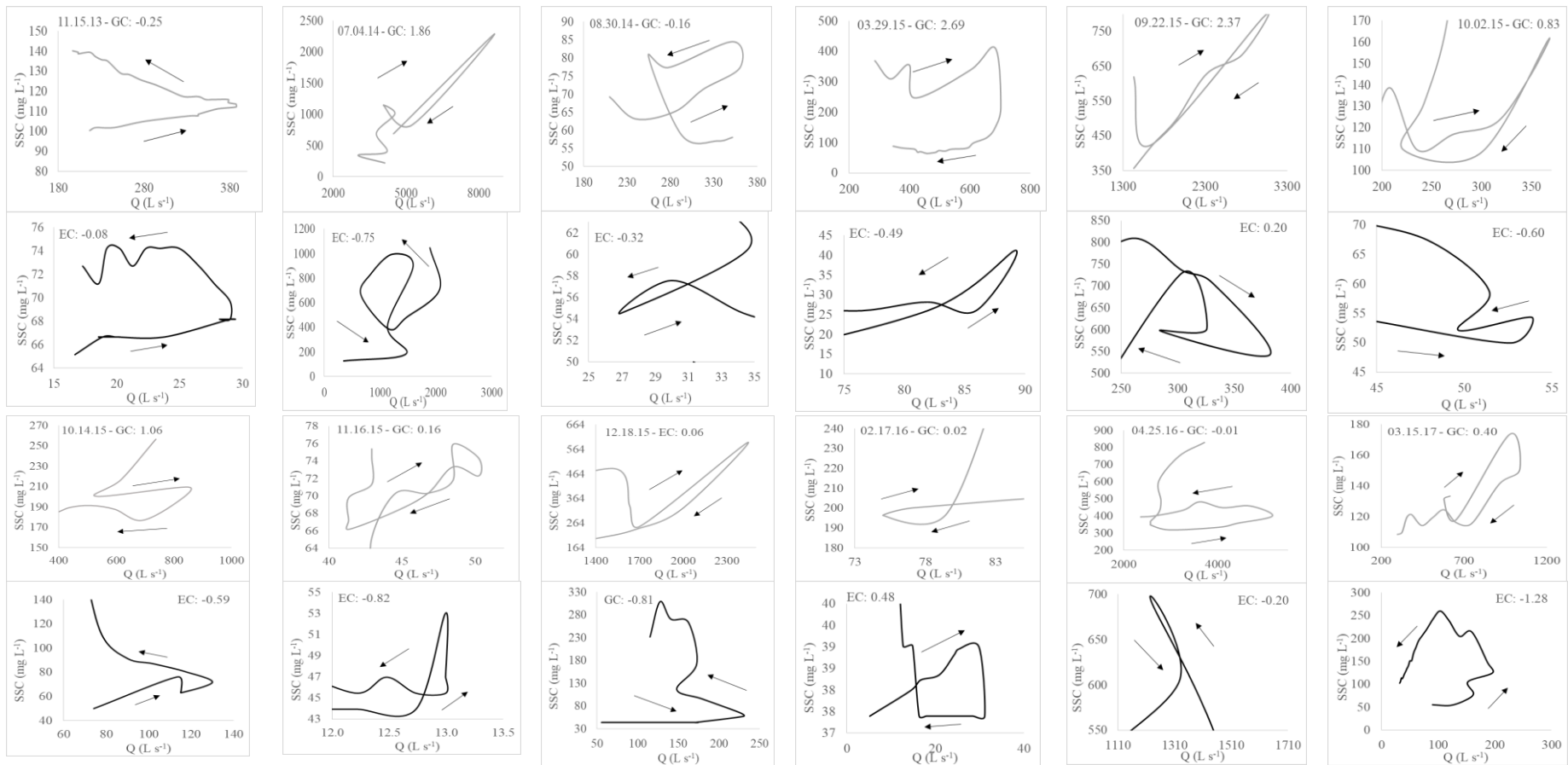


Figure 8 – Hysteresis loops of events in the grassland and eucalyptus catchments.

## 2.4 Discussion

### 2.4.1 Effect of soil use on the hydro-sedimentological variables

Among the variables of hydro-sedimentological process, lower streamflow generally observed in the EC compared to GC can be attributed to greater capacity of rainwater interception by canopy of eucalyptus stand, approximately 13% of rainfall (PELÁEZ, 2014), water infiltration into soil and improved potential for damping floods, when compared to the grazing use in the Pampa biome (REICHERT et al., 2017). Further, the authors verified the range of streamflow with shorter percent time streamflow may indicate lower water infiltration capacity of the soil and greater potential for surface runoff in the grassland catchment when compared to the eucalyptus catchment.

For this study, we observed higher value of runoff in GC compared to EC, where the responses of streamflow by rainfall events were faster than in EC. Similar results were observed by Baumhardt (2014), where the highest peak flows occurred in a catchment covered with grassland compared to eucalyptus stands in the Pampa biome. Also, Almeida et al. (2014) observed eucalyptus plantation provide greater water infiltration into soil compared to grazing areas. Consequently, less water flows outside the catchment, contributing for low peak flow and suspended sediment concentration in EC. Even in the wetter period, between September 2015 and August 2016, when many consecutive rainfall events had a high volume of precipitation, highest water losses and sediment yield were verified in GC. Under such conditions, soil moisture remains high for more days, which provides rapid soil saturation during rainfall events and, consequently, increases generation of runoff and soil loss.

The type of soil cover, the soil characteristics conditioning to erosion have a greater emphasis on: morphology, infiltration capacity, erosion resistance, texture, structure, organic matter content and permeability. In relation to the morphology, the mineralogical composition has a direct influence on the characteristics and properties of the soil that condition the quantity and quality of the sediments yield (MELLO, 2006). In terms of infiltration capacity, Bonan (2002) suggests that low rates of infiltration are responsible for greater outflow and erosion. Thus, poorly structured soils present less physical resistance to soil disintegration by the action of raindrops, and soil particles are thus easily carried under the action of high speed flows (CARVALHO, 2008; WMO, 2003). On the condition of forest use with eucalyptus in the study area, the soils present a better structural condition which favors the water infiltration capacity



in the soil (GUIMARÃES, 2015), attenuating soil condition erosion due to the rapid increase of organic matter in the soil, as in the homogeneous eucalyptus plantations.

Soil cover provided by the crop residues or forest canopy is essential in reducing soil losses due to water erosion, with good efficiency observed already with 30% coverage (RODRIGUES, 2011). Furthermore, the forest canopy acts as a barrier against rainfall that reaches the soil, since rain interception occurs under the forms of interception by canopy, trunk and litter. These processes reduce the amount of precipitation and redistribute it to the ground (CHANG, 2006).

Although the soil surface is more protected under forest plantations, soil tillage, management, harvesting, and construction and maintenance of forest roads increase the susceptibility to erosion in these systems (FERREIRA et al., 2008; LIMA, 1996; OLIVEIRA, 2014; SHERIDAN et al., 2006). As mentioned in the results, harvesting of 20% of the stand with replanting in the sequence did not promote changes in sediment production in the EC. This condition reinforces that the forest harvest, when performed in the staggered way can be considered more sustainable than clear-cutting. In addition to silvicultural practices, some researchers include forest unpaved roads as the main sediment yield in the areas with forestry (CROKE et al., 1999, 2001; HAIRSINE et al., 2002), where in some cases the percentage of the sediment yield corresponds more than 90% (GRACE III et al., 1998; MADEJ, 2001), demonstrating improper road planning. High values of soil loss ( $22 \text{ t ha}^{-1}$ ) and water (44% of the rainfall) were also observed on forest unpaved roads by Oliveira et al. (2014).

In areas with extensive livestock, research developed by Holt et al. (1996) and Müller et al. (2001) condition the worsening of the physical conditions of soils under pasture to the constant trampling of the animals, promoting soil compaction, which is verified by increasing soil bulk density, microporosity and resistance to penetration. Bovine cattle is seen as an important bioerosive agent as it alters the relief forms and accelerates the superface geomorphological processes (THOMAZ, DIAS, 2009). These processes act to reduce the water infiltration into the soil, culminating with a higher percentage of surface runoff.

#### 2.4.2 Sediment yield and transfer for the paired catchments

The higher sediment yield in GC is possibly due to lower rainfall interception and energy dissipation, where pasture seeding increases soil exposure to rain. Moist areas adjacent to the river provide saturated areas that act as sources of rapid surface runoff, being fed by the incident rainfall and subsurface flow of upstream areas (MEDIONDO, TUCCI, 1997).

Modernel et al. (2016) mentioned that soil erosion rates for native grasslands were lower than for croplands in all studies reviewed. For example, in well-managed native grasslands in Uruguay an average erosion rate of  $2.1 \text{ Mg ha}^{-1} \text{ yr}^{-1}$  was reported (GARCÍA PRÉCHAC et al., 2004), and  $6.2 \text{ Mg ha}^{-1} \text{ yr}^{-1}$  were observed on overgrazed grasslands with high levels of bare soil erosion rates (GARCÍA PRÉCHAC, 1992). Erosion rates were observed under degraded grassland with livestock in Brazilian Pampa biome, ranging from  $0.2 \text{ Mg ha}^{-1}$  in one year of monitoring in plots and the suspended sediment yield in the catchment with grassland was  $1.02 \text{ Mg ha}^{-1}$  in one year of monitoring (PELÁEZ, 2014). These results were similar and higher than observed in the present study, where the erosion rates ranging between  $0.32$  and  $1.26 \text{ Mg ha}^{-1} \text{ yr}^{-1}$  in the GC. Cardoso et al. (2004) observed  $0.87 - 66.37 \text{ Mg ha}^{-1} \text{ yr}^{-1}$  in plots without vegetation in soil, and Inácio et al. (2006) verified for bare soil and grassland erosion rates of  $3.7$  and  $0.9 \text{ Mg ha}^{-1}$ , respectively in plots.

In the EC, the suspended sediment yield ranging from  $0.12$  to  $0.40 \text{ Mg ha}^{-1} \text{ yr}^{-1}$  lower than GC. The mean ( $0.26 \text{ Mg ha}^{-1} \text{ yr}^{-1}$ ) in this study was higher than quantified by Peláez (2014)  $0.09 \text{ Mg ha}^{-1} \text{ yr}^{-1}$ , it was similar of data by Ludwig et al. (2005) ( $0.23$  and  $1.7 \text{ Mg ha}^{-1} \text{ yr}^{-1}$  in plots with eucalyptus in Australia) and lower than verified by Cardoso et al. (2004) in Brazil, where they observed  $0.01$  and  $2.38 \text{ Mg ha}^{-1} \text{ yr}^{-1}$  in plots with eucalyptus.

About the hysteresis, the clockwise direction observed in GC has often been associated with rapid delivery of sediment to transport from channel banks to flow, i.e. proximity of the sediment source (e.g. SMITH, DRAGOVICH, 2009). However, this type of loop (CC) occurs when sediments are mobilized, transported and deposited quickly and the main source of sediments can be sediments deposited in the fluvial channel, which are exhausted with the evolution of the event (MINELLA et al., 2011; SEEGER et al., 2004). As mentioned before, in GC the peak flows and high suspended sediment concentration were mostly of short duration, which further demonstrates the rapid flow changes in the drainage network. Accumulated bed sediment in the main drain is directly available for transport during larger events and is resuspended and transported by mobile water (MARTILLA, KLØVE, 2010).

Bank collapses were observed in both areas, during the study period, more frequently in GC near of outlet, which confirmed the findings of hysteresis analysis and indicated the importance of bank stability on suspended sediment sources. In addition, when looking for shade and water, cattle invade legal protection areas and drainage channels, which they use as drinking fountains, forming trails, trampling or feeding on regenerating vegetation (see Appendix A). Bennett et al. (2002) observed that the rivers and natural reservoirs that have

animal watering have their banks unprotected due to the frequent traffic of animals, which also causes silting of rivers, degradation of riparian forests, and their capacity for renewal.

In the EC, anti-clockwise (AC) hysteresis frequently observed in EC, according Martilla and Kløve (2010), the lack of available in-channel bed sediment; they found that bed sediment availability controlled the suspended sediment transport. It means sediment comes from more distances sources, because less bed load was observed in EC than in GC. However, large amounts of lag deposit were observed in the stream channel (see Appendix A). For forested sites, Durlo and Sutli (2012) comment that landslides are caused by wind action on the trees, the addition of weight of the trees to the slopes during rain, the pressure caused by roots of plants, and gravity force. Furthermore, Martilla and Kløve (2010) asserted that the effects of weathering, groundwater seepage, geotechnical instability and erosion conditions on local bank collapse are not well understood in forestry sites, and this topic requires further research. As well as being a significant source of transported sediment, bank erosion can cause structural damage because particles eroded from the bank cannot be replaced. In larger stream systems bank sediment can account for over 50% of the total input (KNIGHTON, 1998).

The rising and falling limb of the events were more pronounced in GC compared to EC. Some hydrographs in GC (Figure 4, events 11.16.15; 02.17.16) with lower rainfall volume had smaller rising and falling limbs due to the slow response to rainfall events, but still the sedigraphs responses were more pronounced for these events. Although the discharge peak continues (as observed in 10.14.15 and 04.25.16), in GC, when the previous peaks was higher than last, the last discharge peak produced a smaller suspended sediment concentration peak, indicating that sediment availability controls suspended sediment transport. The hysteresis loop and simple line were anticlockwise for both areas (see second peak in GC, Figure 4).

This anti-clockwise type was controlled by the spread of the concentration and discharge graph, which ensured that most ratios between these factors on the rising limb were smaller than those on the falling limb (WILLIAMS, 1989). As the first peak had already transported and eroded the available sediment for transport, this second peak suffered from low sediment availability for transport and this mainly controlled the flushed suspended sediment. This shows the importance of bed sediment inter-storm storage on suspended sediment transport in the area drained (MARTILLA, KLØVE; 2010). Furthermore, Lawler et al. (2006) noted anti-clockwise hysteresis produced by biofilms, which caused the delay of stored bed sediment mobilization.

Similar sediment exhaustion has been noted in previous studies (MARTTILA, KLØVE, 2008; MORO, 2011; RODRIGUES, 2011; SMITH, DRAGOVICH, 2009). In relation to values of hysteresis index (HI), for some events rainfall with high intensities it resulted in higher HI for GC with CC direction and for the EC with AC direction. In the literature, hysteresis loop as clockwise type has been observed for high volume rainfall, typical in small catchments (e.g. BARROS; 2012; RICHARDS, MOORE, 2003; RODRIGUES, 2011). According to Rodrigues (2011), the highest values of HI are due to a condition of reduced sediment supply in the falling limb of the sedigraph, possibly related to lower pre-event soil moisture. This observation was more pronounced in CG, with high suspended sediment concentration in the rising section of the sedigraph. The author also mentions that events of greater volume have lower HI, since in events of greater rainfall there is greater sediment supply, a condition observed only in EC, where no sediment supply was evidenced in the falling limb of the sedigraph. By contrast, for the same events in EC, each flow peak was accompanied by suspended sediment concentration, which possibly indicates greater sediment transfer during the consecutive events with high volume. However, water turbidity is also influenced by other constituents, such as the presence of suspended organic carbon or colloidal solid fractions in solution, a condition suggested by Rodrigues (2011) in the catchment covered with eucalyptus.

## **2.5 Conclusions**

Event-scale analysis allowed for better assessment of hydro-sedimentary responses in each catchment. In general, higher water losses by surface runoff and sediment yield occurred in the grassland catchment, being the mean values twice times higher than observed in eucalyptus catchment. Peak discharge was essential in defining on suspended sediment transport processes, and controlling discharge was the key for effective water management and protection in erosion-sensitive areas.

Sediment transfer patterns were distinct between studied catchments, where the response to rainfall was faster in grassland catchment. The dynamic of suspended sediment transport during rainfall events was described by hysteresis loops, suggesting that in many cases the transported suspended sediment originated in the channel bank. This condition may be related to sediment deposition in the channel by runoff and from cattle trampling, in the catchment with grassland, and from the collapse of channel banks, in the catchment with eucalyptus.

## 2.6 References

- ASSOCIAÇÃO GAÚCHA DE EMPRESAS FLORESTAIS. AGEFLOR. Disponível em <<http://www.ageflor.com.br/>>. Acesso em: 12 abr. 2017.
- ALMEIDA, A. Q. D. E.; RIBEIRO, A.; RODY, Y. P. Modeling of water infiltration in soil cultivated with eucalyptus and pasture. **Revista Caatinga**, Mossoró, v. 27, n. 1, p. 148 – 153, jan. – mar., 2014
- ALVARES, C. A., et al. Köppen's climate classification map for Brazil. **Meteorologische Zeitschrift**, 22:711-728, 2013.
- ANDRESSIAN, V. Waters and forests: from historical controversy to scientific debate. **Journal of Hydrology**. V. 291: p. 1-27. 2004.
- BARROS, C. A. P. **Comportamento hidrossedimentológico de uma bacia hidrográfica rural utilizando técnicas de monitoramento e modelagem** [Dissertação]. Santa Maria: Universidade Federal de Santa Maria; 2012.
- BAUMHARDT, E. **Balanço hídrico de microbacia com eucalipto e pastagem nativa na região da campanha do RS**. 2010. 139 f. Dissertação (Mestrado em Engenharia Civil) – Universidade Federal de Santa Maria, Santa Maria, 2010.
- BAUMHARDT, E. **Hidrologia de bacia de cabeceira com eucaliptocultura e campo nativo na região da campanha gaúcha**. 2014. 166 f. Tese (Doutorado em Engenharia Florestal) – Universidade Federal de Santa Maria, Santa Maria, 2014.
- BENETT, C.; ALMEIDA, M.; CASTILHO, M. W. V. Gestão de recursos naturais: Sítio São Brás, município de Carlinda, MT?. **Revista de Biologia e Ciências da Terra**. Universidade Federal da Paraíba, Campina Grande, v. 2, n. 1, 2002.
- BOLDRINI, I. I.; et al. **Bioma Pampa: diversidade florística e fisionômica**. Porto Alegre, editora Pallotti, 2010. 64 p.
- BONAN, G. B. **Ecological Climatology: Concepts and Applications**. Inglaterra: Ed: Cambridge University Press, 678p. 2002.
- CÂMARA, C. D.; LIMA, W. de P.; ZÁKIA, M. J. B. Critérios e indicadores hidrológicos de monitoramento em microbacias. In: **As Florestas Plantadas e a Água...** São Carlos: RiMa, Cap VIII, p. 107-140. 2006.
- CANTALICE, J. R., et al. Relationship between bedload and suspended sediment in the sand-bed Exu River, in the semi-arid region of Brazil. **Hydrological Sciences Journal**. doi: 10.1080/02626667.2013.839875. 2014.
- CARDOSO, D. P et al. Erosão hídrica avaliada pela alteração na superfície do solo com sistemas florestais. **Scientia Forestalis**, n. 66. p 25-37, dez. 2004.
- CARVALHO, N. de O. **Hidrossedimentologia prática**. 2ª ed., rev., atual e ampliada. Rio de Janeiro: Interciência, 599p. 2008.
- CHANG, M. **Forest Hydrology: An introduction to water and forests**. United States: Taylor e Francis. 474 p. 2006.
- CROKE, J., HAIRSINE, P., FOGARTY, P. Sediment transport, redistribution and storage on logged forest hillslopes in south-eastern Australia. **Hydrological Processes**. 13 (17), 2705–2720. 1999.
- CROKE J.; MOCKLER S. Gully initiation and road-to-stream linkage in a forested catchment, southeastern Australia. **Earth Surface Processes and Landforms**, Vol. 26, No. 2, pp. 205–217. 2001.

CRUZ, J. C. et al. Qualitative characteristics of water resulting from the introduction of eucalyptus silviculture in Pampa Biome, RS. **Revista Brasileira de Recursos Hídricos**, v. 21, n. 3, 2016.

DURLO, M; SUTILI, F. **Bioengenharia: Manejo Biotécnico de Cursos de Água**. Santa Maria; Edição do Autor, 189p, 2012.

EDER, A., et al. Comparative calculation of suspended sediment loads with respect to hysteresis effects (in the Petzenkirchen catchment, Austria). **Journal of Hydrology**. 389:168–176. 2010.

EDWARDS, T. E.; GLYSSON, G. D. **Field methods for measurement of fluvial sediment**. **US Geological Survey Techniques of Water Resources Investigations**, Book 3. US Geological Survey. 1999.

EMPRESA BRASILEIRA DE PESQUISA AGROPECUÁRIA - EMBRAPA. **Sistema brasileiro de classificação de solos**. 2.ed. Rio de Janeiro, 306p. 2006.

FERREIRA, A. G.; GONÇALVES, A. C.; DIAS, S. S. Avaliação da sustentabilidade dos sistemas florestais em função da erosão. **Silva Lusitana**, Oeiras, v. 16, p. 55-67, jun. 2008.

GRACE III, J.M.; et al. Evaluation of erosion control techniques on forest roads. **Transactions of the ASAE**, St Joseph, v.41, n.2, p.383-391, 1998.

GRAY, M.J.R. **Sediment data collection techniques**. U. S. Geological Survey Training Course. Castle Rock and Vancouver, W.A. 2005.

GERMER, S. et al.. Implications of long-term land-use change for the hydrology and solute budgets of small catchments in Amazonia. **Journal of Hydrology**, 364, 349-363. 2009.

GOMI, T., MOORE, R.D., HASSAN, M. Suspended sediment dynamics in small forested streams of the Pacific Northwest. **Journal of the American Water Resources Association**. 41 (4), 877–898. 2005.

GARCÍA PRÉCHAC, F. **Guía para la toma de decisiones en conservación de suelos: 3a. aproximación** Montevideo (Uruguay): INIA, 63 p. 1992.

GARCÍA PRÉCHAC F, et al. Integrating no-till into crop–pasture rotations in Uruguay. **Soil Tillage Research**. 77 1–13. 2004.

GUSH, M.B. et al. A new approach to modeling streamflow reductions resulting from commercial afforestation in South Africa. **Southern African Forestry Journal** 196: 27–36. 2002.

GUIMARÃES, D. V. **Erosão hídrica em sistemas florestais no extremo sul da Bahia**. 92 f. 2015. Dissertação (Mestre em Recursos Ambientais e Uso da Terra). Universidade Federal de Lavras. Lavras, 2015.

HAIRSINE, P. B. et al. Modelling plumes of overland flow from logging tracks. **Hydrological Processes**, v. 16, n. 12, p. 2311–2327, 2002.

HOLT, J.A., BRISTOW, K.L., McIVOR, J.G. The effects of grazing pressure on soil animals and hydraulic properties of two soils in semi-arid tropical Queensland. **Australian Journal of Soil Research**. v. 34, p. 69-79, 1996.

INÁCIO, E. S. B. et al. Erosão hídrica em sistema agro - florestal no ribeirão Salomea, sul da Bahia. **CEPLAC – artigos técnicos**. Disponível em: <[http://www.ceplac.gov.br/radar\\_artigos3.htm](http://www.ceplac.gov.br/radar_artigos3.htm)>. Acesso em: 11 jul. 2006.

KNIGHTON, D., **Fluvial Forms and Processes, A New Perspective**. Oxford University Press Inc., New York. 383 p. 1998.

KOITER, A.J., et al. The behavioural characteristics of sediment properties and their implications for sediment fingerprinting as an approach for identifying sediment sources in river basins. **Earth-Science Reviews** 125: 24-42. DOI: 10.1016/j.earscirev.2013.05.009. 2013.

- KRUEGER, T., et al., Uncertainties in data and models to describe event dynamics of agricultural sediment and phosphorus transfer. **Journal of Environmental Quality**. 38 (3), 1137–1148. 2009.
- LAWLER, D.M.; et al. Turbidity dynamics during spring storm events in an urban headwater river system: The Upper Tame, West Midlands, UK. **Sci. Total Environ.** 360, 109–126. 2006.
- LENZI, M. A.; MAO, L.; COMITI, F. Interannual variation of suspended sediment load and sediment yield in an alpine catchment. **Hydrological Sciences** 48(6), 889–915. 2003.
- LIMA, W. de P. **Impacto ambiental do eucalipto**. 2. ed. São Paulo: EDUSP, 301 p. 1996.
- LUDWIG, J.A., et al. Vegetation patches and runoff-erosion as interacting ecohydrological processes in semiarid landscapes. **Ecology** 86, 288–297. 2005.
- MAHMOODABADI, M.; SAJJADI, S. A. Effects of rain intensity, slope gradient and particle size distribution on the relative contributions of splash and wash loads to rain-induced erosion. **Geomorphology**. v. 253: p.159–167. DOI: 10.1016/j.geomorph.2015.10.010. 2016.
- MADEJ, M. A. Erosion and sediment delivery following removal of forest roads. **Earth Surface Processes and Landforms**, Vol. 26, No. 2, pp. 175–190. 2001.
- MARTTILA, H.; KLØVE, B. Dynamics of erosion and suspended sediment transport from drained peatland forestry. **Journal of Hydrology**, v. 388, n. 3–4, p. 414–425, 2010.
- MARTINEZ-MENA M, et al. Influence of vegetal cover on sediment particle size distribution in natural rainfall conditions in a semiarid environment. **Catena** 38:175–190. 1999.
- MEDIONDO, E. M.; TUCCI, C. E. M.. Escalas Hidrológicas. I. Conceitos. RBRH – **Revista Brasileira de Recursos Hídricos**, v. 2, n. 1, p. 59-79, jan./jun., 1997.
- MELLO, N. A. de. Relação entre a fração mineral do solo e qualidade de sedimento - o solo como fonte de sedimentos (p. 38-82). In: **Qualidade dos sedimentos**. POLETO, C. e MERTEN, G. H. (org.). Porto Alegre: ABRH, 397p. 2006.
- MINELLA, J. P. G. **Utilização de técnicas hidrossedimentométricas combinadas com a identificação de fontes de sedimentos para avaliar o efeito do uso e do manejo do solo nos recursos hídricos de uma bacia hidrográfica**. 2007. 172 f. Tese (Doutorado em Recursos Hídricos e Saneamento) – Universidade Federal do Rio Grande do Sul, Porto Alegre, 2007.
- MINELLA, J. P. G.; MERTEN, G. H. & MAGNOGO, P. F. (2011) Qualitative and quantitative analysis of hysteresis between sediment concentration and flow rate during hydrologic events. **Revista Brasileira de Engenharia Agrícola e Ambiental** 15(12), 1306–1313 (in Portuguese).
- MINISTÉRIO DO MEIO AMBIENTE. MMA. Disponível em: <<http://www.mma.gov.br/biomas/pampa>>. Acesso em: 22 de jan. de 2018.
- MORENO, J.A. **Clima do Rio Grande do Sul**. Secretaria da Agricultura. Porto Alegre, 73p, 1961.
- MORALES, B.P., **Atributos do solo e produtividade de Eucalyptus saligna e Eucalyptus dunni no Sul do Rio Grande do Sul**. 2013. 161p. Dissertação (Mestrado em Engenharia Civil) – Universidade Federal de Santa Maria, Santa Maria, 2013.
- MODERNEI, P. et al. Land use change and ecosystem service provision in Pampas and Campos grasslands of southern South America. **Environmental Research Letters**, v. 11, n. 11, p. 113002, 2016.
- MÜLLER, M.M.L.; CECCON, G.; ROSOLEM, C.A. Influência da compactação do solo em subsuperfície sobre o crescimento aéreo e radicular de plantas de adubação verde de inverno. **Revista Brasileira de Ciência do Solo**, 25:531-538, 2001.
- MORGAN, R.P. **Soil erosion and conservation**, 3rd ed. Malden, MA: Blackwell Publishing. 316 p. 2005.

- MODERNEL, P. et al. Land use change and ecosystem service provision in Pampas and Campos grasslands of southern South America. **Environmental Research Letters**, v. 11, n. 11, p. 113002, 2016.
- MUGGLER, C.C.; PAPE T. & BUURMAN, P. Laser grain-size determination in soil genetic studies. 2. Clay content, clay formation, and aggregation in some Brazilian oxisols. **Soil Science**, 162:219-228, 1997.
- NABINGER, C., MORAES, A., MARASCHIN, G.E. **Campos in Southern Brazil**. In: Lemaire, G., et al. (Eds.), *Grassland Ecology- sology and Grazing Ecology*. CAB International, pp. 355–376. 2000.
- OLIVEIRA, A. H. **Erosão hídrica em florestas de eucalipto na região sudeste do Rio Grande do Sul**. 2008. 62 f. Dissertação (Mestrado em Ciência do Solo) – Universidade Federal de Lavras., Minas Gerais. 2008.
- OLIVEIRA, A. H. **Erosão hídrica e seus componentes na sub-bacia hidrográfica do horto florestal Terra Dura**. 2011. 179 f. Tese (Doutorado em Ciência do Solo) – Universidade Federal de Lavras., Minas Gerais. 2011.
- OLIVEIRA, L. C. et al. Erosão hídrica em plantio de pinus, em estrada florestal e em campo nativo. **Floresta**, Curitiba, PR, v. 44, n. 2, p. 239 - 248, abr. / jun. 2014.
- OVERBECK, G. E. et al. Brazil's neglected biome: the south brazilian campos perspect. **Plant Ecology, Evolution and Systematics**. 9 101–16. 2007.
- PELÁEZ, J.J.Z. **Hidrologia comparativa em bacias hidrográficas com eucalipto e campo**. 2014. 156p. Tese (Doutorado em Engenharia Florestal) - Universidade Federal de Santa Maria, Santa Maria, 2014.
- PILLAR, V.D.; et al. **Campos Sulinos conservação e uso sustentável da biodiversidade**. Brasília: MMA, 403 p. 2009.
- PINESE JÚNIOR, J. F.; CRUZ, L. M.; RODRIGUES, S. C. Monitoramento de erosão laminar em diferentes usos da terra, Uberlândia – MG. **Sociedade e Natureza**, Uberlândia, 20 (2): 157-175. 2008.
- PIRES, L. S.; et al. Erosão hídrica pós-plantio em florestas de eucalipto na região centro-leste de Minas Gerais. **Pesquisa Agropecuária Brasileira**, Brasília, v. 41, n. 4, p. 687-695, abr., 2006.
- RAMGRAB, G.E; et al. Geological Map of Brazil the Millionth, Geographic Information Systems Geology program. Brasília Brazil, CPRM, 2004. Disponível in:<<http://www.cprm.gov.br/publique/cgi/cgilua.exe/sys/start.htm?infoid=298&sid=26>> Acesso em 17 Aug. 2017.
- REICHERT, J. M. et al. Agricultural and Forest Meteorology Water balance in paired watersheds with eucalyptus and degraded grassland in Pampa biome. **Agricultural and Forest Meteorology**, v. 237–238, p. 282–295, 2017.
- RICHARDS, G., MOORE, R.D., Suspended sediment dynamics in a steep, glacier- fed mountain stream, Place Creek, Canada. **Hydrological Processes**. 17, 1733–1753. 2003.
- RIO GRANDE DO SUL. Resolução CONSEMA nº 187, de 11 de abril de 2008. Aprova o zoneamento ambiental para a atividade de silvicultura no estado do Rio Grande do Sul. **Diário Oficial do Estado do Rio Grande do Sul**. Porto Alegre, RS, abr., 2008.
- RODRIGUES, M. F. **Monitoramento e Modelagem dos processos hidrossedimentológicos em bacias hidrográficas florestais no sul do Brasil**. 2011. 209 f. Dissertação (Mestrado em Engenharia Florestal) – Universidade Federal de Santa Maria, Santa Maria, 2011.
- RODRIGUES, M. F. et al. Hydrosedimentology of nested subtropical watersheds with native and eucalyptus forests. **Journal of Soils and Sediments**, v. 14, n. 7, p. 1311–1324, 2014.
- RODRIGUES, M.F. et al. Coarse and fine sediment sources in nested watersheds with eucalyptus forest. **Land Degradation e Development**. <https://doi.org/10.1002/ldr.2977>. 2018.



SECRETARIA ESTADUAL DO MEIO AMBIENTE. SEMA. Disponível em <<http://www.sema.rs.gov.br/bacia-hidrografica-do-vacacai-vacacai-mirim> acesso em 2017>. Acesso em Mai. 12; 2017.

SEEGER, M.; et al. Catchment soil moisture and rainfall characteristics as determinant factors for discharge/suspended sediment hysteretic loops in a small headwater catchment in the Spanish pyrenees. **Journal of Hydrology**, v.288, p.299-311, 2004.

SHREVE, E.A.; DOWNS, A.C. **Quality-Assurance Plan for the Analysis of Fluvial Sediment by the U. S. Geological Survey Kentucky Water Science Center Sediment Laboratory**, U.S., Geological Survey Open-File Report, 28p. 2005.

SHERIDAN, G. J, et al. The effect of truck traffic and road water content on sediment delivery from unpaved forest roads. **Hydrological Processes**. 20:1683–1699. 2006.

STRAHLER, A. N. Quantitative analysis of watershed geomorphology. **Transaction of American Geophysical Union**, Washington, v. 38, n. 6, p. 913-920, Jul., 1957.

SMITH, H., DRAGOVICH, D. Interpreting sediment delivery processes using suspended sediment-discharge hysteresis patterns from nested upland catchment, south-eastern Australia. **Hydrological Processes**. 23, 2415–2426. 2009.

SILVEIRA, L.; ALONSO, J. Runoff modifications due to the conversion of natural grasslands to forests in a large basin in Uruguay. **Hydrological Processes**. v. 329, n. October 2008, p. 320–329, 2009.

SILVEIRA, L. et al. Effects of afforestation on groundwater recharge and water budgets in the western region of Uruguay. **Hydrological Processes** 30(20). DOI: 10.1002/hyp.10952. June 2016.

THOMAZ, E. L.; DIAS, W. A. Bioerosão - Evolução do rebanho bovino brasileiro e implicações nos processos geomorfológicos. **Revista Brasileira de Geomorfologia**, v. 10, n. 2, p. 3–11, 2009.

UNITED STATES DEPARTMENT OF AGRICULTURE. USDA. **Soil Survey Staff. Soil taxonomy: a basic system of soil classification for making and interpreting soil surveys**. 2nd ed. U.S. Department of Agriculture/Natural Resources Conservations Service, Washington, Agriculture Handbook. 871pp. 1999.

VALENTE, M. L; et al. Influential factors in surface water quality in catchments within the pampa biome with different land use. **Revista Árvore**, v. 39, n. 6, p. 1135–1145, 2015.

VALENTE, M. L; CALIL, N., F. O papel das florestas integrado aos recursos hídricos cap 1 **In: Procedimentos e Atualidades Florestais**. 196p. 2016.

VERCRUYSSSE, K.; GRABOWSKI, R. C.; RICKSON, R. J. Suspended sediment transport dynamics in rivers: Multi-scale drivers of temporal variation. **Earth-Science Reviews**, v. 166, p. 38–52, 2017.

VITAL, A. R. T.; et al. Biogeoquímica de uma microbacia após o corte raso de uma plantação de eucalipto de 7 anos de idade. **Scientia Forestalis**. n. 55, p. 17-28,jun. 1999.

WALLING, D.E.; WEBB, B.W. Sediment availability and the prediction of storm- period sediment yields. In: Walling, D.E. (Ed.), Recent Developments in the Explanation and Prediction of Erosion and Sediment Yield. **IAHS Press**, Wallingford, pp. 327–337 (IAHS Publications No. 137). 1982.

WILLIAMS, G.P., Sediment concentration versus water discharge during single hydrological events in rivers. **Journal of Hydrology**. 111, 89–106. 1989.

WORLD METEOROLOGICAL ORGANIZATION – WMO. **Manual on sediment management and measurement**. Geneva: Secretariat of the World Meteorological Organization. Operational Hydrology Report No. 47. 159p. 2003.

### 3 ARTICLE II: COMBINATION OF SPECTROCOLORIMETRY AND CONVENTIONAL METHODS FOR IDENTIFYING SEDIMENT SOURCES IN TWO CATCHMENTS IN THE PAMPA BIOME

#### Abstract

Modification of land use soil and sediment fluxes can result in increased sedimentation and turbidity on water bodies with detrimental impacts. Source estimates are difficult to obtain using traditional monitoring techniques, but sediment source fingerprinting or tracing procedures, have emerged as a potentially valuable alternative. We investigate the relative contribution of sediment source in two paired catchments using different conventional and alternative fingerprinting tracers combinations. The conventional approach was based on multiple-parameters used geochemical (G), radionuclides (R) and stable isotopes (S) parameters and the alternative approach based in UV-VIS-based color parameters (V). The sources sediments were conducted in two paired catchments in Brazilian Pampa biome. One area covered with commercial eucalyptus (EC-0.83 km<sup>2</sup>) and other with grassland and livestock farming (GC-1.10 km<sup>2</sup>) localized in the Brazilian Pampa biome. The results using different combinations of tracers parameters provided that areas with commercial eucalyptus plantations contribute with less sediment yield in relation to the grassland use, where in the EC, the mean magnitude corresponded to: channel (81%) > eucalyptus (16%) > unpaved roads (3%) and in the GC was: oats (49%) > channel (26%) ≥ degraded natural field (25%) with relative mean error <15 % for both catchments. The results show how selective was the number of tracers parameters in each area, being very important to work with a large database of variables. Thus, the combination of different groups of tracers used in the conventional and alternative fingerprinting approaches resulted in different set of variables in the discriminant analysis for each area. The results verified in the EC were similar for the combinations GSRV, GSV and GS and G. Whereas for GC, the best results of sediment source were obtained only with the UV-VIS-based color parameters analysis by the alternative approach. The results evidenced the importance of analyzing a large number of variables and how divergent was the selection tracers parameters in each area study.

**Keywords:** Soil erosion; *Eucalyptus* spp.; Sediment fingerprinting; Artificial mixture; Spectroscopy.

### 3.1 Introduction

Soil erosion is a major process of land degradation worldwide. In the Pampa biome in Southern Brazil, the soils have sedimentary rocks as parent material, generating with sandy to medium texture (ROESCH et al., 2009), which conditions greater physical fragility to erosive processes. The complexity in the field-catchment-river sediment transfer system makes estimation of sediment origin, transport and deposition quite challenging. The identification of areas that contribute to soil loss of at the catchment scale contributes to the understanding of hydro-sedimentological processes, since sediments are influenced by the physical and chemical properties of their sources areas. Investigations using the fingerprinting method have been greatly improved over the last decades, which had its first applications in the 70's (COLLINS et al., 2010b; KOITER et al., 2013; SMITH, BLAKE, 2014; TIECHER, 2015; WALLING, 2013; WOLMAN, 1977).

The understanding of the sediment sources and their spatial and temporal variations constitutes a prerequisite for designing effective management measures in order to reduce the supply of sediment and contaminants to the river systems (BROSINSKY et al., 2014; COOPER et al., 2014; LE GALL et al., 2016; TIECHER et al., 2016).

The most frequently used tracers in the conventional method are radionuclides (e.g.  $^{137}\text{Cs}$  and unsupported  $^{210}\text{Pb}_{\text{ex}}$ ), various geochemical elements and organic tracers (EVRARD et al., 2013; LACEBY et al., 2016; 2017; MABIT et al., 2008; MINELLA et al., 2008; SCHULLER et al., 2013). A composite fingerprinting in combination with a multivariate mixing model is able to determine the quantitative contribution of sources, and this procedure has been successfully applied to a range of environments. However, the application of this technique faces some methodological constraints, as labour and costs for the analysis can be very high and about the statistical procedure not considering the inherent variability of the different sediment source properties (COLLINS, WALLING, 2004; VERHEYEN et al., 2014).

Most studies performed in sediment-sources identification in Brazil has been investigated predominantly in agricultural catchments (e.g. FRANZ et al., 2014; LE GALL et al., 2016; MIGUEL et al., 2014a, b; MINELLA et al., 2008, 2009 and 2014; TIECHER et al., 2014; 2015; 2016; 2017a,b and 2018) and in forested catchment (RODRIGUES et al., 2018). Tiecher et al. (2017) investigated the sediment source contribution in two paired agricultural catchments with different proportions of riparian vegetation and wetlands and similar proportion of crop fields, by using the fingerprinting approach, where they found an average of

sediment sources in descending order of contribution: streambanks > grasslands > crop fields > unpaved roads in one catchment, and unpaved roads>grasslands>streambanks>crop fields for the other.

The sediment source fingerprinting research in Brazilian catchments has mainly focused on hydrological and erosion processes and on the estimation of erosion rates (MERTEN et al., 2015; MERTEN, MINELLA, 2013; MINELLA et al., 2014). Tiecher et al. (2015) verified source contributions ranging from 57% to 64% for croplands, from 23% to 36% for unpaved roads, and from 20% to 36% for channel banks. For one eucalyptus forested catchment, Rodrigues et al (2018) found the main relative contribution sediment was the stream channel using the geochemical variables.

Although the soil surface is better protected under forest plantation, soil tillage, management, harvesting, construction and maintenance of forest roads increase the susceptibility to erosion in these systems (FERREIRA et al., 2008; LIMA, 1996; OLIVEIRA et al., 2014; SHERIDAN et al., 2006). Forest roads were identified as the main sediment sources in forested areas (CROKE et al., 1999; CROKE, MOCKLER, 2001; HAIRSINE et al., 2002) and, in cases with inadequate road planning, the source contribution corresponds to more than 90% of the sediment produced (GRACE III et al., 1998; MADEJ, 2001). High soil loss (22 t ha<sup>-1</sup>) and runoff (44% of rainfall) values were also observed on forest roads by Oliveira et al. (2014). Furthermore, Griebeler et al. (2005) demonstrated that the largest portion of sediment produced on the road surface has particle size less than 2 mm, which happens to be the most detrimental to water resources.

The use of the technique has also been efficient in areas with pasture and cattle raising (COLLINS et al., 1997, 2010; OWENS et al., 2000). Sediment mobilization in pasture and livestock areas is commonly related to soil compaction as a result of animal trampling. However, when grazing areas have a good soil management, low soil loss rates are verified (MOTHA et al., 2002; NOSRATI et al., 2011).

Fingerprinting approach using visible and spectrophotometry is an alternative method for determining sediment sources in river catchments (e.g. EVRARD et al., 2013; LEGOUT et al., 2013; MARTINEZ-CARRERAS et al., 2010; TIECHER et al., 2015; VERHEYEN et al., 2014). Spectroscopy is rapid, inexpensive, nondestructive and straightforward technique, and is commonly used in the visible (VIS), near infrared (NIR) and mid-infrared (MIR) ranges to quantify soil properties (VISCARA ROSSEL et al., 2006). VIS based-color parameters allow for an increased physically-based characterization of soil and sediment color, wherein the use of color coefficients can be use not only as a qualitative descriptor but also as a quantitative

measure for soil and sediments (ERSKINE, 2013; FOSTER, LEES, 2000; MARTINEZ-CARRERAS et al., 2010; TIECHER et al., 2015). The use of VIS-based-color parameters and near-infrared diffuse reflectance (NIR) spectroscopy combined to geochemical tracers were applied for Tiecher et al. (2016; 2017) to provide results with an even higher accuracy.

There are still challenges in each fingerprinting variable group. For properties to be effective tracers of sediment, they must differentiate between sediment sources while behaving conservatively (WALLING et al., 1993). This is because the conservation of properties has strong correlation with the type of material being transported, since erosion and transport processes are selective with regard to the particle size of the material affected. For example, Laceby et al. (2017) concluded that sediment source fingerprinting researchers have recently tended to avoid in-depth examinations of fundamental topics such as the impact of organic matter on biogeochemical properties, which tracer properties are non-conservative (e.g. soluble, reactive), and what is the impact of particle size on tracer property predictability. Erskine (2013) concluded that changes in soil color with sediment transport are poorly known, and further work is clearly required to better understand the limitations of soil color as a tracer. Although sediment source tracing techniques based on geochemical and radiometric fingerprinting approaches is advanced, Blake et al. (2012) mention limitations in terms of the potential for source discrimination, because these approaches cannot provide crucial crop-specific information on sediment source. They comment that compound specific stable isotope analyses have the potential to elucidate processes in hydro-geomorphological studies, but it has remained largely unexplored. Lastly, Koiter et al. (2013) suggest that the application of statistical approaches without consideration of how unique sediment fingerprints have developed and how robust they are within the environment is a major limitation of many recent studies. It is recommended to use a large number of tracer elements as well as to evaluate the different combinations between them for analysis aiming to reduce the mathematical uncertainties in the determination (COLLINS, WALLING, 2002; TIECHER et al., 2015; YU, OLDFIELD, 1989).

Thus, there are few studies with different parameters combinations of fingerprinting approach in Brazil. Also, there are no studies in the Pampa biome in catchments with grassland or commercial eucalyptus plantations. This study aimed to investigate the relative contribution of sediment source in two paired catchments, with different land uses (eucalyptus plantation and livestock farming) in the Pampa biome, using different conventional and alternative fingerprinting tracers combinations.

## 3.2 Materials and methods

### 3.2.1 Source material sampling

Potential sediment source types were identified by observing the sediment mobilization and transport processes operating in the eucalyptus and grassland catchments during storm events. Three main sediment source types were identified in each catchment as follows: in the eucalyptus catchment - eucalyptus stands (ES), unpaved roads (UR) and stream channels (SC) and in the grassland catchment - oats fields (OF), pasture field (PF) and stream channels (SC), according Figure 1.

Source material sampling was collected between May 2015 and January 2016. A plastic spatula was used to collect samples and avoid potential metal contamination by scraping the top layer of soil (2–3 cm), where each source sample was composed at least ten sub-samples. Afterwards, all samples were oven-dried at low temperature (<40 °C) to avoid possible decomposition of organic matter bound to clay minerals with swelling layers (REMUSAT et al., 2012) and sieved to 0.063 mm for further analysis.

River sediment samples were collected between March 2014 and February 2017 at the catchment outlets following four strategies: (i) - *suspended matter samples* were collected with a US-DH-48 sampler (3/16 "diameter) during rainfall events. In addition, a large volume of river water (50 to 200 liters) was collected during events to evaluate the potential intra-event variation of sediment source contributions; (ii) - *time-integrated suspended sediment* samples were collected through the deployment of two sediment traps consisting of a 75 mm diameter polyethylene pipe with 80 cm in length in each catchment; (iii) - *bed load sediment* samples were collected with a US-BLH-84 sampler, in total, 20 to 40 sub-samples were composited to provide individual samples, as recommended by Edward and Glysson (1999) and (iv) - *lag deposits* were collected after the storm-events in the vicinity of catchment outlets, following the method proposed by Horowitz (1999). After, all samples were evaporated by the method of Shreve and Downs (2005) and sieved to 0.063 mm for further analysis.

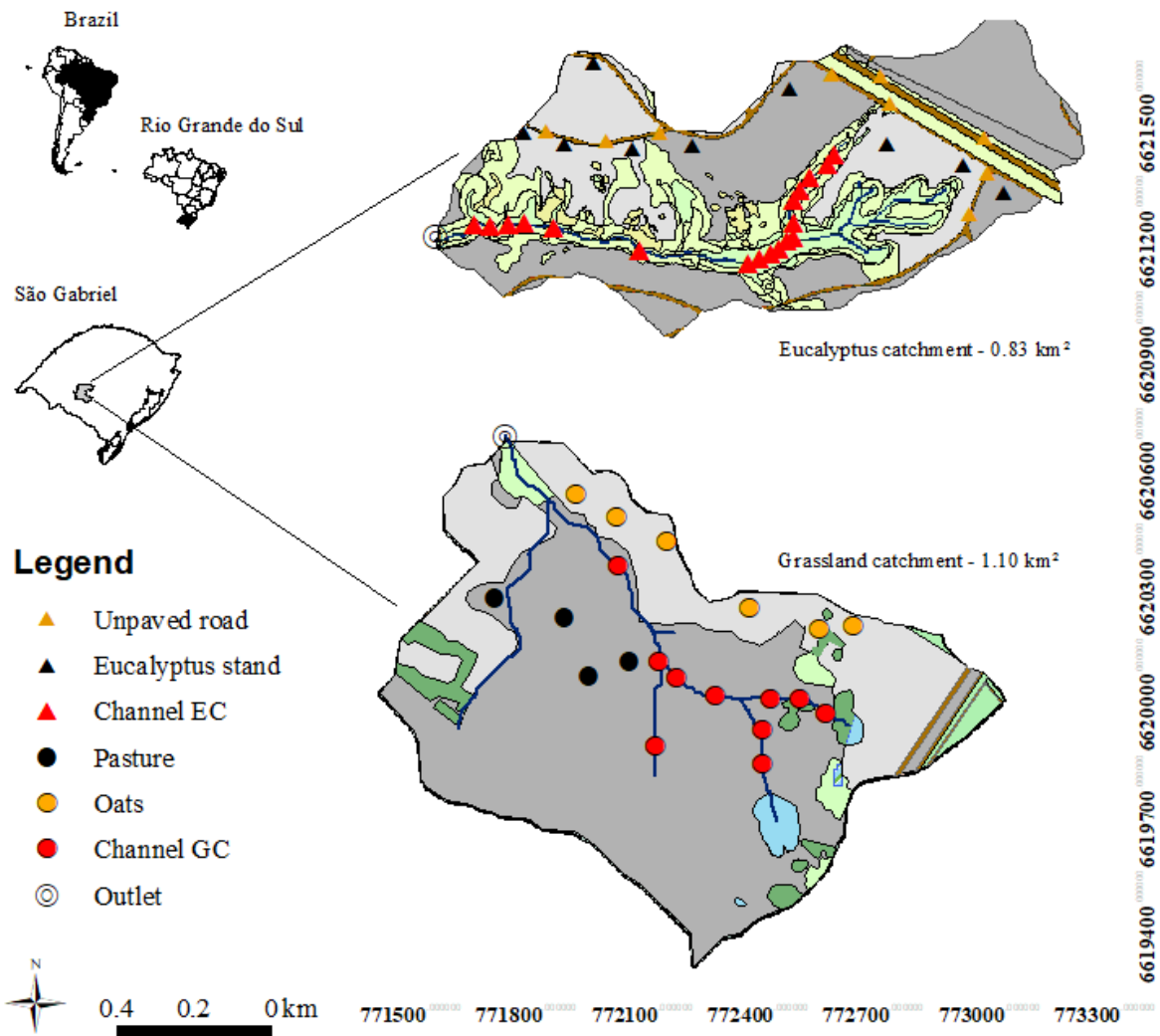


Figure 1 – The location of the sampling sites in each land use in the eucalyptus and grassland catchments.

### 3.2.2 Laboratory analysis

The soil and sediment samples were submitted for the geochemical analysis: Al, As, B, Ba, Be, Ca, Cd, Co, Cr, Cu, Fe, Hg, La, Li, K, Mg, Mn, Mo, Na, Ni, Pb, Se, Si, Sb, Sr, Te, Ti, Va e Zn, were estimated by ICP-OES after microwave assisted digestion for 9.5 min at 182 °C with concentrated HCl and HNO<sub>3</sub> in the ratio 3:1 (aqua regia) at the *Laboratório de Química e Fertilidade do Solo*, UFSM, Brazil.

For fallout radionuclide measurements, the <sup>137</sup>Cs activity was determined by gamma spectrometry using low background N and P type GeHP detectors (Canberra and Ortec) at the Laboratoire des Sciences du Climat et de l'Environnement, in Gif-sur-Yvette, France. Measured activities were decay-corrected to the sampling date and provided with 2σ-errors. Also, <sup>210</sup>Pb<sub>ex</sub>, <sup>226</sup>Ra and <sup>234</sup>Th were measurements.

Isotopes  $\delta^{13}\text{C}$ ,  $\delta^{15}\text{N}$  and total carbon and nitrogen analyses were made by ISO/IEC 17025, according to Guidelines to Uncertainty in Measurement, at Institute of Research for Development, Paris, France.

Spectrocolorimetric measures were taken at Université Grenoble Alpes, France, using a portable diffuse reflectance spectrophotometer (Konica Minolta 2600d) integrating its measurement on a 3-mm radius circle. The spectrophotometer was installed upside-down, face-up, and the tubes containing the samples were placed on the measuring cell. Thus, the measurement was taken directly through the base of the tube. The minimum amount of sample was roughly 100 mg (LEGOUT et al., 2013). Three measurements were taken on each sample because of the rather small measuring area, and to account for the possible heterogeneity within the samples. During a measurement, the spectrophotometer emits a standard Xenon arc light source and measures the ratio between the light reflected from the sample and from a calibrated white standard. UV–VIS diffuse reflectance was measured between 360 and 740 nm with a 10-nm resolution. Raw data collected were the spectral reflectance percentage for each of the 39-wavelength class. From these raw data we also derived eight components of various colorimetry models (VISCARA ROSSEL et al., 2006). XYZ tristimulus values were calculated based on the color-matching functions defined in 1931 by the International Commission on Illumination (CIE, 1931). We then transformed the standardised tristimulus to the CIE  $L^*a^*b^*$  and the CIE  $L^*u^*v^*$  cartesian coordinate systems using the equations given in CIE (1978). The spectrophotometer was calibrated before each set of measurements by making a zero and a white calibration. Control measurements were also taken regularly during and at the end of a set of measurements; the latter consisted of measurements on red, green and yellow panels as well as six contrasting soil samples.

### 3.2.3 Sediment source discrimination and apportionment

First, was identifying outlier samples and variables with sediment concentrations lying outside the range of sources, some tracers and samples were excluded from the next analyses, as recommended by Smith and Blake (2014), known as “range test”. After, tracer selection based on Kruskal–Wallis H-test ( $p \geq 0.05$ ) was applied followed of selection of the best set of tracers using discriminant analyses. After, different combinations based on the selected variables were performed for the discriminant analysis. The variables by the conventional method were: geochemical elements (G), stable isotopes (S) and fallout radionuclides (R), for alternative approach was the VIS-based-color parameters (V). From this, five combinations



were made each catchment (e.g. GSRV, GSV, GS, GSR, G and V), and finally the use of a mixed linear model to calculate the sediment source contribution was applied.

Subsequently, the two-stage procedure proposed by Collins et al. (1997) was used to identify composite fingerprints capable of discriminating the samples collected to represent individual sediment sources. The first step of the statistical analysis was performed to establish the set of properties with the ability to discriminate among the sediment sources by the application of two sequential tests: (a) a non-parametric test of Kruskal–Wallis (H) and (b) a multivariate discriminant function. The H test allows testing the null hypothesis that the sources are from the same population. This test defines which soil properties are statistically different among the sediment sources. When one soil property is statistically different it can be used as tracer. The H test is applied to each soil property, verifying its ability to discriminate individual sources, according to Equation (1):

$$H = \frac{12}{n(n+1)} \sum_{s=1}^k \frac{R_s^2}{n_i} - 3(n+1) \quad (1)$$

where: “ $R_s$ ” is the rank sum occupied by the source “ $s$ ”, “ $n_i$ ” is the number of observations in each source; “ $n$ ” is the sum of the “ $n_i$ ’s”; and “ $k$ ” is the number of sources.

Subsequently, was performed a multivariate discriminant function analyses (DFA) in the backward mode to determine the minimum number of variables that maximizes the discrimination among the sources. DFA analysis was performed according the different combinations, as mentioned before. The DFA analysis was performed only with variables showing differences among sources by the H test. The multivariate discriminant function is based on Wilks' Lambda ( $\Lambda^*$ ) value from the analysis of variance, where the criterion used by the statistical model is the minimization of  $\Lambda^*$  (Equation 2).  $\Lambda^*$  of 1 occurs if all the group means are the same while a low  $\Lambda^*$  value means that the variability within the groups is small compared to the total variability,

$$\Lambda^* = \frac{|W|}{|B+W|} \quad (2)$$

where  $|W|$  is the determinant of the matrix of sums of squares due to the error, while  $|B+W|$  represents the determinant of the matrix of the total sum of squares. At each step, the property which minimized the overall Wilks' Lambda was entered. The maximum significance of F to enter a property was 0.15. The minimum significance of F to remove a property was 0.15.

After defining the set of properties by minimizing, the contribution of each sediment source in the composition of sediment was determined (Equation 3) as the mathematical

relationship between the proportions of contribution of each source and geochemical properties in the sources and in the sediment (WALLING, WOODWARD, 1995).

$$y_i = \sum_{s=1}^n a_{is} P_s \quad (s = 1, 2, \dots, n) \quad e \quad (i = 1, 2, \dots, m) \quad (3)$$

where: “ $y_i$ ”: is the value of the property, “ $i$ ” obtained in sediment; “ $a_{is}$ ” are the linear model coefficients (concentration of the soil geochemical property in source “ $s$ ”); and “ $P_s$ ” is the proportion of mass from the source “ $s$ ”, which may be presented as a set of linear functions of  $m$  properties and  $n$  sources.

No weighting factors, organic matter, or particle size were corrected. The mixing model was run using Matlab® software. The solution was found by an iterative process aiming at minimizing the value of  $R$  (f mincon) (Equation 4). In the minimization process,  $P$  values are subject to two constraints: to be greater than or equal to zero and less than or equal to 1 (Equation 5), and the sum of  $P$  values must to be equal to 1 (Equation 6). The iterative process ends when the differences between modeled and measured chemical concentrations in sediment are minimized.

$$R = \left( \sum_{i=1}^n \left\{ \frac{(c_i - (\sum_{s=1}^m P_s S_{si}))^2}{c_i} \right\} \right) \quad (4)$$

$$0 \leq P_s \leq 1 \quad (5)$$

$$\sum_{s=1}^n P_s = 1 \quad (6)$$

where: “ $P_s$ ” is the optimized percentage contribution from source category “ $s$ ”, “ $c_i$ ” is the concentration of fingerprint property, “ $i$ ” in the sediment, “ $S_{si}$ ” is the mean concentration of fingerprint property “ $i$ ” in source category “ $s$ ”, “ $n$ ” is the number of fingerprint properties, and “ $m$ ” is the number of sediment source categories.

The optimization process (Equation 4) was checked whether it provided acceptable results of the relative contribution from the sediment sources. The evaluation of the results was made by comparing the concentration of fingerprint property used in the sediment and the value predicted by the model based on the proportion calculated for each source. Then, with the values of relative error of each geochemical property, a mean (RME) was calculated to provide a unique value associated with each sample of suspended sediment (Equation 7). When the result of RME is less than 15% it indicates the model found a feasible solution of  $P_s$  values (relative contributions of each source) from the minimization procedure (Equation 4) (WALLING, COLLINS, 2000).

$$ERM = \left( \sum_{i=1}^n \left\{ \frac{(C_i - (\sum_{s=1}^m P_s S_{si}))}{n} \right\} \right) \quad (7)$$

The statistical procedure used greatly differs for UV-VIS by the partial least squares regression models (PLSR). Briefly, the steps used in the alternative method were i) principal component analyses to reduce the number of variables, ii) discriminant analyses to determine the tracer potential of the spectroscopic analysis, and finally iii) the use of partial least square regression based on mixtures of the sediment sources in various weight proportions (Figure 2) to calculate the sediment source contribution.

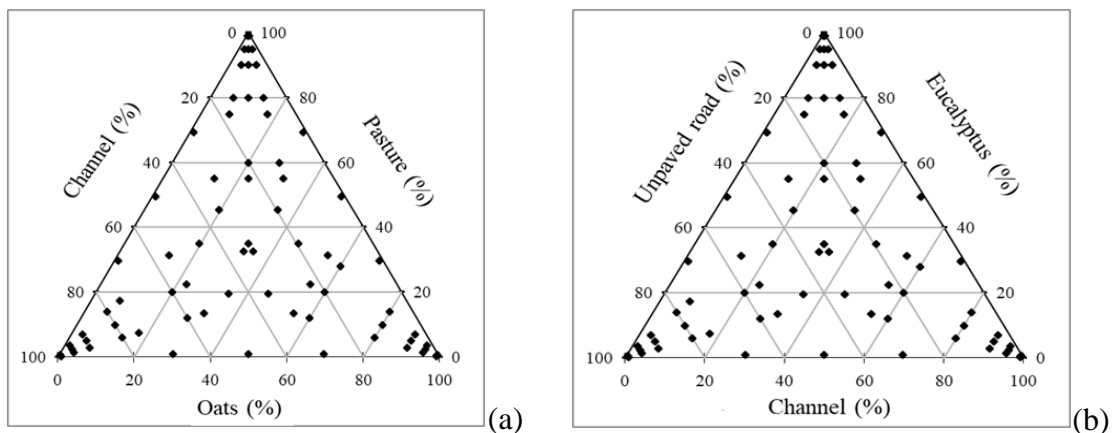


Figure 2 – Ternary diagram with the position of the experimental mixtures prepared for the PLSR-UV-VIS model calibration for GC (a) and EC (b).

In addition, inferences in soil composition based on ratios of absorption bands in UV-VIS-spectra was made. Absorption in the VIS spectra (360-740 nm) was used to discriminate iron oxides (e.g. hematite) and iron oxy-hydroxides (e.g. goethite) in soils. The proportions of hematite (Hr) and goethite (Gt) were estimated according to the methodology employed by Caner et al. (2011) and Fritsch et al. (2005). All the steps are in the Tiecher et al. (2015).

### 3.3 Results

#### 3.3.1 Sediment source discrimination

##### 3.3.1.1 Grassland catchment

Table 1 shows all parameters analyzed for grassland catchment, from forty-two multiple parameters. Thirteen did not pass in the range test, it means that sediment concentration was outside of source, they were not conservative and were thus removed from the next steps. From the geochemical parameters just one was lower than 0.05 according the Kruskal-Wallis

H-test ( $p < 0.05$ ). For radionuclides three were selected, one for stable isotopes and ten for VIS-based-color parameters. Discriminatory power of individual properties ranged from 52 to 74%.

Table 1 – Mean and standard deviation (SD) of parameters used for discriminating land use sources to catchment with grassland, including the significance level indicated by the Kruskal–Wallis test H and range test for sediment.

Variable	Kruskal-Wallis test		Correct clas. DFA (%)	Oats		Pasture		Channel		Sediment		Sed. samples out of source range (%)	
	H-value	p-value*		Mean	SD	Mean	SD	Mean	SD	Mean	SD	Max $\pm$ SD	Min $\pm$ SD
<i>Geochemical (G)</i>				(n=6)		(n=4)		(n=13)		(n=19)		Higher	Lower
B (mg kg <sup>-1</sup> )	8.50	<b>0.01</b>	57	7.3	3.4	5.2	2.7	4.2	2.9	31.2	35.0	38	4
Ba (g kg <sup>-1</sup> )	†	-	-	0.1	0.0	0.1	0.0	0.2	0.1	0.4	0.2	<b>63</b>	0
Be (mg kg <sup>-1</sup> )	†	-	-	1.8	0.5	1.8	0.3	2.4	0.5	4.5	0.7	<b>88</b>	0
Ca (g kg <sup>-1</sup> )	†	-	-	0.2	0.1	0.1	0.0	0.1	0.1	0.9	0.6	<b>46</b>	0
Cd (mg kg <sup>-1</sup> )	†	-	-	0.4	0.2	0.6	0.3	0.5	0.2	1.0	0.4	<b>78</b>	0
Co (mg kg <sup>-1</sup> )	†	-	-	3.1	0.4	2.7	0.8	6.1	4.0	30.1	25.5	<b>46</b>	0
Cr (mg kg <sup>-1</sup> )	2.00	0.37	-	18.6	5.4	21.2	4.0	23.5	6.8	30.7	5.9	8	0
Cu (mg kg <sup>-1</sup> )	0.30	0.88	-	8.6	3.0	7.2	0.3	8.3	3.7	16.3	9.1	38	0
Fe (g kg <sup>-1</sup> )	†	-	-	13.9	3.5	14.0	1.3	14.1	2.8	26.6	6.9	<b>75</b>	4
K (g kg <sup>-1</sup> )	†	-	-	5.1	1.5	5.5	1.3	4.1	1.2	13.4	11.9	<b>53</b>	5
Li (mg kg <sup>-1</sup> )	0.50	0.76	-	20.8	8.7	17.0	4.6	20.9	6.7	29.6	9.2	13	0
Mg (g kg <sup>-1</sup> )	†	-	-	2.1	0.5	1.2	0.1	1.0	0.4	3.6	1.9	<b>54</b>	0
Mn (g kg <sup>-1</sup> )	5.20	0.07	57	0.3	0.1	0.2	0.0	0.4	0.4	1.6	1.1	38	0
Na (mg kg <sup>-1</sup> )	†	-	-	0.1	0.2	0.2	0.1	0.1	0.1	0.8	0.9	<b>44</b>	0
Ni (mg kg <sup>-1</sup> )	0.30	0.85	-	7.7	3.1	8.4	2.3	7.6	3.1	13.4	4.5	33	0
Sr (mg kg <sup>-1</sup> )	†	-	-	10.8	2.8	11.1	0.7	16.8	2.6	84.2	56.1	<b>92</b>	0
Ti (g kg <sup>-1</sup> )	1.30	0.52	-	1.6	0.4	1.6	0.1	1.3	0.8	1.7	0.4	0	0
V (mg kg <sup>-1</sup> )	0.00	0.98	-	41.1	9.9	43.7	5.9	40.6	11.7	52.8	10.4	8	0
Zn (mg kg <sup>-1</sup> )	5.50	0.06	70	19.2	6.8	15.3	2.5	12.9	3.3	36.9	20.9	33	0
<i>Radionuclides (R)</i>				(n=6)		(n=4)		(n=13)		(n=19)		Higher	Lower
<sup>137</sup> Cs (Bq kg <sup>-1</sup> )	12.40	<b>0.00</b>	63	4.4	1.6	4.9	1.2	1.3	0.9	2.8	2.4	1	0
<sup>210</sup> Pb <sub>xs</sub> (Bq kg <sup>-1</sup> )	12.90	<b>0.00</b>	74	114.1	37.1	119.4	33.1	30.2	17.4	184.6	162.6	47	0
<sup>228</sup> Ra (Bq kg <sup>-1</sup> )	5.20	<b>0.07</b>	68	115.0	25.9	83.7	12.6	85.4	10.5	106.3	111.8	23	0
<sup>234</sup> Th (Bq kg <sup>-1</sup> )	2.40	0.31	-	116.8	39.1	84.6	25.7	98.3	17.3	127.9	139.1	44	0
<i>Stable isotopes and organic (S)</i>				(n=6)		(n=4)		(n=13)		(n=19)		Higher	Lower
δ <sup>13</sup> C (‰)	†	-	-	-19.3	0.8	-17.9	0.3	-16.4	1.0	-21.3	1.6	<b>58</b>	0
δ <sup>15</sup> N (‰)	10.00	<b>0.01</b>	57	6.5	0.6	5.1	0.6	7.2	1.1	4.2	1.5	0	33
C (%)	†	-	-	2.8	0.5	3.2	0.2	2.0	0.6	5.9	2.7	<b>78</b>	0
N (%)	†	-	-	0.3	0.0	0.3	0.0	0.2	0.1	0.5	0.2	<b>78</b>	0
<i>VIS-based-color parameters (V)</i>				(n=6)		(n=4)		(n=13)		(n=19)		Higher	Lower
L*	6.10	<b>0.05</b>	52	44.1	1.5	43.6	2.0	42.6	4.7	40.6	6.4	0	11
a*	6.20	<b>0.04</b>	65	7.7	1.7	6.4	0.9	6.5	0.7	7.6	2.0	5	0
b*	10.00	<b>0.01</b>	61	19.0	2.0	18.3	2.0	17.1	2.1	18.5	2.2	0	0
C*	9.10	<b>0.01</b>	61	20.5	2.5	19.3	2.2	18.3	2.2	20.0	2.7	5	0

Table 1 – Continued...

Variable	Kruskal-Wallis test		Correct clas. DFA (%)	Oats		Pasture		Channel		Sediment		Sed. samples out of source range (%)	
	H-value	P-value*		Mean	SD	Mean	SD	Mean	SD	Mean	SD	Max ± SD	Min ± SD
<i>VIS-based-color parameters (V)</i>				(n=6)		(n=4)		(n=13)		(n=19)		Higher	Lower
h	22.10	<b>0.00</b>	70	68.0	2.3	70.8	0.8	69.1	1.3	67.8	2.9	0	5
x	2.20	0.33	-	0.4	0.0	0.4	0.0	0.4	0.0	0.4	0.0	21	0
y	3.40	0.19	-	0.4	0.0	0.4	0.0	0.4	0.0	0.4	0.0	11	0
z	1.70	0.43	-	0.2	0.0	0.2	0.0	0.2	0.0	0.2	0.0	0	16
L	6.10	<b>0.05</b>	52	37.3	1.4	36.8	1.9	36.0	4.3	34.1	5.7	0	11
a	7.10	<b>0.03</b>	65	5.9	1.3	4.8	0.7	4.9	0.6	5.6	1.5	5	0
b	19.50	<b>0.00</b>	57	11.3	0.9	10.9	0.7	10.2	1.3	10.7	1.0	0	0
u*	10.60	<b>0.01</b>	61	20.1	3.2	17.7	2.0	17.2	2.0	18.8	3.5	5	0
v*	18.30	<b>0.00</b>	57	20.8	1.7	20.2	1.5	18.8	2.4	19.9	1.7	0	0
u'	3.40	0.19	-	0.2	0.0	0.2	0.0	0.2	0.0	0.2	0.0	16	0
v'	2.00	0.37	-	0.5	0.0	0.5	0.0	0.5	0.0	0.5	0.0	11	0

†: variable removed after range test; bold values indicate significant  $p < 0.05$  of Kruskal–Wallis H-test; -, not significant.

### 3.3.1.2 Eucalyptus catchment

In the catchment with eucalyptus, from the forty multiple parameters, six did not pass in the range test, it means that sediment concentration was outside of source, were not conservative and were removed from the next steps, according Table 2.

Table 2 – Mean and standard deviation (SD) of parameters used for discriminating land use sources to catchment with eucalyptus, including the significance level indicated by the Kruskal–Wallis test H and range test for sediment.

Variable	Kruskal-Wallis test		Correct clas. DFA (%)	Channel		Unpaved road		Eucalyptus		Sediment		Sed. samples out of source range (%)	
	H-value	P-value *		Mean	SD	Mean	SD	Mean	SD	Mean	SD	Max ± SD	Min ± SD
<i>Geochemical (G)</i>				(n=21)		(n=9)		(n=11)		(n=22)		Higher	Lower
B (mg kg <sup>-1</sup> )	†	-	-	5.2	2.5	5.5	2.0	7.9	2.0	22.1	22.2	<b>44</b>	0
Ba (g kg <sup>-1</sup> )	†	-	-	0.1	0.0	0.1	0.0	0.1	0.0	1.00E+07	1.83E+07	<b>63</b>	0
Be (mg kg <sup>-1</sup> )	13.40	<b>0.00</b>	84	6.4	2.4	2.0	0.5	1.3	0.4	6.9	1.8	4	0
Ca (g kg <sup>-1</sup> )	†	-	-	0.1	0.0	0.1	0.0	0.2	0.1	7.93E+07	1.37E+08	<b>52</b>	0
Co mg kg <sup>-1</sup> )	0.40	0.82	37	5.2	1.3	4.4	1.1	4.7	1.8	9.3	2.4	7	0
Cr (mg kg <sup>-1</sup> )	11.90	<b>0.00</b>	68	16.0	11.1	29.8	6.2	20.8	7.8	23.1	6.3	11	0
Cu (mg kg <sup>-1</sup> )	5.90	<b>0.05</b>	58	17.7	5.5	11.9	2.6	8.2	2.4	23.1	6.7	11	0
Fe (g kg <sup>-1</sup> )	4.10	0.13	42	14.7	1.9	15.5	2.4	11.5	3.9	2.72E+08	4.26E+08	<b>30</b>	0
K (g kg <sup>-1</sup> )	†	-	-	9.4	3.0	6.0	1.2	3.2	1.5	9.73E+07	1.60E+08	<b>44</b>	0
Li (mg kg <sup>-1</sup> )	6.40	<b>0.04</b>	63	35.5	9.4	29.6	8.6	18.6	8.9	40.3	10.0	7	0
Mg (g kg <sup>-1</sup> )	12.10	<b>0.00</b>	58	2.9	0.9	1.5	0.3	1.2	0.5	8.22E+07	1.27E+08	19	0
Mn (g kg <sup>-1</sup> )	8.10	<b>0.02</b>	63	0.3	0.1	0.2	0.1	0.3	0.1	1.03E+08	1.65E+08	<b>37</b>	0
Ni (mg kg <sup>-1</sup> )	4.40	0.11	47	7.4	3.5	11.7	3.3	7.7	3.0	12.0	4.7	0	0
Sr (mg kg <sup>-1</sup> )	†	-	-	14.4	5.3	12.6	2.5	11.6	4.0	74.5	67.8	<b>48</b>	0
Ti (g kg <sup>-1</sup> )	8.80	<b>0.01</b>	63	1.1	0.3	1.6	0.6	1.9	0.6	2.45E+08	3.90E+08	19	0
V (mg kg <sup>-1</sup> )	8.60	<b>0.01</b>	63	28.9	7.2	58.1	13.5	38.7	13.7	39.8	9.2	4	0
Zn (mg kg <sup>-1</sup> )	12.40	<b>0.00</b>	79	35.7	8.6	18.5	3.6	13.1	2.6	44.9	18.3	4	0
<i>Radionuclides (R)</i>				(n=6)		(n=7)		(n=6)		(n=5)		Higher	Lower
<sup>137</sup> Cs (Bq kg <sup>-1</sup> )	6.00	<b>0.05</b>	63	0.8	0.5	1.8	1.2	2.0	0.6	0.8	0.7	0	0
<sup>210</sup> Pb <sub>xs</sub> (Bq kg <sup>-1</sup> )	9.90	<b>0.01</b>	58	21.1	16.9	41.8	30.0	93.0	34.4	115.6	51.1	13	0
<sup>228</sup> Ra (Bq kg <sup>-1</sup> )	†	-	-	110.0	20.8	95.9	28.4	84.2	17.2	184.3	39.2	63	0
<sup>234</sup> Th (Bq kg <sup>-1</sup> )	12.20	<b>0.00</b>	79	199.4	89.3	79.0	14.2	70.7	12.0	193.4	36.3	0	0
<i>Stable isotopes and organic (S)</i>				(n=21)		(n=9)		(n=11)		(n=22)		Higher	Lower
δ <sup>13</sup> C (‰)	5.80	<b>0.05</b>	74	-23.8	2.1	-19.5	1.2	-22.7	1.1	-24.3	1.6	0	0
δ <sup>15</sup> N (‰)	5.60	0.06	63	8.3	1.9	8.2	0.6	6.6	0.8	3.9	0.3	25	0
C (%)	10.60	<b>0.00</b>	47	0.5	0.5	1.8	0.9	2.7	0.9	3.6	1.6	13	0
N (%)	10.10	<b>0.01</b>	47	0.0	0.0	0.2	0.1	0.2	0.1	0.3	0.2	13	0
<i>VIS-based-color parameters (V)</i>				(n=21)		(n=9)		(n=11)		(n=22)		Higher	Lower
L*	77.30	<b>0.00</b>	68	59.0	8.4	39.9	3.3	42.7	4.4	49.3	2.9	0	0
a*	30.50	<b>0.00</b>	63	7.2	1.3	12.2	4.5	7.9	2.4	6.1	0.5	0	0
b*	22.90	<b>0.00</b>	55	21.2	2.8	22.0	4.3	18.1	2.1	14.4	1.4	0	0
C*	21.00	<b>0.00</b>	57	22.4	2.9	25.3	6.0	19.8	2.9	15.6	1.4	0	0
h	68.00	<b>0.00</b>	68	71.3	2.1	62.3	4.5	67.1	3.5	66.2	1.5	0	0
x	40.50	<b>0.00</b>	66	0.4	0.0	0.4	0.0	0.4	0.0	0.4	0.0	0	0
y	24.30	<b>0.00</b>	56	0.4	0.0	0.4	0.0	0.4	0.0	0.4	0.0	0	0

Table 2 – Continued...

Variable	Kruskal-Wallis test		Correct clas. DFA (%)	Channel		Unpaved road		Eucalyptus		Sediment		Sed. samples out of source range (%)	
	H-value	p-value		Mean	SD	Mean	SD	Mean	SD	Mean	SD	Higher	Lower
<i>VIS-based-color parameters (V)</i>				(n=21)		(n=9)		(n=11)		(n=22)			
z	34.90	<b>0.00</b>	64	0.2	0.0	0.2	0.0	0.2	0.0	0.3	0.0	0	0
L	77.30	<b>0.00</b>	65	52.3	8.5	33.5	3.0	36.1	4.0	42.4	2.8	0	0
a	24.20	<b>0.00</b>	56	6.1	1.1	9.2	3.5	5.9	1.6	4.8	0.3	0	0
b	45.00	<b>0.00</b>	65	14.4	2.1	11.9	1.6	10.6	0.5	9.1	0.7	0	0
u*	23.60	<b>0.00</b>	54	21.8	3.1	27.1	8.2	19.5	3.7	15.8	1.1	0	0
v*	42.80	<b>0.00</b>	64	25.5	3.4	21.6	2.8	19.4	1.0	16.4	1.4	0	0
u'	48.30	<b>0.00</b>	66	0.2	0.0	0.3	0.0	0.2	0.0	0.2	0.0	0	0
v'	30.70	<b>0.00</b>	64	0.5	0.0	0.5	0.0	0.5	0.0	0.5	0.0	0	0

†: variable removed with range test; bold values indicate significant  $p < 0.05$  of Kruskal-Wallis H-test; -, not significant.

Thirty variables were selected as potential tracers by applying Kruskal-Wallis H-test ( $p < 0.05$ ), according Table 2. Discriminatory power of individual properties ranged from 42 to 84 %.

### 3.3.2 Discriminant function analysis in the paired catchments

In the catchment with Grassland, the introduction of the properties into the analysis provided progressive reduction in Wilks' lambda value ( $\Lambda^*$ ). Table 3 shows the combination for each parameters group resulted in different final results possible. The combination among all parameters (geochemical, stable isotopes, radionuclides and VIS-based-color parameters = GSRV) had the same cumulative percentage of samples classified correctly that GSR. For GSRV parameters, four elements were selected by DFA analyses, resulting in a final value of the  $\Lambda^*$  parameter of 0.42 with 74 % of source type samples classified correctly. Analyzing only VIS based-color parameters, two properties were classified correctly the samples in 70%. In total, less parameters were selected in GC than EC (Table 4), probably because less parameters were selected in the previous step.

Table 3 – General discriminant analysis tests for different combinations in the catchment with Grassland.

GSRV				
Step	Property select	Discrim. Analysis		Cumulative % of source type samples classified correctly
		Wilks' Lambda	p-level	
1	$\delta^{15}\text{N}$	0.4	< 0.0001	57
2	$^{137}\text{Cs}$	0.45	0.0003	63
3	H	0.65	0.0125	70
4	$^{210}\text{Pb}_{\text{xs}}$	0.42	0.0002	74
GSV				
1	$\delta^{15}\text{N}$	0.4	< 0.0001	57
2	H	0.65	0.0125	70
GS				
1	$\delta^{15}\text{N}$	0.4	< 0.0001	57
GSR				
1	$^{137}\text{Cs}$	0.45	0.0003	63
2	$\delta^{15}\text{N}$	0.4	< 0.0001	57
3	$^{210}\text{Pb}_{\text{xs}}$	0.42	0.0002	74
V				
1	A	0.73	<0.0001	65
2	H	0.64	<0.0001	70

In the eucalyptus catchment (Table 4), the different combinations were similar in correctly classifying, being the lower value for the VIS-based-color combination. The final value of the  $\Lambda^*$  parameter was between 0.33 and 0.40 for DFA using all combinations and just with VIS-based-color parameters, respectively. As the value of  $\Lambda^*$  is the proportion of the total variance due to the error of the source discrimination, the selected variables provided an error of 33 and 40%, for DFA, respectively. It means the set of selected variables explains approximately 67 and 60% of the differences between the sources, for DFA using multiple parameters combinations and VIS-based-color parameters. Also, the uncertainty associated with the discrimination of the source was better for the previous combinations and worse for the VIS-based-color parameters. However, least uncertainty associated with the discrimination of the source was to VIS-based-color parameters in the GC (Tables 3).



Table 4 – General discriminant analysis tests for different combinations in the catchment with eucalyptus.

GSRV				
Step	Property select	Discrim. Analysis		Cumulative % of source type samples classified correctly
		Wilks' Lambda	p-level	
1	Cu	0.53	< 0.0001	47.4
2	<sup>210</sup> Pb <sub>xs</sub>	0.73	0.00	57.9
3	Cu	0.60	< 0.0001	57.9
4	Mg	0.53	< 0.0001	57.9
5	Mn	0.85	0.04	63.2
6	Ti	0.82	0.02	63.2
7	V	0.60	< 0.0001	63.2
8	v*	0.64	0.00	63.8
9	H	0.53	< 0.0001	68.1
10	δ13C	0.52	< 0.0001	73.7
11	Zn	0.51	< 0.0001	78.9
12	Be	0.33	< 0.0001	84.2
GSV				
1	C	0.53	< 0.0001	47.4
2	Cu	0.60	< 0.0001	57.9
3	Mg	0.53	< 0.0001	57.9
4	Li	0.69	0.00	63.2
5	Mn	0.85	0.04	63.2
6	Ti	0.82	0.02	63.2
7	V	0.60	< 0.0001	63.2
8	v'	0.76	0.01	63.8
9	H	0.53	< 0.0001	68.1
10	δ13C	0.52	< 0.0001	73.7
11	Zn	0.51	< 0.0001	78.9
12	Be	0.33	< 0.0001	84.2
GS				
1	C	0.53	< 0.0001	47.4
2	Cu	0.60	< 0.0001	57.9
3	Mg	0.53	< 0.0001	57.9
4	Li	0.69	0.00	63.2
5	Mn	0.85	0.04	63.2
6	Ti	0.82	0.02	63.2
7	V	0.60	< 0.0001	63.2
8	δ13C	0.52	< 0.0001	73.7
9	Zn	0.51	< 0.0001	78.9
10	Be	0.33	< 0.0001	84.2
G				
1	Cu	0.60	< 0.0001	57.9
2	Mg	0.53	< 0.0001	57.9
3	Li	0.69	0.00	63.2

Table 4 – Continued...

Step	Property select	Discrim. Analysis		Cumulative % of source type samples classified correctly
		Wilks' Lambda	p-level	
G				
4	Mn	0.85	0.04	63.2
5	Ti	0.82	0.02	63.2
6	V	0.60	< 0.0001	63.2
7	Zn	0.51	< 0.0001	78.9
8	Be	0.33	< 0.0001	84.2
V				
1	y	0.84	0.02	56.0
2	h	0.50	< 0.0001	68.1
3	L*	0.40	< 0.0001	68.3

In GC, sediment-sources were separated by a significant Mahalanobis distance of  $11.4 \pm 6.1$  for combination among GSRV,  $4.0 \pm 2.4$  for GSV,  $3.0 \pm 2.5$  for GS,  $9.4 \pm 6.1$  for GSR and  $10.9 \pm 4.2$  for VIS-based-color parameters (see Table 5 and Figure 3). Although the distances among all sources were significantly different, the scatter of points within each group introduces a source of uncertainty; when a sample is classified correctly, it is important to consider the distance to the group central point (Figure 3). Among the different combinations, the lowest uncertainty associated with the discrimination of the source (%) was verified for VIS-based-color parameters in the catchment with grassland.

Sediment-sources in the EC were separated by a significant Mahalanobis distance of  $11.0 \pm 1.1$  for combination among GSRV,  $14.8 \pm 3.9$  for GSV,  $14.6 \pm 4.0$  for GS,  $10.9 \pm 5.3$  for G (geochemical) and  $6.8 \pm 2.7$  for VIS-based-color parameters (see Table 6 and Figure 3). As mentioned before, even though the distances among all sources were significantly different the scatter of points within each group introduces a source of uncertainty; when a sample is classified correctly, it is important to consider the distance to the group central point.

Table 5 – Discriminant analysis output for the different parameters fingerprinting combinations groups in the grassland catchment.

DFA output	GSRV	GSV	GS	GSR	VIS
Wilks' lambda	0.045	0.128	0.312	1.144	0.809
Variance due to differences among sources (%)					
Degree of freedom	14;28	10;32	4;38	8;36	4;142
Fcalculated	7.378	5.734	7.513	6.012	3.96
Fcritical	0.521	0.465	0.263	0.422	0.27
p-value	< 0.0001	< 0.0001	0.000	< 0.0001	0.0044
F-values					
Oats vs. Pasture	2.2	5.2	6.4	2.2	17.7
Oats vs. Channel	10.0	2.6	2.4	10.3	12.1
Channel vs. Pasture	9.0	8.7	17.5	12.4	21.7
p-levels					
Oats vs. Pasture	0.13	0.0	0.0	0.1	3.54E-12
Oats vs. Channel	0.00	0.1	0.1	0.0	3.74E-09
Channel vs. Pasture	0.00	0.0	0.0	0.0	5.45E-14
Squared Mahalanobis distances					
Oats vs. Pasture	4.5	4.6	2.7	3.2	14.0
Oats vs. Channel	13.7	1.3	0.6	9.8	6.2
Channel vs. Pasture	16.1	6.0	5.7	15.4	12.7
Average	11.4	4.0	3.0	9.4	10.9
Source type classified correctly					
Oats	83.3	50.0	66.7	66.7	94.4
Pasture	75.0	100.0	75.0	75.0	93.3
Channel	100.0	69.2	69.2	100.0	85.7
Total	89.5	69.6	69.6	84.2	89.3
Uncertainty associated with the discrimination of the source (%)					
Oats	15.4	20.5	52.1	16.0	0.8
Pasture	7.2	20.7	17.6	16.5	0.9
Channel	6.1	27.8	33.5	5.6	0.8
Average	9.5	23.0	34.4	12.7	0.8

Table 6 – Discriminant analysis output of different parameters fingerprinting combinations groups in the eucalyptus catchment.

DFA output	GSRV	GSV	GS	G	VIS
Wilks' lambda	0.049	0.062	0.063	0.098	0.283
Variance due to differences among sources (%)					
Degrees of freedom	30;48	28;50	24;54	20;58	6;84
Fcalculated	5.618	5.396	6.706	6.343	12.34
Fcritical	0.643	0.636	0.619	0.596	0.36
p-value	< 0.0001	< 0.0001	< 0.0001	< 0.0001	< 0.0001
F-values					
Eucalyptus vs. Channel	7.6	6.6	8.4	8.7	13.9
Eucalyptus vs. Unpaved road	7.7	2.7	3.3	2.1	8.2
Channel vs. Unpaved road	9.1	5.5	6.9	7.9	26.1
p-levels					
Eucalyptus vs. Channel	3.18E-02	2.35E-05	2.73E-06	2.92E-06	1.90E-13
Eucalyptus vs. Unpaved road	3.16E-02	1.54E-02	5.18E-03	6.67E-02	3.06E-08
Channel vs. Unpaved road	2.30E-02	1.06E-04	1.68E-05	7.38E-06	0.00E+00
Squared Mahalanobis distances					
Eucalyptus vs. Channel	12.2	17.4	17.4	13.7	7.4
Eucalyptus vs. Unpaved road	11.0	10.3	10.0	4.7	9.2
Channel vs. Unpaved road	9.9	16.7	16.4	14.2	3.8
Average	11.0	14.8	14.6	10.9	6.8
Source type classified correctly					
Channel	100.0	85.7	81.0	95.2	66.7
Unpaved road	100.0	88.9	88.9	88.9	66.7
Eucalyptus	100.0	90.9	90.9	72.7	77.8
Total	100.0	87.8	85.4	87.8	69.5
Uncertainty associated with the discrimination of the source (%)					
Channel	0.0	4.8	1.8	7.9	27.5
Unpaved road	0.0	6.7	5.3	12.0	38.4
Eucalyptus	0.0	3.6	4.5	6.9	37.6
Average	0.0	5.0	3.9	8.9	34.5

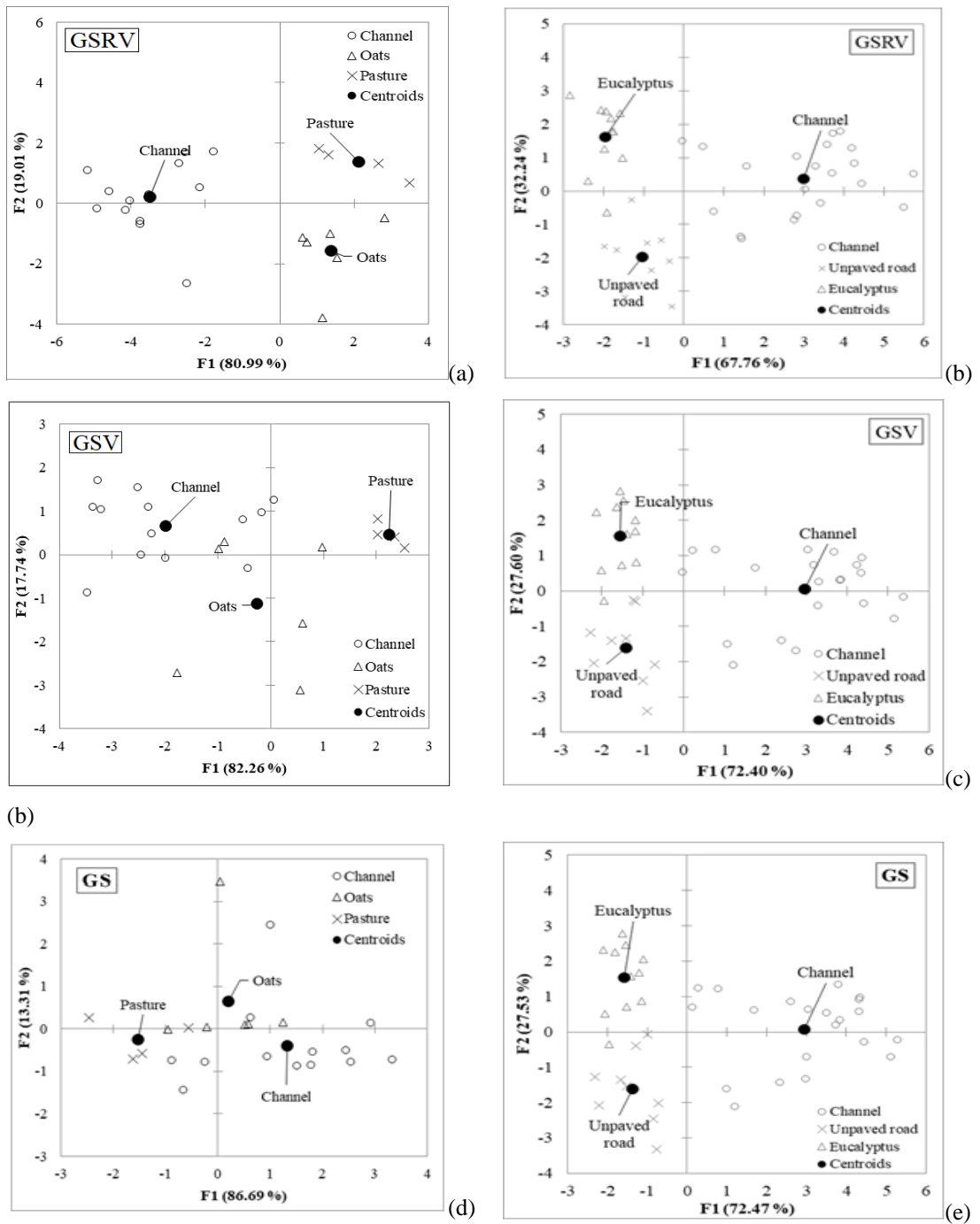


Figure 3 – Scatterplot of the first and second discriminant functions from stepwise discriminant function analysis for GSRV in the GC (a) and EC (b), GSV (c, d), GS (e, f), GSR (g), G (h) and V (I, j) of sources samples in the catchments with grassland and eucalyptus.

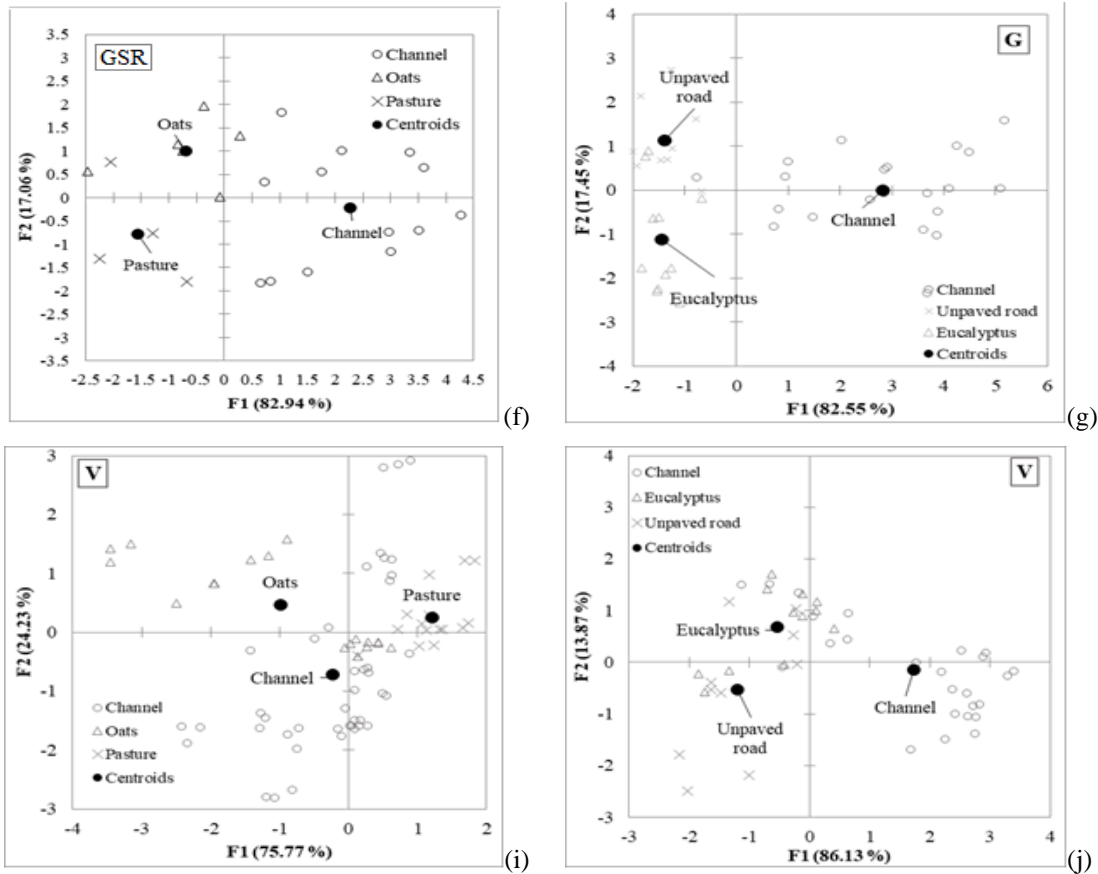


Figure 3 – Continued...

### 3.3.3 Source apportionment

In the grassland catchment, most of sediment results show lower error for the VIS-based-color parameters, which better discriminated the sources compared to others combinations (Table 7). The results agree with the best precision of the variables select for this combination, which provided the lower uncertainty observed in the discriminant analysis output. The mean of sediment source magnitude in the grassland catchment was oats > stream channel  $\geq$  pasture, with relative mean error (RME) < 15%.

In the catchment with eucalyptus (Table 8), lower errors were verified for VIS-based-color parameters for all results of sediment samples. However, it was not the best for the correct classification during the discrimination analysis. Thus, the best classification was verified for each combination and also the discrimination among sources were similar for them, less for the VIS-based-color parameters alone. The magnitude of sediment source for different combinations (GSRV, GSV, GS and G) was similar, being respectively: stream channel > eucalyptus > unpaved road. with the relative contribution < 15%.

Table 7 – Sediment source contribution predicted by the different approaches in grassland catchment.

Sediment	GSRV	GSV	GS	GSR	UV- VIS- PLSR	V	GSRV	GSV	GS	GSR	UV- VIS- PLSR	V	GSRV	GSV	GS	GSR	UV- VIS- PLSR	V	GSRV	GSV	GS	GSR	V	
	Oats contribution (%)						Pasture contribution (%)						Channel contribution (%)						RME (%)					
	Event 14.06.13	-	0	0	-	118.2	-	100	100	-	-68.9	-	0	0	-	31.3	-	>15	>15	-				
Event 14.06.29	-	0	0	-	-	0	-	100	100	-	-	53.6	-	0	0	-	-	46.4	-	>15	>15	-	0.2	
Event 14.07.04	-	0	0	-	40.1	36	-	100	100	-	-95.3	31.2	-	0	0	-	162.1	32.9	-	0.2	0.3	-	0.6	
Event 14.07.04	36.3	0	0	36.1	18.8	97.9	60.8	100	100	61	37.2	0	2.9	0	0	2.9	66.9	2.2	7.9	0.2	0.1	10.5	0.5	
Event 14.10.30	-	0	0	-	43.5	96.6	-	100	100	-	-44	0	-	0	0	-	85.4	3.4	-	0.7	0.8	-	0.6	
Event 14.12.21	0	0	0	0	76.4	31.4	93.6	100	100	93.6	-5.9	34	6.5	0	0	6.4	53.6	34.7	>15	>15	>15	>15	0.1	
Event 15.10.07	0	0	0	0	131.4	0	100	100	100	100	-43.6	53.3	0	0	0	0	-15.3	46.7	>15	>15	>15	>15	0.3	
Event 15.10.08	-	0	0	-	17.3	33	-	100	100	-	20.6	33	-	0	0	-	68.3	34	-	>15	>15	-	0	
Event 16.03.31	0	0	0	0	-0.2	32.1	100	100	100	100	-7.7	33.6	0	0	0	0	112.6	34.3	>15	>15	>15	>15	0.1	
Lag deposit 14.08.20	-	19.8	19.2	-	59.6	35.9	-	80.2	80.9	-	-35.2	31.3	-	0	0	-	86.6	32.9	-	0.1	0.2	-	0.6	
Lag deposit 15.11.24	0	0	0	0	66.7	0	0	100	100	0	-35.7	58.3	100	0	0	100	84.7	41.8	>15	4.1	8	>15	10.3	
Lag deposit 16.02.03	26.2	0	0	26.1	32.1	34.8	34.9	100	100	35	5.2	31.9	38.9	0	0	38.9	68.3	33.4	2	0.8	1.4	2.6	0.2	
Lag deposit 16.05.11	0	0	0	0	0.3	33.4	1.4	100	100	1.4	85	32.8	98.6	0	0	98.6	45	33.9	>15	0.9	1.7	>15	0	
Trap 14.05.05	-	0	0	-	35	34	-	100	100	-	98.4	32.3	-	0	0	-	1.5	33.7	-	0.7	0.7	-	0.2	
Trap 14.08.14	-	0	0	-	41.3	30.2	-	100	100	-	-49.4	34.7	-	0	0	-	16.4	35.2	-	3.6	7.1	-	0.4	
Trap 15.03.19	-	0	0	-	57.4	100	-	100	100	-	50.1	0	-	0	0	-	1.5	0	-	>15	>15	-	11.7	
Trap 15.07.17	-	0	0	-	89.3	93.6	-	100	100	-	36.8	0	-	0	0	-	-15.8	6.4	-	6.9	13.3	-	0.3	
Trap 16.03.31	0	0	0	0	-9.4	95.6	52.8	100	100	52.8	64.7	0	47.2	0	0	47.2	40.7	4.5	>15	2.1	3.9	>15	0.4	
Trap 16.10.12	0	0	0	0	-16.4	93.4	86.8	100	100	86.9	37.6	0	13.2	0	0	13.1	103.7	6.6	6.1	0.4	0.4	8	9	
Mean	6.94	1.04	1.01	6.91	44.52	48.77	58.92	98.96	98.99	58.97	2.77	25.56	34.14	0	0	34.12	55.42	25.72	5.33	1.73	3.16	7.03	1.97	

Table 8 – Sediment source contribution predicted by the different approaches in eucalyptus catchment.

Sediment	GSRV	GSV	GS	G	UV- VIS- PLSR	V	GSRV	GSV	GS	G	UV- VIS- PLSR	V	GSRV	GSV	GS	G	UV- VIS- PLSR	V	GSRV	GSV	GS	G	V				
	Channel contribution (%)						Unpaved road contribution (%)						Eucalyptus contribution (%)						RME (%)								
Event 14.09.10	-	93.1	88.9	95.3	8.2	-	-	6.9	4	4.7	57.5	-	-	0	7.2	0	91.4	-	-	>15	>15	12.5	-				
Event 14.10.30	-	100	100	100	17.1	34.4	-	0	0	0	24.1	32.1	-	0	0	0	106.2	33.5	-	>15	>15	13.9	0.1				
Event 16.01.08	-	94	100	100	-	-	-	6	0	0	-	-	-	0	0	0	-	-	-	10.7	12.6	6.3	-				
Event 16.07.06	-	100	100	100	59.8	-	-	0	0	0	12.7	-	-	0	0	0	59.8	-	-	>15	>15	20	-				
Event 16.10.18	-	100	100	100	30.3	36.6	-	0	0	0	-7.8	30.9	-	0	0	0	89.7	32.5	-	>15	>15	>15	0.3				
Lag deposit 14.07.05	54.2	74.7	74.7	87.7	40.1	30.3	0	0	0	1.3	-14.5	35.2	45.8	25.3	25.3	11.1	91.6	34.5	13.2	3	3.5	2.5	0.3				
Lag deposit 14.08.20	50.3	58.8	58.9	68.4	27.5	-	0	0	0	11.3	15.3	-	49.7	41.2	41.2	20.3	77.9	-	12.3	>15	>15	>15	-				
Lag deposit 14.09.20	-	82.2	82.4	66.5	55.5	57.5	-	17.8	17.6	0.3	-4.9	17.3	-	0	0	33.3	49.1	25.2	-	>15	>15	>15	0.1				
Lag deposit 14.12.20	-	57	57.1	60.8	25.8	34	-	0	0	0	-4.3	32.3	-	43	42.9	39.2	76	33.7	-	>15	>15	>15	0				
Lag deposit 15.03.12	-	87.9	88.3	87.3	38.9	37	-	11.5	10.6	10.4	15.1	30.5	-	0.6	1.1	2.3	75.5	32.5	-	0.7	0.8	1	0.3				
Lag deposit 15.06.18	-	83.7	84.3	95.1	28.3	12.1	-	2.5	0	4.9	-20.6	47	-	13.8	15.8	0	84	40.9	-	3.7	4.3	1.3	0				
Lag deposit 15.09.15	75	74.7	75	84.6	56.6	-	3	0	0	5.5	-25.1	-	22	25.3	25	9.9	59.7	-	4.6	4	4.6	3.5	-				
Lag deposit 15.11.24	-	75.3	75.3	82.7	-	36.9	-	0	0	0	-	30.6	-	24.7	24.7	17.3	-	32.6	-	1.3	1.5	1.3	0.3				
Lag deposit 16.02.03	-	63	63.2	75.5	6.8	34.1	-	15.6	15.2	24.6	3.1	32.3	-	21.4	21.6	0	112.5	33.7	-	>15	>15	>15	0				
Lag deposit 16.05.11	-	90	90.2	83.8	27.2	-	-	7.1	6.4	0.2	-15.6	-	-	2.9	3.3	16	90.9	-	-	2.2	2.6	2.7	-				
Lag deposit 16.06.23	-	64.4	64.5	72.9	58.4	34.5	-	0	0	10.4	0.4	32.1	-	35.6	35.5	16.7	40.2	33.5	-	>15	>15	>15	0				
Lag deposit 16.11.15	-	89.5	89.6	72.8	48.2	-	-	0	0	0	-11.8	-	-	10.5	10.5	27.2	40.1	-	-	2.9	3.4	2	-				
Trap 14.02.12	-	100	100	100	33.7	13.8	-	0	0	0	34.9	44.7	-	0	0	0	49.1	41.6	-	>15	>15	>15	0				
Trap 14.05.05	76.6	100	100	100	50.2	58.3	0	0	0	0	45.3	15.7	23.4	0	0	0	50.6	26	19	14.7	>15	12.5	0				
Trap 15.03.19	-	100	100	100	-	-	-	0	0	0	-	-	-	0	0	0	-	-	-	15.8	>15	10.7	-				
Trap 15.07.17	-	100	100	100	-	31.1	-	0	0	0	-	34.5	-	0	0	0	-	34.4	-	>15	>15	14.6	0.2				
Trap 16.03.31	73.9	87.4	87.7	96.2	53.4	-	0	7.9	7.4	3.8	-4.3	-	26.1	4.6	4.9	0	74.5	-	14.6	8.4	9.9	5.5	-				
Mean	66	85.3	85.5	87.7	37	34.7	0.6	3.4	2.8	3.5	5.5	31.9	33.4	11.3	11.8	8.8	73.3	33.4	12.7	6.1	4.8	7.4	0.1				



## UV-VIS Partial least squares regression

Figure 4 shows the performance of the PLSR-UV-VIS constructed independently for the three source materials.

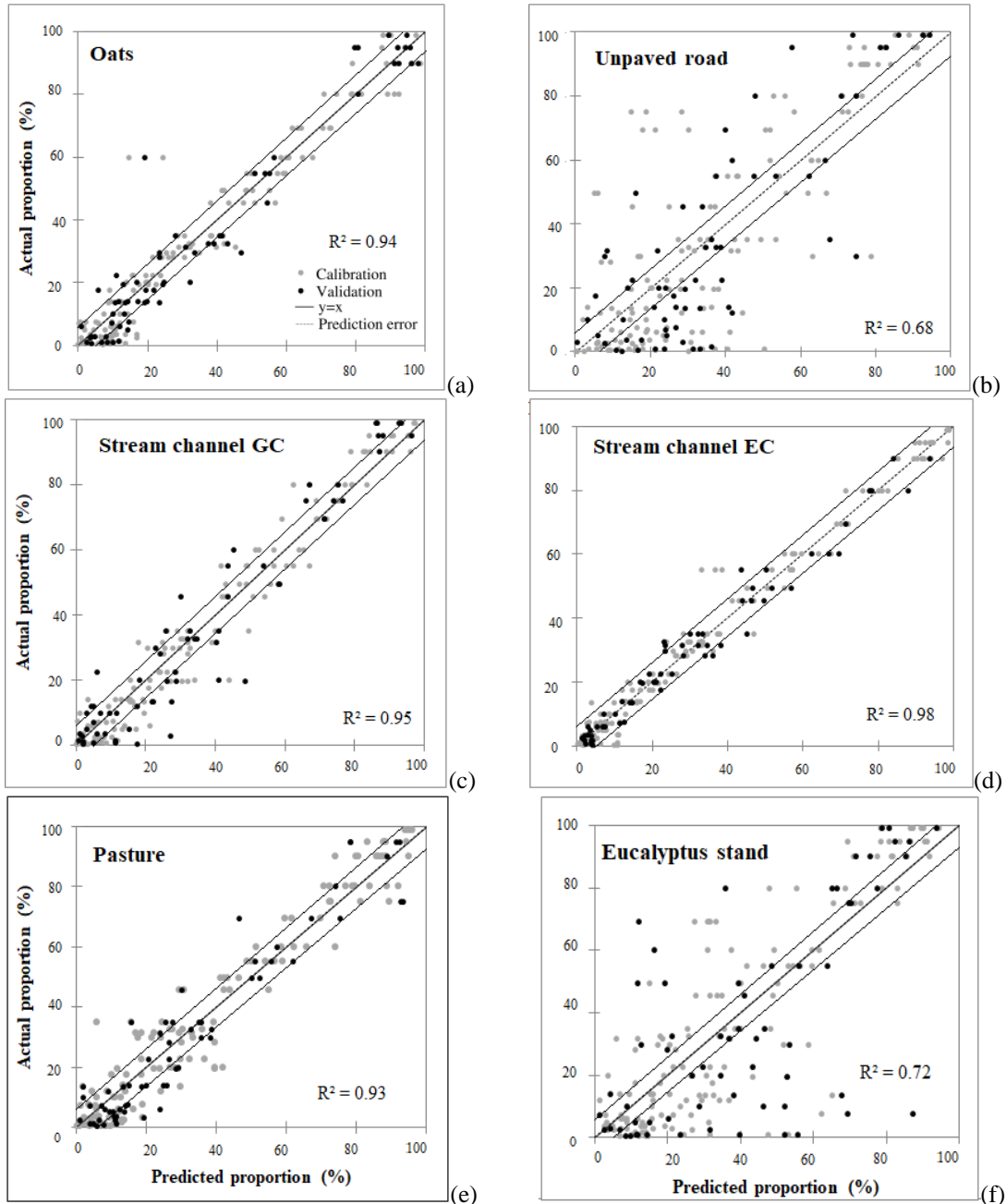


Figure 4 – The relationship between actual proportion and sources predicted by PLSR-UV-VIS models for oats (a), unpaved roads (b), stream channel GC (c) and EC (d) and pasture (e) and eucalyptus stand (f). Dotted lines are the confidence limit (95%).

In GC, the determination coefficients were similar for each model (0.94; 0.95 and 0.94), whereas the root mean square errors were slightly different with values of 0.07, 0.06 and 0.08, for oats, channel and pasture, respectively. For EG, the determination coefficients were

not similar among each model (0.68; 0.72 and 0.98), whereas the root mean square errors were slightly different with values of 0.19, 0.17 and 0.04, for unpaved road, eucalyptus stand and stream channel, respectively.

Using the whole data set used in the construction of the partial least-squares regression models (training and validation) led to a median sum of the three predicted source proportions of 100.0% with minimum sums of 90% and maximum sums of 111% for the GC and the values of minimum and maximum sums of 79% and 126% for the EC, meaning the model was better for the GC due to lower variation. The sums were only representative for laboratory mixtures made with the three source materials sieved to 0.063 mm. The error could also propagate in the models because of the spatial variability of the source material signature as mentioned by Martínez-Carreras et al. (2010a) and Poulenard et al. (2012). Even if the variability of the colorimetric parameters within a group of source material samples was rather low (see Figure 3), the errors generated were assessed by this spatial variability, as suggested by Legout et al. (2013). As mentioned by Collins et al. (2012), the uncertainty associated with the spectrophotometric fingerprinting procedure could be considered as rather high, in comparison with errors reported by some studies that used the “conventional” fingerprinting approach based on geochemistry and radionuclide properties.

#### 3.3.4 UV–VIS Reflectance spectra and characterization

Spectra were very similar between suspended sediments and sediment sources for each catchment (Figure 5). Several absorption bands in the UV–VIS spectra related mainly to iron oxides were found in all soil and sediment samples, as observed in the Figure 5c,d and Table 9, that present several ratios between different absorption bands of the UV–VIS spectrum.

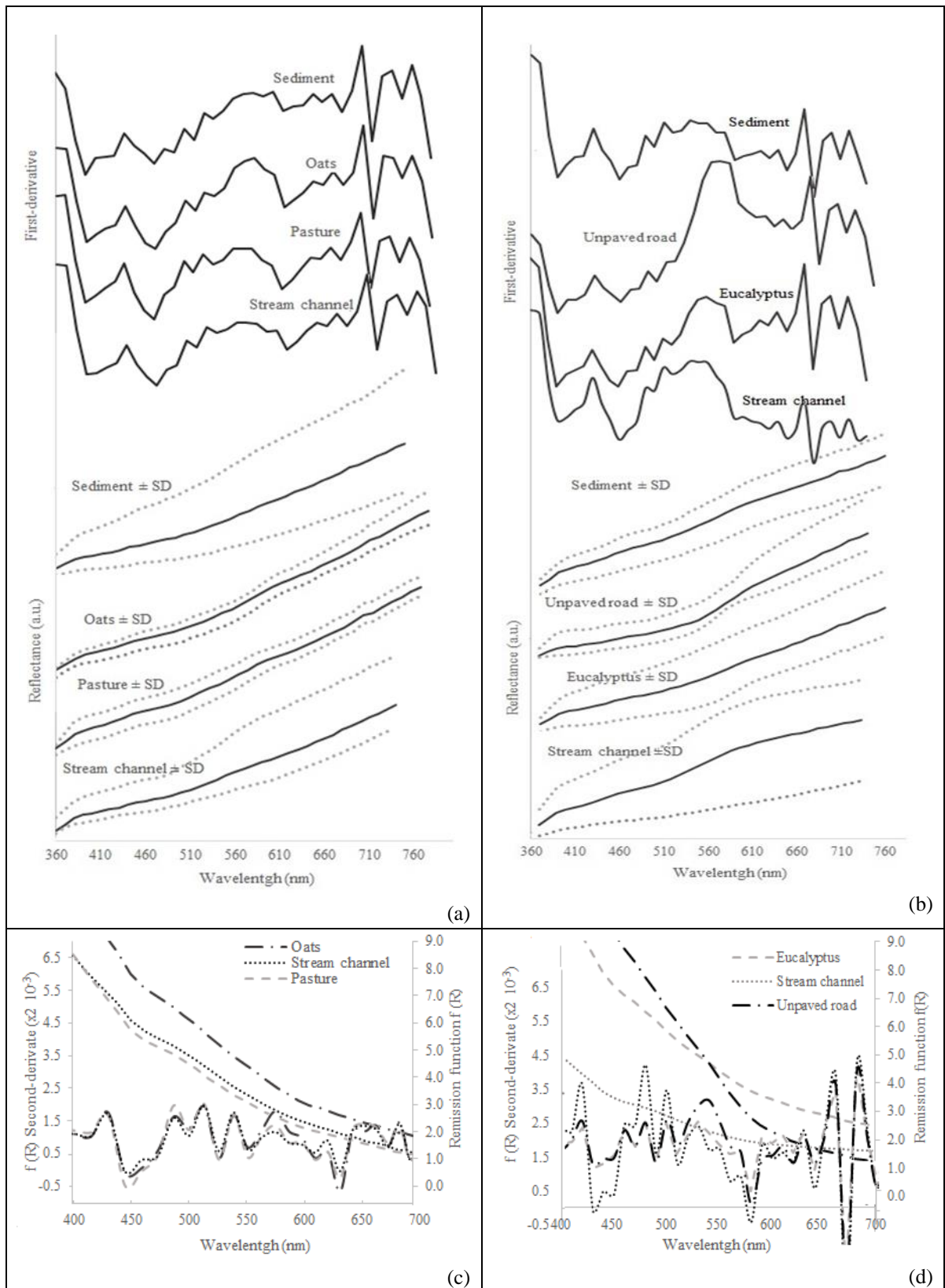


Figure 5 – First-derivative UV–VIS reflectance spectra in the GC (a) and EC (b), and second-derivative spectra of the remission function  $f(R)$  from reflectance spectroscopy curves of soil constituents in the sediment source in the GC (c) and in the EC (d).

Table 9 – UV–VIS spectra ratios for organic and mineral soil components in the catchments.

Grassland catchment					
UV-VIS parameter	Wavelength (nm)	Soil constituent	Oats	Pasture	Stream channel
Iron oxides					
A1	420/450	SET Gt goethite	0.82±0.76	0.82±0.72	0.87±0.74
A2	480/510	EPT Gt goethite	0.85±0.81	0.86±0.78	0.89±0.78
A3	535/575	EPT Hm hematite	0.82±0.72	0.84±0.75	0.86±0.74
Hr (%)	A3/(A1+A3)	-	0.51±0.50	0.50±0.46	0.51±0.49
Organic compounds					
E4/E6	465/665	Organic matter	0.45±0.30	0.46±0.21	0.49±0.29
Eucalyptus catchment					
UV-VIS parameter	Wavelength (nm)	Soil constituent	Eucalyptus	Unpaved road	Stream channel
Iron oxides					
A1	420/450	SET Gt goethite	0.85±0.72	0.87±0.67	0.84±0.67
A2	480/510	EPT Gt goethite	0.87±0.81	0.87±0.78	0.89±0.75
A3	535/575	EPT Hm hematite	0.838±0.62	0.83±0.48	0.85±0.67
Hr (%)	A3/(A1+A3)	-	0.50±0.46	0.50±0.39	0.51±0.48
Organic compounds					
E4/E6	465/665	Organic matter	0.46±0.21	0.44±0.12	0.57±0.26

SET, single electron transition; EPT, electron pair transition; Gt, goethite; Hm, hematite; A, amplitudes of the SET and the EPT of the diffuse reflectance spectra illustrated in Figure 5; Hr, proportion of Hm in the Fe-oxides pool.

The second-derivative curves of remission functions in the visible range of fine earth samples displayed three major absorption bands commonly assigned to Fe-oxide. The first band at low wavelength (A1 in Table 9) corresponds to a single electron transition of Fe in goethite (CANER et al., 2011; TIECHER et al., 2015). The two others (A2 and A3 in Table 9) correspond to an electron pair transition, which there is not differences in the values found among the land uses for each catchment (Table 2). This procedure enabled the estimation of the proportion of hematite (Hr) in the pool of Fe-oxides (hematite + goethite). Also, Table 9 shows the similarity of hematite in different land use for organic components.

### 3.4 Discussion

#### 3.4.1 Sediment source apportionment

In the grassland catchment, the magnitude of sediment source was oats > stream channel ≥ pasture, with relative mean error (RME) <15%. Studies in the rural catchments in northern RS State indicated that cropland (91±15%) was the main source of sediment, as

opposed to very low channel bank contributions ( $5\pm 2\%$ ) (TIECHER et al., 2017). The predominance of oats field sediment is compatible with the importance of this source in the catchment area and with the high erosion rates compared to eucalyptus catchment. Furthermore, it is in agreement with previous results obtained for crop fields. In Brazil, agricultural activities are among those that most disturb the environment, accelerating the transfer of sediments into water bodies (TIECHER et al., 2015). Also, Anache et al. (2017), when revising data from Brazil, observed half of the studied crops showed higher soil loss than grasslands and pasture, while crops with more canopy had lower soil loss.

In areas with extensive livestock, Holt et al. (1996) and Müller et al. (2001) condition the worsening of the physical conditions of soils under pasture to the constant trampling of the animals, promoting soil compaction, which is verified by increasing soil bulk density, micro porosity and resistance to penetration. Bovine cattle is seen as an important bioerosive agent as it alters the relief forms and accelerates the superficial geomorphological processes (THOMAZ, DIAS, 2009). These processes act to reduce the infiltration of water into the soil, culminating with a higher percentage of surface runoff.

In the catchment with eucalyptus, the discrimination analysis of source shows that the magnitude of sediment source was: stream channel > eucalyptus > unpaved road, with the relative error < 15%. Stream bank collapses were observed in both areas, during the study period, more frequently in GC near of outlet, which indicates the importance of bank stability on suspended sediment sources. Furthermore, when seeking shade and water, cattle invade legal protection areas and drainage channels, which they use as drinking, trampling or feeding on regenerating vegetation (see Appendix A). Benett et al. (2002) observed that the rivers and natural reservoirs that have animal watering have their banks unprotected due to the frequent traffic of animals, which also causes silting of rivers, degradation of riparian forests and their capacity for renewal.

In the EC, large amounts of lag deposit were verified in the stream channel (see Appendix A). For forested sites, Durlo and Sutili (2012) comment that these landslides are caused by wind action on the trees, the addition of the weight of the trees to the slopes during rain, pressure caused by roots of plants, and gravity force. Furthermore, Martilla and Kløve (2010) asserted that the effects of weathering, groundwater seepage, and geotechnical instability and erosion conditions on local bank collapse are not well understood in forestry sites, and this topic requires further research. Besides being a significant source of transported sediment, bank erosion can cause structural damage because particles eroded from the bank

cannot be replaced. In larger stream systems, bank sediment can account for over 50% of the total input (KNIGHTON, 1998). In one forested catchment, Rodrigues et al (2018) found the major sediment contribution from stream channel, indicating that management actions should be focused on more proximal sources instead of eucalyptus stands. Despite the low sediment contribution from eucalyptus stands and watercourse bank protection by riparian vegetation, higher contribution of banks for sediment yield highlights the fragility of the soils, independent of the riparian vegetation land use area or the type of riparian vegetation.

The contribution of eucalyptus stands to sediment yield shows the effectiveness of surface litter and canopy protection (RODRIGUES et al., 2018), runoff control (MELLO et al., 2007) and, consequently, erosion control in areas cropped to eucalyptus. Thus, under the condition of the forest use with eucalyptus in the study area, it is believed that the soils present a better structural condition which favors water infiltration capacity in the soil (GUIMARÃES, 2015), attenuating the soil erosion condition to the rapid increase of organic matter in the soil, as in homogeneous eucalyptus plantations.

In forested catchments, the forest canopy acts as a barrier against the precipitation that reaches the soil, reducing the amount of rainfall and redistribute it to the ground (CHANG, 2006). Soil cover, provided by the crop residues and by forest canopy, is fundamental in reducing soil losses due to water erosion, with good efficiency already with 30% coverage (RODRIGUES, 2011). Comparing suspended sediment yield among undisturbed forest sites, Zimmermann et al. (2012) clearly indicate that hydrological characteristics strongly influence suspended sediment dynamics in forested areas. In other words, although there is no doubt that vegetation reduces erosion to some degree and that forests cannot impede erosion completely where a pronounced soil anisotropy (expressed as the change of the saturated hydraulic conductivity with depth) favors the activation of surface flow paths. Also, they suggest that their estimates place the monitoring site near the high-end of reported suspended-sediment yields, and lend credence to the notion that low yields reflect primarily the dominance of vertical flow paths and not necessarily and exclusively the kind of vegetative cover.

Although the soil surface is more protected under forest plantations, soil tillage, management, harvesting, and construction and maintenance of forest roads increase the susceptibility to erosion in these systems (FERREIRA et al., 2008; LIMA, 1996; OLIVEIRA, 2014; SHERIDAN et al., 2006). In the present area with eucalyptus, the harvest of 20% of the field with replanting in the sequence did not promote changes in the sediment production in the EC. This condition reinforces that the forest harvest, when carried out in the staggered way, can be considered more sustainable than clear-cutting.

The low contribution of unpaved roads shows small influence to sediment deposit, possibly due to the small area of this land use. Usually, maintenance of forest unpaved roads increases the susceptibility of these areas to soil erosion (CROKE et al., 1999, 2001; FERREIRA et al., 2008; HAIRSINE et al., 2002; LIMA, 1996; OLIVEIRA, 2014; SHERIDAN et al., 2006). In some cases, the percentage of sediment yield corresponds to more than 90% of the sediment produced from forest roads (GRACE III et al., 1998; MADEJ, 2001), as a result of inadequate planning. Tiecher et al. (2014) observed that the main sediment source was unpaved road in periods with rainfall according to long-term climate average, but the main sediment-source changed to crop fields with extreme rainfall events (about four times higher than long-term average). However, in the study area we observed reduced need for maintenance and absence of new road construction for most of the study period. Also, Ramos-Scharrón and LaFevor (2016) mentioned that water infiltration and erosion dynamics in unpaved roads are related to small sediment contribution, as infiltration in unpaved roads was about 25% of that in forest soil, generates runoff by an increased frequency of 10 times and with very-fast runoff generation and soil loss rates decrease as surface loose materials were washed away during a rainstorm (CAO et al., 2015).

#### 3.4.2 Sediment tracing methods

In the grassland catchment, better results for discrimination among source was verified from VIS-based-color parameters. In general, the low concentrations in geochemical elements made it difficult to outline significant composition differences among different types of sources (land use soil). In contrast, low activities in fallout radionuclides ( $^{137}\text{Cs}$  and  $^{210}\text{Pb}_{\text{xs}}$ ) provided a better way to discriminate among different sources when low-background and efficient gamma spectrometry detectors are available to conduct measurements. The results obtained in this study confirmed the preliminary observations made by Evrard et al. (2010; 2013). However, this was shown only for two samples of event 14.07.04 and lag deposit 16.02.03 (Table 7), considering the combinations with fallout radionuclides (GSRV and GSR).

However, in the eucalyptus catchment, more geochemical elements could discriminate better the different sources than fallout radionuclides. The selection of multiple parameters combination, especially due to the large number of geochemical elements selected in this catchment in relation the GC, emphasizes that the sediment-source signatures imprinted in soils of the catchment are different among sources due to land use, management and relief position, and these differences are also observed in sediment properties (RODRIGUES et al., 2018).

Because of these assumptions and statistical procedures, the selected properties used to identify sediment sources in the eucalyptus and grassland catchments were different. Also, in EC, the sediment source ascription was not evaluated for color parameters alone because it was not possible to discriminate the sediment sources using only the color parameters. This uncertainty associated by spectrophotometric procedure could be considered rather high in comparison with errors reported by some studies that used the multiple-parameters, as fingerprinting approach based on geochemistry and radionuclide properties (COLLINS et al., 2012).

However, comparison of the results provided by different combinations cannot provide independent validation of the color-based fingerprinting, since different combinations use the same fundamental approach and the results involve considerable uncertainty. The results from this study shows the better discrimination consistency among different approaches when comparing suspended sediment source ascriptions based on spectral color parameters to ascriptions based on classical fingerprinting parameters (geochemistry and radionuclides) for three small catchments (MARTÍNEZ-CARRERAS et al., 2010).

The best combination for EC show the final set of tracers comprised trace elements including isotopes, geochemical and radionuclides. The advantages of using composite signatures including tracers from several groups or sets of tracer properties have been previously emphasized (EVRARD et al., 2010; MARTÍNEZ-CARRERAS et al., 2010; OLLEY, CAITCHEON, 2000; WALLING, 2005). These tracers selected, especially for radionuclides, require a long time for analysis, are expensive and require more quantity of sample compared to spectrophotometric analysis, which turn research not feasible depending on the available financial resources. However, in the grassland catchment, most of sediment results show that lower error was verified for VIS-based-color parameters and it could better discriminate the sources than by the others combinations. The results show that, although the study areas have similar soils, different land uses and hydrological dynamic conditions lead to different tracer selection.

### **3.5 Conclusions**

Areas with commercial eucalyptus plantations contribute with less sediment yield compared to traditional use of the region (grassland with extensive cattle). The mean magnitude corresponded to channel (81%) > eucalyptus (16%) > unpaved roads (3%). By contrast, in the



GC, the source magnitude corresponded to oats (49%) > channel (26%) ≥ degraded natural field (25%) with relative mean error <15 % for both catchments.

The discriminant analysis for each catchment was peculiar, that is, the results show how selective was the number of tracer parameters, being very important to work with a large database. Thus, the combination of different groups of tracers used in the conventional and alternative fingerprinting approaches resulted in different set of variables in the discriminant analysis for each area. The results in the EC were similar for the combinations GSRV, GSV and GS and G (where, G: geochemical, S: stable isotopes, R: radionuclides and V: UV-VIS-based color parameters). For GC, the best results of sediment source were obtained only with the UV-VIS-based color parameters analysis by the alternative approach.

The results evidenced the importance of analyzing a large number of variables and how complex is the identification of sediment sources for each area, since, for the study case, although the areas present the same classes of soil, the different soil uses may have interfered in the variables selection.

### 3.6 References

- ALVARES, C. A., et al. Köppen's climate classification map for Brazil. **Meteorologische Zeitschrift**, 22:711-728, 2013.
- ANACHE, J. A. A. et al. Runoff and soil erosion plot-scale studies under natural rainfall: A meta-analysis of the Brazilian experience. **Catena**, v. 152, p. 29–39, 2017.
- BRACKEN, L.J. et al. Sediment connectivity: a framework for understanding sediment transfer at multiple scales. **Earth Surface Processes and Landforms**. 40:177–188. <http://dx.doi.org/10.1002/esp.3635>. 2015.
- BROSINSKY, A., et al. Spectral fingerprinting: sediment source discrimination and contribution modelling of artificial mixtures based on VNIR–SWIR spectral properties. **Journal Soils Sediments** 14, 1949–1964. 2014.
- CANER, L., et al. Accumulation of organo-metallic complexes in laterites and the formation of Aluandic Andosols in the Nilgiri Hills (southern India): similarities and differences with Umbric Podzols. **European Journal of Soil Science**. 62, 754–764. 2011.
- CAO, L., et al. 2015. Modeling interrill erosion on unpaved roads in the Loess Plateau of China. *Land Degradation & Development* 26: 825-832. DOI: 10.1002/ldr.2253
- CHANG, M. **Forest Hydrology: An introduction to water and forests**. United States: Taylor e Francis. 474 p. 2006.
- COLLINS A. L., et al. Apportioning catchment scale sediment sources using a modified composite fingerprinting technique incorporating property weightings and prior information. **Geoderma**, v. 155, n. 3–4, pp. 249–261. 2010.
- COLLINS A.L., et al. Sediment source tracing in a lowland agricultural catchment in southern England using a modified procedure combining statistical analysis and numerical modelling. **Science of the Total Environment**. v. 414: p.301–317. 2012.

COLLINS, A. L.; WALLING, D. Selecting fingerprint properties for discriminating potential suspended sediment sources in river basins. **Journal of Hydrology**, v. 261, n. 1-4, p. 218–244, abr. 2002.

COLLINS, A. L.; WALLING, D. E.; LEEKS, G. J. L. Source type ascription for fluvial suspended sediment based on a quantitative composite fingerprinting technique. **Catena**, v. 29, n. 1, p. 1–27, mar. 1997.

COMMISSION INTERNATIONALE DE L'ECLAIRAGE. CIE. **CIE Proceedings**. Cambridge University Press, Cambridge. 1931.

COMMISSION INTERNATIONALE DE L'ECLAIRAGE. CIE. **Recommendations on Uniform Color Spaces, Color Differences, and Psychometric Color Terms**. Colorimetry CIE, Paris Suppl. no. 2 to Publication no. 15. 1978.

COOPER, R.J., et al. Sensitivity of fluvial sediment source apportionment to mixing model assumptions: a Bayesian model comparison. **Water Resources Research**. 50, 9031–9047. 2014.

CROKE, J.; HAIRSINE, P.; FOGARTY, P. Sediment transport, redistribution and storage on logged forest hillslopes in south-eastern Australia. **Hydrological Processes**. 13 (17), 2705–2720. 1999b.

CROKE J.; MOCKLER S. Gully initiation and road-to-stream linkage in a forested catchment, southeastern Australia. **Earth Surface Processes and Landforms**, Vol. 26, No. 2, pp. 205–217. 2001.

DURLO, M; SUTILI, F. **Bioengenharia: Manejo Biotécnico de Cursos de Água**. Santa Maria; Edição do Autor, 189p, 2012.

EDWARDS, T. E.; GLYSSON, G. D. **Field methods for measurement of fluvial sediment**. **US Geological Survey Techniques of Water Resources Investigations**, Book 3. US Geological Survey. 1999.

ERSKINE, W. D. Soil color as a tracer of sediment dispersion from erosion of forest roads in Chichester State Forest, NSW, Australia. **Hydrological Processes**, v. 27, n. 6, p. 933–942, 2013.

EVARD, O., et al. A comparison of management approaches to control muddy floods in Central Belgium, Northern France and Southern **Land Degradation & Development**. 21, 322–335. doi:<http://dx.doi.org/10.1002/ldr.1006>. 2010.

EVARD, O. et al. Tracing sediment sources in a tropical highland catchment of central Mexico by using conventional and alternative fingerprinting methods. **Hydrological Processes**, v. 27, n. 6, p. 911–922, 2013.

FRANZ, C. et al. Sediments in urban river basins: identification of sediment sources within the Lago Paranoá catchment, Brasília DF, Brazil - using the fingerprinting approach. **The Science of the total environment**, v. 466-467, p. 513–23, 1 jan. 2014.

FERREIRA, A. G.; GONÇALVES, A. C.; DIAS, S. S. Avaliação da sustentabilidade dos sistemas florestais em função da erosão. **Silva Lusitana**, Oeiras, v. 16, p. 55-67, jun. 2008.

FRYIRS, K., (Dis)connectivity in catchment sediment cascades: a fresh look at the sediment delivery problem. **Earth Surf. Process. Landf.** 38, 30e46. State of Science Series. 2013.

FOSTER I.D.L., LEES J.A. Tracers in geomorphology: theory and applications in tracing fine particulate sediments. In: Foster IDL, editor. **Tracers in geomorphology**. Chichester, UK: Wiley; p. 3-20. 2000.

GRACE III, J.M.; et al. Evaluation of erosion control techniques on forest roads. **Transactions of the ASAE**, St Joseph, v.41, n.2, p.383-391, 1998.

GRIEBELER, N. P.; et al. Equipamento para determinação da erodibilidade e tensão crítica de cisalhamento do solo em canais de estradas. **Revista Brasileira de Engenharia Agrícola e Ambiental**. vol.9 no.2. 2005.

GUIMARÃES, D. V. **Erosão hídrica em sistemas florestais no extremo sul da Bahia**. 92 f. 2015. Dissertação (Mestre em Recursos Ambientais e Uso da Terra). Universidade Federal de Lavras. Lavras, 2015.

- HAIRSINE, P.B., et al. Modelling plumes of overland flow from logging tracks. **Hydrological Processes** 16 (12), 2311–2327. 2002.
- HOROWITZ, A. J. et al. Variations in trace element geochemistry in the Seine River Basin based on floodplain deposits and bed sediments Abstract : **Hydrological Processes**, v. 13, n. October 1998, p. 1329–1340, 1999.
- HOLT, J.A., BRISTOW, K.L., McIVOR, J.G. The effects of grazing pressure on soil animals and hydraulic properties of two soils in semi-arid tropical Queensland. . **Australian Journal of Soil Research**. v. 34, p. 69-79, 1996.
- LACEBY, J. P. et al. Do forests represent a long-term source of contaminated particulate matter in the Fukushima Prefecture? **Journal of Environmental Management**, v. 183, p. 742–753, 2016.
- LACEBY, J. P. et al. The challenges and opportunities of addressing particle size effects in sediment source fingerprinting: A review. **Earth-Science Reviews**, v. 169, n. April, p. 85–103, 2017.
- LE, GALL, M. et al. Science of the Total Environment Quantifying sediment sources in a lowland agricultural catchment pond using  $^{137}\text{Cs}$  activities and radiogenic  $^{87}\text{Sr} / ^{86}\text{Sr}$  ratios. **Science of the total environment**. v. 567, p. 968–980, 2016.
- LE GALL, M. et al. Tracing Sediment Sources in a Subtropical Agricultural Catchment of Southern Brazil Cultivated With Conventional and Conservation Farming Practices. **Land Degradation & Development** v. 28, n. 4, p. 1426–1436, 2017.
- LEGOUT, C. et al. Quantifying suspended sediment sources during runoff events in headwater catchments using spectrophotometry. **Journal of Soils and Sediments**, v. 13, n. 8, p. 1478–1492, 2013.
- LIMA, W. de P. **Impacto ambiental do eucalipto**. 2. ed. São Paulo: EDUSP, 301 p. 1996.
- KNIGHTON, D., 1998. **Fluvial Forms and Processes: A New Perspective**. Arnold, London, United Kingdom.
- KOITER, A. J. et al. Investigating the role of connectivity and scale in assessing the sources of sediment in an agricultural watershed in the Canadian prairies using sediment source fingerprinting ing. p. **J Soils Sediments**. 1676–1691, 2013.
- MABIT L, BENMANSOUR M, WALLING DE. 2008. Comparative advantages and limitations of the fallout radionuclides  $^{137}\text{Cs}$ ,  $^{210}\text{Pb}_{\text{ex}}$  and  $^7\text{Be}$  for assessing soil erosion and sedimentation. **Journal of Environmental Radioactivity** 99: 1799–1807.
- MADEJ, M. A. Erosion and sediment delivery following removal of forest roads. **Earth Surface Processes and Landforms**, Vol. 26, No. 2, pp. 175–190. 2001.
- MARTÍNEZ-CARRERAS, N., et al. The use of sediment color measured by diffuse reflectance spectrometry to determine sediment sources: application to the Attert River catchment (Luxembourg). **Journal of Hydrology**. 382, 49–63. 2010.
- MIGUEL, P. et al. Variáveis mineralógicas preditoras de fontes de produção de sedimentos, em uma bacia hidrográfica Do Rio Grande Do Sul. **Revista Brasileira de Ciência do Solo**, v. 38, n. 3, p. 783–796, 2014a.
- MIGUEL, P. et al. Identificação de fontes de produção de sedimentos em uma bacia hidrográfica de encosta. **Revista Brasileira de Ciencia do Solo**, v. 38, n. 2, p. 585–598, 2014b.
- MINELLA, J. P. G. **Utilização de técnicas hidrossedimentométricas combinadas com a identificação de fontes de sedimentos para avaliar o efeito do uso e do manejo do solo nos recursos hídricos de uma bacia hidrográfica**. 2007. 172 f. Tese (Doutorado em Recursos Hídricos e Saneamento) – Universidade Federal do Rio Grande do Sul, Porto Alegre, 2007
- MINELLA, J. P. G.; MERTEN, G. H.; CLARKE, R. T. Método “fingerprinting” para identificação de fontes de sedimentos em bacia hidrográfica rural. **Revista Brasileira de Engenharia Agrícola e Ambiental**, v. 13, n. 5, p. 633–638, 2009.

MINELLA, J.P.G., WALLING, D.E., MERTEN, G.H., Combining sediment source tracing techniques with traditional monitoring to assess the impact of improved land management on catchment sediment yields. **Journal of Hydrology**. 348, 546–563. 2008.

MINELLA, J.P.G., WALLING, D.E., MERTEN, G.H., Establishing a sediment budget for a small agricultural catchment in southern Brazil, to support the development of effective sediment management strategies. **J. Hydrol.** 519, 2189–2201. 2014.

MERTEN, G.H. et al. No-till surface runoff and soil losses in southern Brazil. **Soil and Tillage Research** 152:85–93. DOI:10.1016/j.still.2015.03.014. 2015.

MERTEN, G.H.; MINELLA, J.P.G. The expansion of Brazilian agriculture: soil erosion scenarios. **International Soil and Water Conservation Research** 1: 37–48. DOI:10.1016/s2095-6339(15)30029-0. 2013

MELLO, C. R.; LIMA, J. M.; SILVA, A. M. Simulação do deflúvio e vazão de pico em microbacia hidrográfica com escoamento efêmero. **Revista Brasileira de Engenharia Agrícola e Ambiental**, v. 11, n. 4, p. 410–419, 2007.

MÜLLER, M.M.L.; CECCON, G. & ROSOLEM, C.A. Influência da compactação do solo em subsuperfície sobre o crescimento aéreo e radicular de plantas de adubação verde de inverno. **Revista Brasileira de Ciência do Solo**, 25:531-538, 2001.

MOTHA J. A., et al. Tracer properties of eroded sediment and source material. **Hydrological Processes**, v. 16, n. 10, pp. 1983–2000. 2002.

NOSRATI K., et al. An exploratory study on the use of enzyme activities as sediment tracers: biochemical fingerprints? **International Journal of Sediment Research**, Vol. 26, No. 2, pp. 136–151. 2011.

OLIVEIRA, L. C. et al. Erosão hídrica em plantio de pinus, em estrada florestal e em campo nativo. **Floresta**, Curitiba, PR, v. 44, n. 2, p. 239 - 248, abr. / jun. 2014. OLIVIRA 201

OWENS, P.N.; WALLING, D.E.; LEEKS, G.J.L. Tracing fluvial suspended sediment sources in the catchment of the River Tweed, Scotland, using composite fingerprints and a numerical mixing model. In: **Tracers in Geomorphology**, Foster IDL (Ed.) John Wiley and Sons Ltd: Chichester; 291–308. 2000.

OLLEY, J.; CAITCHEON, G. Major element chemistry of sediments from the Darling-Barwon River and its tributaries: Implications for sediment and phosphorous sources. **Hydrological Process**. 14, 1159–1175. 2000.

PELÁEZ, J.J.Z. **Hidrologia comparativa em bacias hidrográficas com eucalipto e campo**. 156p. Tese (Doutorado em Engenharia Florestal) - Universidade Federal de Santa Maria, Santa Maria, 2014.

POULENARD J, et al. Tracing sediment sources during floods using Diffuse Reflectance Infrared Fourier Transform Spectrometry (DRIFTS): a case study in a highly erosive mountainous catchment (Southern French Alps). **Journal of Hydrology**. 414-415: 452-462. DOI: 10.1016/j.jhydrol.2011.11.022. 2012.

RAMOS-SCHARRÓN, C.E., LA FEVOR, M. C. The role of unpaved roads as active source areas of precipitation excess in small watersheds drained by ephemeral streams in the Northeastern Caribbean. **Journal of Hydrology**. v. 533: p.168-179. DOI: 10.1016/j.jhydrol.2015.11.051. 2016.

REMUSAT, L., et al. 2012. NanoSIMS study of organic matter associated with soil aggregates: advantages, limitations, and combination with STXM. **Environ. Sci. Technol.** 46, 3943e3949.

RODRIGUES, M. F. **Monitoramento e Modelagem dos processos hidrossedimentológicos em bacias hidrográficas florestais no sul do Brasil**. 209 f. Dissertação (Mestrado em Engenharia Florestal) – Universidade Federal de Santa Maria, Santa Maria, 2011.

RODRIGUES, M. F. **Dinâmica hidrossedimentológica de pequenas bacias hidrográficas florestais**. 2015. 126f. Tese (Doutorado em Engenharia Florestal) – Universidade Federal de Santa Maria, Santa Maria, 2015.

RODRIGUES, M.F. et al. Coarse and fine sediment sources in nested watersheds with eucalyptus forest. **Land Degradation e Development**. <https://doi.org/10.1002/ldr.2977>. 2018.

ROESCH, L.F.W., et al. The Brazilian Pampa: a fragile biome. **Diversity**. 1: 182-198. 2009.

SCHULLER, P. et al. Using  $^{137}\text{Cs}$  and  $^{210}\text{Pb}_{\text{ex}}$  and other sediment source fingerprinting s to document suspended sediment sources in small forested catchments in south-central Chile. **Journal of environmental radioactivity**, v. 124, p. 147–59, out. 2013.

SHREVE, E.A.; DOWNS, A.C. **Quality-Assurance Plan for the Analysis of Fluvial Sediment by the U. S. Geological Survey Kentucky Water Science Center Sediment Laboratory**, U.S., Geological Survey Open-File Report, 28p. 2005.

SHERIDAN, G. J, et al. The effect of truck traffic and road water content on sediment delivery from unpaved forest roads. **Hydrol Process** 20:1683–1699. 2006.

SMITH, H.G.; BLAKE, W.H., Sediment fingerprinting in agricultural catchments: a critical re-examination of source discrimination and data corrections. **Geomorphology** 204, 177–191. <http://dx.doi.org/10.1016/j.geomorph.2013.08.003>. 2014.

THOMAZ, E. L.; DIAS, W. A. Bioerosão - Evolução do rebanho bovino brasileiro e implicações nos processos geomorfológicos. **Revista Brasileira de Geomorfologia**, v. 10, n. 2, p. 3–11, 2009.

TIECHER, T. et al. Alternative method to trace sediment sources in a subtropical rural catchment of southern Brazil by using near-infrared spectroscopy. **EGU General Assembly 2014**, held 27 April - 2 May, 2014 in Vienna, Austria, id.594. 2014.

TIECHER, T. et al. Combining visible-based-color parameters and geochemical tracers to improve sediment source discrimination and apportionment. **Science of the Total Environment**, v. 527–528, p. 135–149, 2015.

TIECHER, T. **Fingerprinting Sediment Sources in Agricultural Catchments in Southern Brazil**. 2015. 307 f. These. (Doctor in Soil Science and Doctor in Sciences of the Earth and the Universe, Space). Universidade Federal de Santa Maria, Santa Maria, e University of Poitiers, France. 2015.

TIECHER, T. et al. Tracing sediment sources in a subtropical rural catchment of southern Brazil by using geochemical tracers and near-infrared spectroscopy. **Soil and Tillage Research**, v. 155, p. 478–491, 2016.

TIECHER, T. et al. Quantifying land use contributions to suspended sediment in a large cultivated catchment of Southern Brazil (Guaporé River, Rio Grande do Sul). **Agriculture, Ecosystems and Environment**, v. 237, p. 95–108, 2017a.

TIECHER, T. et al. Tracing sediment sources in two paired agricultural catchments with different riparian forest and wetland proportion in southern Brazil. **Geoderma** (Amsterdam), v. 285, p. 225-239, 2017b.

TIECHER, T. et al. Fingerprinting sediment sources in a large agricultural catchment under no-tillage in southern Brazil (conceição river). **Land degradation e development**, v. 1, p. 1, 2018.

VERHEYEN, D. et al. The use of visible and near-infrared reflectance measurements for identifying the source of suspended sediment in rivers and comparison with geochemical fingerprinting ing. **Journal of Soils and Sediments**, v. 14, n. 11, p. 1869–1885, 2014.

VISCARRA ROSSEL, R.A.; MCGLYNN, R.; MCBRATNEY, A. Determining the composition of mineral-organic mixes using UV–vis-NIR diffuse reflectance spectroscopy. **Geoderma** 137:70–82. 2006.

WALLING D.E. Tracing suspended sediment sources in catchments and river systems. **Science of the Total Environment** 344:159–184. (2005).

WALLING, D.E.; COLLINS, A.L. **Integrated assessment of catchment sediment budgets: A technical manual**. Exeter, University of Exeter, 2000. 168p.

WALLING, D.E., WOODWARD, J.C., NICHOLAS, A.P., A multi-parameter approach to fingerprinting suspended-sediment sources. In: Peters, N.E., et al. (Eds.), **Tracers in Hydrology**. IAHS Publication No. 215 IAHS Press, Wallingford, pp. 329–338. 1993.

WALLING, D.E.; WOODWARD, J.C. **Tracing sources of suspended sediment in river basins**: A case study of the River Culm, Devon, UK. *Marine and Freshwater Research*, 46:327-336, 1995.

WOLMAN, M.G. Changing needs and opportunities in the sediment field. *Water Resources Research* 13:50–54. 1977.

YU, L.; OLDFIELD, F. A multivariate mixing model for identifying sediment source from magnetic measurements. *Quaternary Research*, v. 32, n. 2, p. 168–181, set. 1989.

ZIMMERMANN, A.; FRANCKE, T.; ELSENBEER, H. Forests and erosion: Insights from a study of suspended-sediment dynamics in an overland flow-prone rainforest catchment. *Journal of Hydrology*, v. 428–429, p. 170–181, 2012.

## 4 ARTICLE III: QUANTIFYING SURFACE AND SUBSURFACE EROSION PROCESSES USING SEDIMENT TRACING IN PAIRED RURAL CATCHMENTS IN THE PAMPA BIOME

### Abstract

Although the protective role of surface litter cover and canopy for partial soil protection and erosion control is known for a long time, little research has been conducted on the processes hydro-sedimentological involved. The aim of this chapter was to identify the dominant erosion process for two sediment-size fractions ( $<0.063$  mm) by using the conventional multiple parameters fingerprinting approach (including fallout radionuclides, geochemical elements and stable isotopes and UV-VIS-based color parameters), and for coarse sediment (0.063-2 mm) using geochemical properties. This analysis were employed to calculate proportional contributions of surface and subsurface sediment in a catchment covered with eucalyptus (0.83 km<sup>2</sup>) and other with grassland (1.10 km<sup>2</sup>) in Brazilian Pampa biome. The dominant erosion process for fine sediment ( $<0.063$  mm), in the both catchments, was the subsurface source, being important the use of a large number of variables for the discrimination of this fraction. The discrimination for the coarse fraction (0.063 - 2 mm) based only on the geochemical variables was not possible for the study areas. These results indicate that management actions should be focused on the channel or in the riparian areas in both catchments.

**Keywords:** Soil erosion; Sediment tracing; Size fraction; *Eucalyptus* spp.; Fingerprinting.

### 4.1 Introduction

Land use change and soil management practices can adversely affect water resources and erosion processes from cultivated areas in catchments, resulting from interactions among diverse environmental factors. In Brazilian Pampa biome, the expansion of forest commercial areas with fast-growing species, e.g. eucalyptus, is a response to the increased demand for forest products. The effects of *Eucalyptus* spp. plantation on water and land resources are not well known, and there are uncertainties about the ability of production land to support planted forests without degrading those natural (REICHERT et al., 2017; RODRIGUES et al., 2014).

Different use soil (e.g. crops, soil tillage, vegetation cover) can significantly increase runoff and soil erosion rates on hillslopes, which may have result in higher sediment yields recorded at catchment outlets. Sediment in suspension and bedload sediment cause environmental problems and the identification of source sediment is important to manage the areas more susceptible. The excess of fine sediment particles (<0.063 mm) supplied by water erosion to rivers are detrimental to water quality, stream environments and the resulting higher turbidity recorded in the water courses may lead to an increased sedimentation in river channels, which generates numerous impacts (HOROWITZ, 2008).

Bed sediment load (0.063-2 mm) are also important fraction of sediment, but the identification of coarse-sediment sources have received little attention (D'HAEN et al., 2012; DÉTRICHÉ et al., 2010; GRIEBELER et al., 2005; LIÉBAULT et al., 2012; PELÁEZ, 2014; RODRIGUES et al., 2018). Most of the sediment which enters the system is not transported all the way to the catchment outlet (CAITCHEON et al., 2012), and thus sediment yield at the outlet of a catchment represents a small portion of the total sediment yield (RODRIGUES, 2015). Thus, the knowledge of sediment source variations can provide the necessary information to formulate more conclusive statements about factors driving variations during transport, and one approach to retrieve this kind of information is sediment fingerprinting (VERCRUYSSSE et al., 2017).

Fingerprinting approach is often used to identify the contribution of different uses soil and lithologies (POULENARD et al., 2009). Tracer properties are grouped into six different classes of parameters: mineralogical, magnetic, geochemical, organic, radiometers, isotopes and physical (MINELLA, 2007). Sediment properties successfully being used as source fingerprints include a wide range of geochemical parameters, isotopic signatures, radionuclides and sediment color and compound specific stable isotopes, as we can see for some studies in forested catchments used as tracers: color (ERSKINE, 2013; FOSTER, LEES, 2000); radionuclides (MATISSOFF et al., 2002; NAGLE et al., 2004; SCHULLER et al., 2013; WALLBRINK et al., 2003; WILKINSON et al., 2009); isotopes (BLAKE et al., 2012; GIBBS, 2008); geochemical (CARTER et al., 2003; KRAUSE et al., 2003; MOTHA et al., 2004) and organic (MABIT et al., 2008; WALLING, 2003). However, the use of a large number of tracer elements is recommended for analysis aiming to reduce the mathematical uncertainties in determining (COLLINS, WALLING, 2002; YU, OLDFIELD, 1989).

The choice of discriminant properties is often guided by the sources supplying sediment. For example, fallout radionuclides discriminate between surface and subsurface sources (EVRARD et al., 2013; LE GALL et al., 2016; OWENS et al., 2012). Fallout



radionuclides ( $^{137}\text{Cs}$ ,  $^{210}\text{Pb}_{\text{ex}}$ ) were used to examine surface and sub-surface sources of post-fire fine sediment (<63 mm) exported from a small catchment (136 ha) in the wet eucalypt forest mountain environment of north-eastern Victoria (SMITH et al., 2011b). The dominance of surface sources can be associated with extensive interrill or rill erosion, whereas subsurface sources are mainly mobilized by gully and bank channel erosion processes (LACEBY, 2012; SLIMANE et al., 2013).

The contributions of surface and subsurface soil sources to stream sediment exports at the catchment outlet can be discriminated by measuring the properties; e.g. activity of  $^{137}\text{Cs}$  (LE GALL et al., 2016; OLLEY et al., 2013; RIBOLZI et al., 2017) and carbon and nitrogen stable isotopes ( $\delta^{13}\text{C}$ ,  $\delta^{15}\text{N}$ ) (EVRARD et al., 2013; LACEBY, 2012; LACEBY et al., 2016; 2017). Thus, the use of fingerprinting techniques based on fallout radionuclides alone or in combination with other tracers has proven to be effective in discriminating between subsoil and topsoil sources (CAITCHEON et al., 2012; FOUCHER et al., 2015; LE GALL, 2016; SMITH et al. 2012; WALLING, 2005) because fallout radionuclides are commonly found in higher concentrations in surface materials (within the top 5 cm) or in undisturbed areas such as forests (MATISOFF et al., 2002), whereas they are depleted in subsurface materials making them useful in distinguishing surface and subsurface materials (OLLEY et al., 2012). Also, soil organic carbon, nitrogen, stable isotopes  $\delta^{13}\text{C}$  and  $\delta^{15}\text{N}$  and fallout radionuclides are potential alternatives to discriminate surface and subsurface soil contributions to sediment (LACEBY et al., 2016).

Soil geochemical properties have frequently been incorporated in multi-tracer fingerprinting studies of sediment sources. The range of potential tracer properties used typically includes various metals (including Al, Cd, Co, Cr, Cu, Fe, Mn, Ni, Pb, Sr and Zn), base cations (Ca, K, Mg and Na) and nutrients (N, P and C) (WALLING et al., 2008). According Smith et al. (2012), the selection of a specific geochemical property as part of the final set of tracers used in source ascription is dependent upon establishing statistical differences between target sources for a given study catchment, because these differences relate to natural or human-impacted processes and controlling factors affecting the development of soil profiles. Thus, geochemical source signatures may differ as a result of modifications to the soil surface. For example, cultivation mixes surface and subsurface soil to produce a different geochemical signature compared with undisturbed pasture or forest soils (WALLING, 2005).

In Brazil, fingerprinting techniques have been successfully applied to determine the sources of suspended sediments, most of them in rivers of southern Brazil (e.g. FRANZ et al.,

2013; 2014; LE GALL et al., 2017; MIGUEL et al., 2014; MINELLA., 2007; POLETO et al., 2009; RODRIGUES et al., 2018; TIECHER et al., 2014; 2015; 2017). In Rio Grande do Sul State, most of them were conducted in the northern part, where clayey soils and soybean largely dominates as major crop. In contrast, almost no information is available about sediment source contributions of fine and coarse sediment in the southern part of the State (Pampa biome) where the soil is fragile and the native grasslands are progressively replaced with livestock farming, soybean, eucalyptus plantations and others crops.

The objective of the current chapter is to discriminate the dominant erosion process for two sediment-sizes ( $<0.063$  mm and  $0.063-2$  mm) in two paired catchments with different land use soil (grassland and eucalyptus forestry) in the Pampa biome.

## **4.2 Materials and methods**

### 4.2.1 Source material and sediment sampling

Source material sampling was collected between May 2015 and January 2016. Before sampling, potential sediment sources mobilization and transport were observed during storm events, and soil sampling was restricted to areas sensitive to erosion and potentially connected to the river network. Surface soil and subsurface channel bank samples were collected to characterize potential sources (Figure 1), by scraping the top 2–3 cm layer of soil.

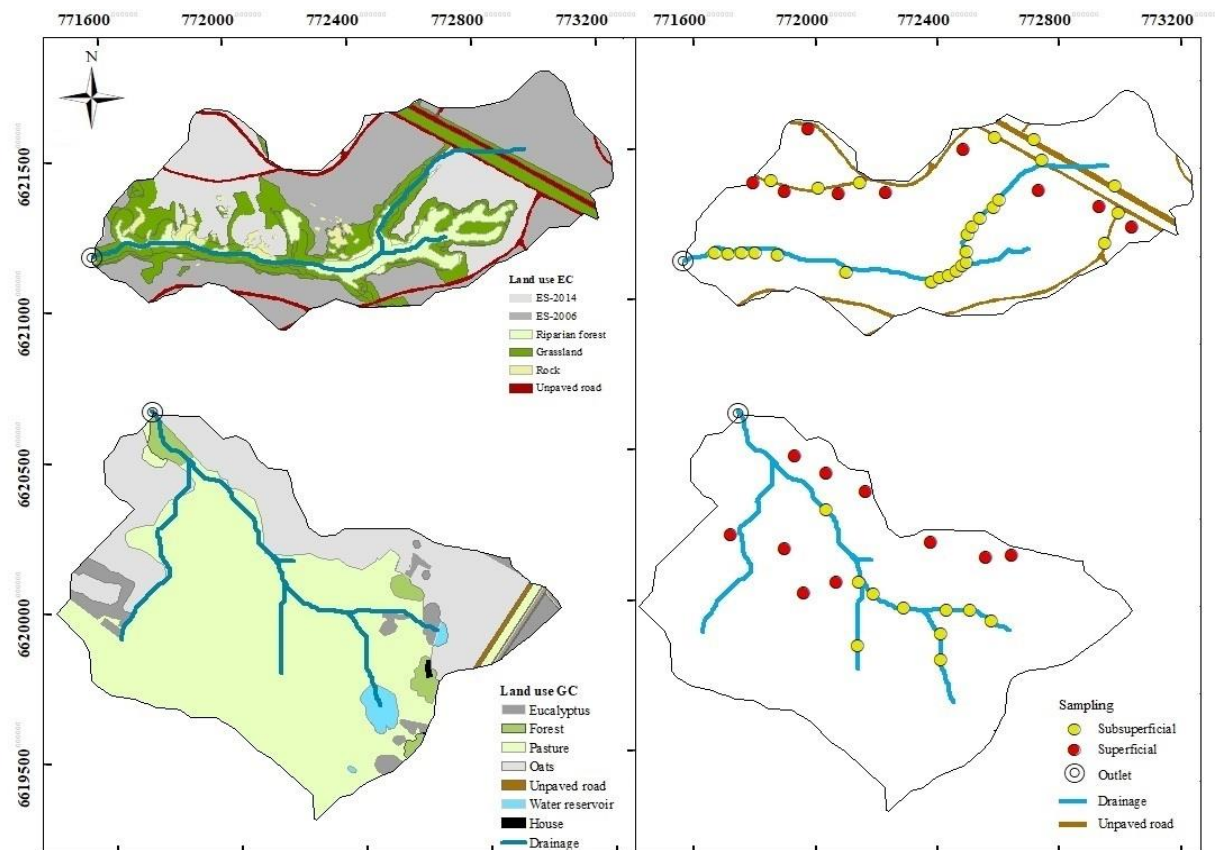


Figure 1 – Surface and subsurface sampling in the eucalyptus and grassland catchments. (\*Eucalyptus stand (ES) planted in 2006 and 2014)

In the eucalyptus catchment, the surface sampling was composed of commercial eucalyptus stand use, whereas unpaved road and stream channel composed the subsurface sampling. In the grassland catchment, the surface was composed of oats and pasture field, whereas the subsurface was composed of stream channel. Each source sample was composed of at least ten sub-samples. A plastic spatula was used to collect samples and avoid potential metal contamination. River sediment samples were collected between March of 2014 and February of 2017 at the catchment outlets following four strategies: (i) suspended matter samples, (ii) time-integrated suspended sediment, (iii) bed load sediment, and (iv) lag deposits.

All collected samples were oven-dried at low temperature (<40 °C) to avoid possible decomposition of organic matter bound to clay minerals with swelling layers (REMUSAT et al., 2012) and sieved to 2 mm and 0.063 mm for further analysis.

#### 4.2.2 Laboratory analysis

Table 1 summarizes all the parameter analyses, including fallout radionuclides, isotopes, geochemical elements and VIS-based-color parameters for fine (<0.063 mm) and

coarse (0.063-2 mm) source material and sediment. More details of analysis methods for fine fraction in the Chapter 2.

Table 1 – Fingerprinting properties used in each fraction of analysis.

Fraction	Fingerprinting Parameter	Sample Mass (g)	Laboratory	Method
<b>0.063 mm</b>	UV-VIS–based color	~0.1	IGE (UGA)	Spectrophotometer
	Al, As, B, Ba, Be, Ca, Cd, Co, Cr, Cu, Fe, Hg, La, Li, K, Mg, Mn, Mo, Na, Ni, Pb, Se, Si, Sb, Sr, Te, Ti, Va and Zn	~0.2	LAAR (UFSM)	Inductively coupled plasma–mass spectroscopy (ICP-OES) – Method 511P
	$^{137}\text{Cs}$ , $^{210}\text{Pb}_{\text{ex}}$ , $^{226}\text{Ra}$ , $^{234}\text{Th}$ and K(%)	3~5	LSCE (CNRS)	Gamma spectrometry using low background N and P type GeHP detectors (Canberra and Ortec)
	$\delta^{13}\text{C}$ , $\delta^{15}\text{N}$ and total carbon (C%) and nitrogen (N%)	~0.1	IRD	ISO/IEC17025 according to GUM - Guidelines to Uncertainty in Measurement
<b>0.063-2 mm</b>	Sc, $\text{TiO}_2$ , V, Cr, $\text{MnO}$ , $\text{Fe}_2\text{O}_3$ , Co, Ni, Cu, Zn, Ga, As, Rb, Sr, Y, Zr, Nb, Mo, Sn, Sb, Cs, Ba, La, Ce, Pb, Th, U.	10 g	LMI (UFSM)	XRF – GEO-QUANT T®

Note: IGE: Institut des Géosciences de l'Environnement/Université Grenoble Alpes; LQFS: Laboratório de Química e Fertilidade do Solo; LAAR: Laboratório de Análises de Águas Rurais; LSCE: Laboratoire des Sciences du Climat et de l'Environnement, Gif-Sur-Yvette, France; IRD: Institute of Research for Development, Paris, France; LMI: Laboratório de Materiais Inorgânicos.

For coarse fraction, the X-ray fluorescence (XRF) analysis was performed using samples with 0.063-2.00 mm size due the difficulty in analyzing chemical composition of coarse soil and sediments. According Rodrigues (2015), it is an adequate analytical technique to perform elemental analysis in coarse soil and sediments because XRF combines highest accuracy and precision with simple and fast sample preparation for the non-destructive quantitative analysis of elements from Beryllium (Be) to Uranium (U), in the concentration range from 100% down to the sub-ppm-level. Thus, soil and sediment samples were thoroughly homogenized grinded/milled and sieved into a fine, loose, powder state, with final particle sizes of <math>53\ \mu\text{m}</math>. Also, after grinding/milling and sieving procedures, ~ 2.7 g (9 pastilles) of powdery binder ("Mahlhilfe") containing cellulose was weighed into 9 g of each sample. Subsequently, for make the measure of elements, 10 g of the mixture (sample + binding material) was homogenized, placed into deformable aluminium cups (40 mm of diameter) and compacted using a hydraulic press with a pressure of 15 Mgf during 2 minutes.

### 4.2.3 Sediment fingerprinting using a mixing model

The statistical methodology was the same for both fractions sizes. After identifying outlier samples and variables with sediment concentrations lying outside the range of sources, some tracers and samples were excluded from the next analyses, as recommended by Smith and Blake (2014), known as the “range test”.

The statistical procedure used greatly differs for multiple-parameters and UV-VIS-based color. Briefly, the steps used were: i) tracer selection based on Mann-Whitney (U test) Equation 1, ii) selection of the best set of tracers using discriminant analyses and finally iii) the use of a mixed linear model to calculate the sediment source contribution. More detailed description of each statistical step is in the Chapter 2.

$$U_1 = R_1 - \frac{n_1(n_1+1)}{2} \quad \text{or} \quad U_2 = R_2 - \frac{n_2(n_2+1)}{2} \quad (1)$$

Where: “R” is the rank sum occupied by the source, “n” is the number of observations in each source.

## 4.3 Results

### 4.3.1 Fine sediment in the paired catchments

#### 4.3.1.1 Discrimination of sediment sources

For fine sediment in the catchment with grassland (Table 2), from all properties analyzed (42), thirteen did not pass in the range test, it means that sediment concentration was outside of source, they were not conservative and were removed from the next steps. From the geochemical (G) parameters three was lower than 0.05 according the Mann Whitney U-Test ( $p < 0.05$ ). For radionuclides (R) two were selected, one for stable isotopes and organic (S) and seven for VIS-based-color parameters (V). Discriminatory power of individual properties ranged from 43 to 95%.

Table 2 – Mean and standard deviation (SD) of parameters used for discriminating land use sources to catchment with grassland, including the significance level indicated by the Mann Whitney U-Test and range test for sediment.

Variable	Mann-Whitney U-test		Correct clas. DFA (%)	Subsurface		Surface		Sediment		Sediment samples out of source range (%)	
	U-value	p-value*		Mean	SD	Mean	SD	Mean	SD	Max $\pm$ SD	Min $\pm$ SD
<i>Geochemical</i>				(n=13)		(n=9)		(n=19)		Higher	Lower
B (mg kg <sup>-1</sup> )	19.0	<b>0.00</b>	61	4.20	2.90	6.50	3.30	31.20	35.00	38	4
Ba (g kg <sup>-1</sup> )	†	-	-	0.20	0.10	0.10	0.00	0.40	0.20	<b>63</b>	0
Be (mg kg <sup>-1</sup> )	†	-	-	2.40	0.50	1.80	0.40	4.50	0.70	<b>88</b>	0
Ca (g kg <sup>-1</sup> )	†	-	-	147.50	0.10	184.50	0.10	851.00	586.00	<b>46</b>	0
Cd (mg kg <sup>-1</sup> )	†	-	-	0.50	0.20	0.40	0.20	1.00	0.40	<b>78</b>	0
Co mg kg <sup>-1</sup> )	†	-	-	6.10	4.00	2.90	0.70	30.10	25.50	<b>46</b>	0
Cr (mg kg <sup>-1</sup> )	45.0	0.21	-	23.50	6.80	19.60	4.70	30.70	5.90	8	0
Cu (mg kg <sup>-1</sup> )	63.0	0.90	-	8.30	3.70	8.10	2.50	16.30	9.10	38	0
Fe (g kg <sup>-1</sup> )	†	-	-	14.10	2.80	13.90	2.80	26.60	6.90	<b>75</b>	4
K (g kg <sup>-1</sup> )	†	-	-	4.10	1.20	5.30	1.40	13.40	11.90	<b>53</b>	5
Li (mg kg <sup>-1</sup> )	58.0	0.66	-	20.90	6.70	19.30	8.00	29.60	9.20	13	0
Mg (g kg <sup>-1</sup> )	†	-	-	1.00	0.40	1.70	0.60	3.60	1.90	<b>54</b>	0
Mn (g kg <sup>-1</sup> )	31.0	<b>0.03</b>	70	0.40	0.40	0.20	0.10	1.60	1.10	38	0
Na (mg kg <sup>-1</sup> )	†	-	-	0.10	0.10	0.10	0.20	0.80	0.90	<b>44</b>	0
Ni (mg kg <sup>-1</sup> )	60.0	0.76	-	7.60	3.10	8.00	2.70	13.40	4.50	33	0
Sr (mg kg <sup>-1</sup> )	†	-	-	16.80	2.60	10.90	2.10	84.20	56.10	<b>92</b>	0
Ti (g kg <sup>-1</sup> )	47.0	0.26	-	1.30	0.80	1.60	0.30	1.70	0.40	0	0
V (mg kg <sup>-1</sup> )	65.0	1.00	-	40.60	11.70	42.10	8.50	52.80	10.40	8	0
Zn (mg kg <sup>-1</sup> )	28.0	<b>0.02</b>	65	12.90	3.30	17.70	6.00	36.90	20.90	33	0
<i>Radionuclides</i>				(n=9)		(n=9)		(n=9)		Higher	Lower
<sup>137</sup> Cs (Bq kg <sup>-1</sup> )	2.0	<b>0.00</b>	84	1.30	0.90	4.60	1.40	2.40	1.20	0	0
<sup>210</sup> Pb <sub>xs</sub> (Bq kg <sup>-1</sup> )	1.0	<b>0.00</b>	95	30.20	17.40	116.20	33.70	162.60	47.30	11	0
<sup>228</sup> Ra (Bq kg <sup>-1</sup> )	28.0	0.17	-	85.40	10.50	102.40	26.20	111.80	22.50	0	0
<sup>234</sup> Th (Bq kg <sup>-1</sup> )	44.0	0.93	-	98.30	17.30	103.90	36.70	139.10	43.90	0	0
<i>Stable isotopes</i>				(n=13)		(n=9)		(n=19)		Higher	Lower
δ13C	†	-	-	-16.40	1.00	-18.80	0.93	-21.30	1.60	<b>58</b>	0
δ15N (‰)	22.0	<b>0.01</b>	82	7.20	1.10	5.90	0.90	3.40	1.60	0	33
C (%)	†	-	-	2.00	0.60	3.00	0.40	6.50	3.10	<b>78</b>	0
N (%)	†	-	-	0.20	0.10	0.30	0.00	0.60	0.30	<b>78</b>	0
<i>VIS-based-color parameters</i>				(n=13)		(n=9)		(n=19)		Higher	Lower
L*	462.0	<b>0.01</b>	43	42.60	4.70	43.90	1.70	39.40	6.60	0	11
a*	687.0	0.95	-	6.50	0.70	7.20	1.60	7.80	2.10	5	0
b*	408.0	<b>0.00</b>	61	17.10	2.10	18.70	2.00	19.00	2.20	0	0
C*	434.0	<b>0.01</b>	65	18.30	2.20	20.00	2.40	20.50	2.80	5	0
h	522.0	0.07	-	69.10	1.30	69.10	2.20	67.90	3.10	0	5
x	641.0	0.58	-	0.40	0.00	0.40	0.00	0.40	0.00	21	0

Table 2 – Continued...

Variable	Mann-Whitney U-test		Correct clas. DFA (%)	Subsurface		Surface		Sediment		Sediment samples out of source range (%)	
	U-value	p-value*		Mean	SD	Mean	SD	Mean	SD	Max ± SD	Min ± SD
<i>VIS-based-color parameters</i>				(n=13)		(n=9)		(n=19)		Higher	Lower
y	527.0	0.08	-	0.40	0.00	0.40	0.00	0.40	0.00	11	0
z	614.0	0.40	-	0.20	0.00	0.20	0.00	0.20	0.00	0	16
L	462.0	<b>0.01</b>	43	36.00	4.30	37.10	1.60	33.20	5.90	0	11
a	620.0	0.44	-	4.90	0.60	5.50	1.20	5.70	1.60	5	0
b	288.0	<b>0.00</b>	61	10.20	1.30	11.10	0.90	10.60	1.00	0	0
u*	452.0	<b>0.01</b>	65	17.20	2.00	19.10	3.00	19.40	3.70	5	0
v*	298.0	<b>0.00</b>	61	18.80	2.40	20.50	1.60	19.70	1.70	0	0
u'	658.0	0.71	-	0.20	0.00	0.20	0.00	0.20	0.00	16	0
v'	576.0	0.21	-	0.50	0.00	0.50	0.00	0.50	0.00	11	0

Note: Bold values indicate significant differences between the sediment sources at  $p < 0.05$ ; -, not significant

In the catchment with eucalyptus (Table 3), for fine sediment, from the forty multiple parameters six did not pass in the range test, it means that sediment concentration was outside of source, were not conservative and were removed from the next steps. Twenty-one were selected as a potential tracers by applying Mann Whitney U-Test ( $p < 0.05$ ). Discriminatory power of individual properties ranged from 53 to 79 %.

Table 3 – Mean and standard deviation (SD) of parameters used for discriminating land use sources to catchment with eucalyptus, including the significance level indicated by the Mann Whitney U-Test and range test for sediment.

Variable	Kruskal-Wallis test		Correct clas. DFA (%)	Subsurface		Surface		Sediment		Sed. samples out of source range (%)	
	H-value	p-value*		Mean	SD	Mean	SD	Mean	SD	Max ± SD	Min ± SD
<i>Geochemical</i>				(n=30)		(n=11)		(n=22)		Higher	Lower
B (mg kg <sup>-1</sup> )	†	-	-	5.30	2.40	7.90	2.00	22.10	22.20	<b>44</b>	0
Ba (g kg <sup>-1</sup> )	†	-	-	0.10	0.00	0.10	0.00	1.00E+07	1.83E+07	<b>63</b>	0
Be (mg kg <sup>-1</sup> )	8.0	<b>0.00</b>	79	5.10	2.70	1.30	0.40	6.90	1.80	4	0
Ca (g kg <sup>-1</sup> )	†	-	-	0.10	0.00	0.20	0.10	7.93E+07	1.37E+08	<b>52</b>	0
Co (mg kg <sup>-1</sup> )	37.0	0.67	63	5.00	1.20	4.70	1.80	9.30	2.40	7	0
Cr (mg kg <sup>-1</sup> )	34.0	0.50	63	20.20	13.30	20.80	7.80	23.10	6.30	11	0
Cu (mg kg <sup>-1</sup> )	18.0	<b>0.04</b>	74	16.00	5.10	8.20	2.40	23.10	6.70	11	0
Fe (g kg <sup>-1</sup> )	18.0	<b>0.04</b>	79	15.00	2.10	11.50	3.90	2.72E+08	4.26E+08	<b>30</b>	0
K (g kg <sup>-1</sup> )	†	-	-	8.40	2.90	3.20	1.50	9.73E+07	1.60E+08	<b>44</b>	0
Li (mg kg <sup>-1</sup> )	15.0	<b>0.02</b>	79	33.80	9.30	18.60	8.90	40.30	10.00	7	0
Mg (g kg <sup>-1</sup> )	15.0	<b>0.02</b>	68	2.50	0.90	1.20	0.50	8.22E+07	1.27E+08	19	0
Mn (g kg <sup>-1</sup> )	30.0	0.31	53	0.30	0.10	0.30	0.10	1.03E+08	1.65E+08	<b>37</b>	0
Ni (mg kg <sup>-1</sup> )	41.0	0.93	63	8.70	4.20	7.70	3.00	12.00	4.70	0	0

Table 3 – Continued...

Variable	Kruskal-Wallis test		Correct clas. DFA (%)	Subsurface		Surface		Sediment		Sed. samples out of source range (%)	
	H-value	p-value *		Mean	SD	Mean	SD	Mean	SD	Max ± SD	Min ± SD
<i>Geochemical</i>				(n=30)		(n=11)		(n=22)		Higher	Lower
Sr (mg kg <sup>-1</sup> )	†	-	-	13.90	4.40	11.60	4.00	74.50	67.80	<b>48</b>	0
Ti (g kg <sup>-1</sup> )	18.0	<b>0.04</b>	68	1.30	0.40	1.90	0.60	2.45E+08	3.90E+08	19	0
V (mg kg <sup>-1</sup> )	41.0	0.93	63	37.60	15.10	38.70	13.70	39.80	9.20	4	0
Zn (mg kg <sup>-1</sup> )	10.0	<b>0.01</b>	79	30.60	9.50	13.10	2.60	44.90	18.30	4	0
<i>Radionuclides</i>				(n=30)		(n=11)		(n=22)		Higher	Lower
<sup>137</sup> Cs (Bq kg <sup>-1</sup> )	21.0	0.08	58	1.30	1.10	2.00	0.60	0.81	0.69	0	0
<sup>210</sup> Pb <sub>xs</sub> (Bq kg <sup>-1</sup> )	7.0	<b>0.00</b>	74	31.50	26.40	93.00	34.40	115.56	51.08	12.5	0
<sup>228</sup> Ra (Bq kg <sup>-1</sup> )	†	-	-	103.00	25.80	84.20	17.20	184.34	39.19	62.5	0
<sup>234</sup> Th (Bq kg <sup>-1</sup> )	14.0	<b>0.02</b>	79	139.20	87.80	70.60	12.00	193.38	36.35	0	0
<i>Stable isotopes</i>				(n=30)		(n=11)		(n=22)		Higher	Lower
δ <sup>13</sup> C (‰)	32.0	0.40	63	-22.50	2.80	-22.70	1.10	-24.30	1.61	0	0
δ <sup>15</sup> N (‰)	14.0	<b>0.02</b>	79	8.30	1.40	6.50	0.80	3.93	0.30	25	0
C (%)	12.0	<b>0.01</b>	68	1.20	1.00	2.70	0.90	3.58	1.65	13	0
N (%)	15.0	<b>0.02</b>	63	0.10	0.10	0.20	0.10	0.32	0.18	13	0
<i>VIS-based-color parameters</i>				(n=30)		(n=11)		(n=22)		Higher	Lower
L*	1044.0	<b>0.00</b>	75	53.20	11.20	42.70	4.40	49.30	2.91	0	0
a*	1622.0	0.21	-	8.70	2.90	7.90	2.30	6.10	0.47	0	0
b*	955.0	<b>0.00</b>	73	21.50	3.30	18.10	2.10	14.37	1.41	0	0
C*	1125.0	<b>0.00</b>	74	23.30	4.00	19.80	2.90	15.64	1.44	0	0
h	1456.0	<b>0.04</b>	75	68.60	4.00	67.10	3.50	66.23	1.45	0	0
x	1785.0	0.62	-	0.40	0.00	0.40	0.00	0.37	0.01	0	0
y	1744.0	0.49	-	0.40	0.00	0.40	0.00	0.37	0.00	0	0
z	1874.0	0.94	-	0.20	0.00	0.20	0.00	0.26	0.01	0	0
L	1044.0	<b>0.00</b>	77	46.60	11.20	36.10	4.00	42.45	2.85	0	0
a	1374.0	<b>0.01</b>	75	7.00	2.10	5.90	1.60	4.78	0.34	0	0
b	594.0	<b>0.00</b>	72	13.60	2.40	10.60	0.50	9.15	0.74	0	0
u*	1180.0	<b>0.00</b>	75	23.40	4.90	19.50	3.70	15.76	1.14	0	0
v*	607.0	<b>0.00</b>	72	24.30	3.80	19.40	1.00	16.40	1.44	0	0
u'	1702.0	0.37	-	0.20	0.00	0.20	0.00	0.22	0.00	0	0
v'	1840.0	0.81	-	0.50	0.00	0.50	0.00	0.50	0.00	0	0

Note: Bold values indicate significant differences between the sediment sources at p<0.05 and -, not significant.

#### 4.3.1.2 Discriminant function analysis

In the grassland catchment (Table 4), for fine sediment, the final set of elements selected by DFA analyses was different for each parameters combination. The combination



among all parameters (geochemical, stable isotopes, radionuclides and VIS-based-color parameters = GSRV) had the similar cumulative percentage of samples classified correctly that GSV, GS and G, between 70-74 %. For GSRV parameters, four elements were selected by DFA analyses, resulting in a final value of the  $\Lambda^*$  parameter of 0.39 with 74 % of source type samples classified correctly. Analyzing only VIS based-color parameters, two properties were classified correctly the samples in 61%. In total, less parameters were selected in GC than in EC, probably because of less parameters selected in the previous step.

As the value of  $\Lambda^*$  is the proportion of the total variance due to the error of the source discrimination, the selected variables provided an error of 39 and 86% for DFA, respectively, for GSRV and V. It means the set of selected variables explains approximately 61 and 14% of the differences between the sources, for DFA using multiple parameters combinations and VIS-based-color parameters. Also, the uncertainty associated with the discrimination of the source was better for the previous combinations and worse for the VIS-based-color parameters.

Table 4 – General discriminant analysis test for fine sediment in the catchment with grassland.

Step	Property select	Discrim. Analysis		Cumulative % of source type samples classified correctly
		Wilks' Lambda	p-level	
GSRV				
1	$\delta^{15}\text{N}$	0.69	0.01	57
2	$^{137}\text{Cs}$	0.43	< 0.0001	63
3	Zn	0.77	0.02	70
4	$^{210}\text{Pb}_{\text{xs}}$	0.39	< 0.0001	74
GSV = GS				
1	$\delta^{15}\text{N}$	0.69	0.01	57
2	Zn	0.77	0.02	70
G				
1	Zn	0.77	0.02	70
V				
1	L*	0.94	0.04	43
2	v*	0.86	0.001	61

In the eucalyptus catchment (Table 5), for fine sediment, the final set of elements selected by DFA analysis was different for each parameters combination. The combination among all parameters (GSRV) had the similar cumulative percentage of samples classified correctly that GSV, GS and G, between 70-74 %. For GSRV parameters, eleven elements were selected by DFA analyses, resulting in a final value of the  $\Lambda^*$  parameter of 0.63 with 79 % of source type samples classified correctly.

Table 5 – General discriminant analysis test for fine sediment in the catchment with eucalyptus.

Step	Property select	Discrim. Analysis		Cumulative % of source type samples classified correctly
		Wilks' Lambda	p-level	
GSRV				
1	C	0.57	< 0.0001	68
2	Mg	0.69	0.00	68
3	Ti	0.84	0.01	68
4	v*	0.66	< 0.0001	72
5	<sup>210</sup> Pb <sub>xs</sub>	0.73	0.00	74
6	Cu	0.64	< 0.0001	74
7	L	0.75	0.00	77
8	<sup>234</sup> Th	0.84	0.01	79
9	Fe	0.81	0.00	79
10	Li	0.66	< 0.0001	79
11	Zn	0.63	< 0.0001	79
GSV				
1	C	0.57	< 0.0001	68
2	Mg	0.69	0.00	68
3	Ti	0.84	0.01	68
4	b*	0.81	0.00	73
5	Cu	0.64	< 0.0001	74
6	Be	0.56	< 0.0001	79
7	Fe	0.81	0.00	79
8	Li	0.66	< 0.0001	79
9	Zn	0.63	< 0.0001	79
GS				
1	C	0.57	< 0.0001	68
2	Mg	0.69	0.00	68
3	Ti	0.84	0.01	68
4	Cu	0.64	< 0.0001	74
5	Be	0.56	< 0.0001	79
6	Fe	0.81	0.00	79
7	Li	0.66	< 0.0001	79
8	Zn	0.63	< 0.0001	79
G				
1	Mg	0.69	0.00	68
2	Ti	0.84	0.01	68
3	Cu	0.64	< 0.0001	74
4	Be	0.56	< 0.0001	79
5	Fe	0.81	0.00	79
6	Li	0.66	< 0.0001	79
7	Zn	0.63	< 0.0001	79
V				
1	L	0.75	0.00	65
2	b	0.64	< 0.0001	65

Analyzing only VIS based-color parameters, two properties were classified correctly the samples in 65%. In general, the final value of the  $\Lambda^*$  parameter was between 0.63 and 0.64, for DFA using all combinations. It means that selection of variables provided an error of 63%, respectively, and the set of selected variables explains approximately 37% of the differences between the sources.

#### 4.3.1.3 Source apportionment

In the grassland catchment (Table 6.), only the geochemical combination results were divergent from others combinations, probably because just one variable was selected in the DFA. In general, the subsurface source was the main sediment source for fine sediment fractions, with relative mean error (RME) <15% for all combinations less for geochemical combination.

Table 6 – Relative contribution of fine sediment source in the catchment with grassland.

Sediment	GSRV	GSV = GS	G	V	GSRV	GSV = GS	G	V	GSRV	GSV = GS	G	V
	Subsurface contribution (%)				Surface contribution (%)				RME (%)			
Event 14.06.13	-	100	0	-	-	0	100	-	-	>15	>15	-
Event 14.06.29	100	100	0	50	0	0	100	50	10	>15	>15	0.1
Event 14.07.04	-	100	0	55.1	-	0	100	44.9	-	6.1	6.8	5.3
Event 14.07.04	100	100	0	50.3	0	0	100	49.7	>15	12.2	>15	0.3
Event 14.10.30	-	100	0	58.2	-	0	100	41.8	-	>15	>15	3.9
Event 14.12.21	97.2	100	0	55.8	2.8	0	100	44.2	>15	>15	>15	1.1
Event 15.10.07	100	100	0	56.1	0	0	100	44	>15	>15	>15	0.7
Event 15.10.08	-	100	0	50.6	-	0	100	49.4	-	>15	>15	0
Event 16.01.18	-	100	0	0	-	0	100	100	-	>15	>15	1.3
Lag deposit 14.08.20	57.5	100	4.8	49.8	42.6	0	95.2	50.2	>15	1.2	0	0.2
Lag deposit 15.11.24	-	100	0	47.5	-	0	100	52.5	-	6.9	3.2	0.7
Lag deposit 16.02.03	100	100	0	100	0	0	100	0	7.5	7.2	4.7	4.2
Lag deposit 16.05.11	-	100	0	56.4	-	0	100	43.6	-	>15	10.1	0.8
Trap 14.05.05	-	100	0	100	-	0	100	0	-	6.3	5.4	13.7
Trap 14.08.14	-	100	0	50.9	-	0	100	49.1	-	15	7	0.2
Trap 15.03.19	-	100	0	40.5	-	0	100	59.5	-	>15	>15	1.4
Trap 15.07.17	1.6	100	0	100	98.4	0	100	0	>15	>15	>15	9.1
Trap 16.03.31	67.9	100	0	52	32.1	0	100	48	4.3	9.1	1.8	2.5
Trap 16.10.12	0	100	0	53.8	100	0	100	46.2	>15	3.9	2	2.5
Mean	69.4	100	0.3	57.1	30.7	0	99.7	43	7.3	7.5	4.6	2.7

In the eucalyptus catchment (Table 7), in general, fine sediment have the mainly source the subsurface for the GSRV, GSV, GS and G combinations. The VIS-based-color parameters shows the surface as the main sediment source.

Table 7 – Relative contribution of fine sediment source in the catchment with Eucalyptus.

Sediment	GSRV	GSV	GS	G	V	GSRV	GSV	GS	G	V	GSRV	GSV	GS	G	V
	Subsurface contribution (%)					Surface contribution (%)					RME (%)				
Event 14.09.10	-	100	100	100	-	-	0	0	0	-	-	>15	>15	11.9	-
Event 14.10.30	-	100	100	100	0	-	0	0	0	100	-	>15	>15	12.9	10.8
Event 16.01.08	-	100	100	100	-	-	0	0	0	-	-	14.9	13.4	11.1	-
Event 16.07.06	-	100	100	100	-	-	0	0	0	-	-	>15	>15	>15	-
Event 16.10.18	-	100	100	100	0	-	0	0	0	100	-	>15	>15	>15	3.6
Lag deposit 14.07.05	65.5	90.3	93.1	100	0	34.5	9.7	6.9	0	100	13.8	4.4	3.7	1.9	5.4
Lag deposit 14.08.20	63.4	70.2	73.7	90.8	-	36.7	29.8	26.3	9.2	-	>15	>15	>15	>15	-
Lag deposit 14.09.20	-	100	100	85.4	0	-	0	0	14.6	100	-	>15	>15	>15	4.4
Lag deposit 14.12.20	-	65.5	71	77.2	44.9	-	34.5	29	22.8	55.1	-	>15	>15	>15	1.7
Lag deposit 15.03.12	-	100	100	100	0	-	0	0	0	100	-	6.6	2	1.6	4.7
Lag deposit 15.06.18	-	98.7	100	100	0	-	1.3	0	0	100	-	8.4	5.3	2.8	0.7
Lag deposit 15.09.15	92.8	87.7	94.5	100	-	7.2	12.4	5.6	0	-	5.5	7.8	4.5	2.4	-
Lag deposit 15.11.24	-	90.8	93.3	100	0	-	9.2	6.7	0	100	-	3	2	1.5	3.5
Lag deposit 16.02.03	-	79.5	85.1	100	8.9	-	20.5	14.9	0	91.1	-	>15	>15	>15	0.9
Lag deposit 16.05.11	-	100	100	100	-	-	0	0	0	-	-	3.8	2.7	1.6	-
Lag deposit 16.06.23	-	77.4	80.4	96.1	8.4	-	22.6	19.6	3.9	91.6	-	>15	>15	>15	1.1
Lag deposit 16.11.15	-	100	100	91	-	-	0	0	9	-	-	6.6	3.8	1.5	-
Trap 14.02.12	-	100	100	100	0	-	0	0	0	100	-	>15	>15	>15	1.8
Trap 14.05.05	85.9	100	100	100	49.8	14.2	0	0	0	50.2	>15	>15	>15	13.8	0.9
Trap 15.03.19	-	100	100	100	-	-	0	0	0	-	-	>15	>15	12.4	-
Trap 15.07.17	-	100	100	100	0	-	0	0	0	100	-	>15	>15	14	7.3
Trap 16.03.31	91.9	100	100	100	-	8.1	0	0	0	-	12.8	10.9	10.3	5.5	-
Mean	79.9	93.6	95.1	97.3	8.6	20.1	6.4	5.0	2.7	91.4	10.7	7.4	5.3	6.8	3.6

#### 4.3.2 Coarse sediment in the paired catchments

##### 4.3.2.1 Discrimination of sediment sources

For coarse sediment in GC (Table 8), eighteen properties analyzed passed in the range test, and six were selected as potential tracers by applying Mann-Whitney U-test ( $p < 0.05$ ). The discriminatory power of individual properties ranged from 71 to 83%.

Table 8 – Mean and standard deviation (SD) of coarse sediment tracers used for discriminating surface and subsurface soil sources to catchment with grassland, including the significance level indicated by the Mann-Whitney U-test and range test.

Variable	Mann-Whitney U-test		Correct clas. DFA (%)	Subsurface		Surface		Sediment		Sediment samples out of source range (%)	
	U-value	p-value*		Mean	SD	Mean	SD	Mean	SD	Max ± SD	Min ± SD
				(n=12)		(n=11)		(n=12)		Higher	Lower
As (mg kg <sup>-1</sup> )	31.5	<b>0.02</b>	71	16.0	2.5	13.0	2.5	11.5	5.7	0	0
Ba (g kg <sup>-1</sup> )	32.0	<b>0.02</b>	75	0.2	0.0	0.2	0.0	0.3	0.0	8	0
Co (mg kg <sup>-1</sup> )	55.5	0.35	-	9.0	3.3	10.0	4.2	9.0	9.6	0	0
Cr (g kg <sup>-1</sup> )	26.0	<b>0.01</b>	83	0.7	0.0	1.2	0.0	1.2	0.0	0	0
Cs (mg kg <sup>-1</sup> )	52.5	0.26	-	7.0	2.5	6.0	2.8	4.0	2.0	0	0
Cu (mg kg <sup>-1</sup> )	30.0	<b>0.02</b>	79	24.0	5.7	36.0	14.8	33.0	8.4	0	0
Ga (mg kg <sup>-1</sup> )	66.0	0.75	-	11.0	3.3	11.0	4.2	7.0	2.1	0	0
Mo (mg kg <sup>-1</sup> )	43.5	0.10	78	58.0	12.7	86.0	42.6	90.0	32.9	0	0
Nb (mg kg <sup>-1</sup> )	64.5	0.68	-	14.0	4.4	15.0	8.6	6.5	2.2	0	0
Ni (g kg <sup>-1</sup> )	29.0	<b>0.01</b>	75	0.3	0.0	0.5	0.0	0.5	0.0	0	0
Pb (mg kg <sup>-1</sup> )	63.0	0.62	-	28.0	6.3	25.0	17.1	17.0	4.7	0	0
Rb (mg kg <sup>-1</sup> )	70.0	0.93	-	85.0	18.0	87.0	43.3	71.5	15.6	0	0
Sn (mg kg <sup>-1</sup> )	62.5	0.60	-	3.0	1.8	4.0	2.2	2.9	1.6	0	0
Sr (mg kg <sup>-1</sup> )	47.5	0.16	-	27.0	7.2	22.0	8.0	43.0	10.3	42	0
V (mg kg <sup>-1</sup> )	29.5	<b>0.01</b>	75	47.0	14.5	36.0	12.0	18.5	12.8	0	0
Y (mg kg <sup>-1</sup> )	52.5	0.27	-	35.0	9.8	28.0	11.8	15.0	5.1	0	0
Zn (mg kg <sup>-1</sup> )	62.0	0.58	-	27.0	6.4	25.0	8.8	15.0	10.6	0	0
Zr (mg kg <sup>-1</sup> )	63.0	0.62	-	209.0	45.3	175.0	59.5	68.5	19.9	25	0

Note: Bold values indicate significant differences between the sediment sources at \*p<0.15; -, not significant and \* Cs and Pb corrected.

For coarse sediment in EC, from nineteen properties analyzed, ten were selected as a potential by applying Mann-Whitney U-test (p<0.05) (Table 9). Discriminant function analysis shows the discriminatory power of individual properties ranged from 61 to 76%.

Table 9 – Mean and standard deviation (SD) of coarse sediment tracers used for discriminating surface and subsurface soil sources to catchment with eucalyptus, including the significance level indicated by the by the Mann-Whitney U-test and range test.

Variable	Mann-Whitney U-test		Correct clas. DFA (%)	Subsurface		Surface		Sediment		Sediment samples out of source range (%)	
	U-value	p-value*		Mean	SD	Mean	SD	Mean	SD	Max ± SD	Min ± SD
				(n=25)	(n=13)	(n=15)	Higher	Lower			
As (mg kg <sup>-1</sup> )	98.5	<b>0.05</b>	61	13.4	4.2	14.6	2.8	11.0	0.5	0	0
Ba (g kg <sup>-1</sup> )	71.0	<b>0.00</b>	66	0.3	0.2	0.2	0.0	0.4	0.0	0	0
Co (mg kg <sup>-1</sup> )	91.5	<b>0.03</b>	66	8.8	4.8	11.7	4.3	6.5	2.2	0	0
Cr (g kg <sup>-1</sup> )	98.5	<b>0.05</b>	74	1.0	0.7	1.5	0.9	1.0	0.2	0	0
Cs (mg kg <sup>-1</sup> )	137.0	0.43	-	7.6	2.9	6.4	2.8	4.1	1.4	0	0
Cu (mg kg <sup>-1</sup> )	104.0	0.07	68	32.8	13.9	40.8	16.8	31.0	7.2	0	0
Ga (mg kg <sup>-1</sup> )	78.5	<b>0.01</b>	76	19.6	6.2	12.8	2.6	8.0	0.5	0	0
MnO (mg kg <sup>-1</sup> )	138.0	0.45	-	0.0	0.0	0.0	0.0	0.0	0.0	0	0
Mo (mg kg <sup>-1</sup> )	101.0	0.06	66	54.4	18.3	50.9	21.0	84.5	22.2	0	0
Nb (mg kg <sup>-1</sup> )	134.0	0.38	-	19.1	5.1	14.8	3.6	7.0	1.6	0	0
Ni (g kg <sup>-1</sup> )	130.0	0.31	-	0.4	0.3	0.6	0.3	0.5	0.1	0	0
Pb (mg kg <sup>-1</sup> )	108.5	0.10	66	31.8	8.2	31.9	15.7	23.5	5.1	0	0
Rb (g kg <sup>-1</sup> )	70.5	<b>0.00</b>	61	0.2	0.1	0.1	0.1	0.1	0.0	0	0
Sn (mg kg <sup>-1</sup> )	82.0	<b>0.01</b>	74	4.4	1.6	2.8	1.2	3.0	1.7	13	0
Sr (mg kg <sup>-1</sup> )	108.5	0.10	63	49.7	25.3	26.4	4.8	51.0	3.8	0	0
V (mg kg <sup>-1</sup> )	59.5	<b>0.00</b>	66	38.6	24.8	40.2	17.4	10.5	2.6	0	0
Y (mg kg <sup>-1</sup> )	138.0	0.45	-	36.7	9.0	27.5	5.9	15.0	2.3	0	0
Zn (mg kg <sup>-1</sup> )	67.5	<b>0.00</b>	66	41.4	15.8	27.2	6.8	12.5	2.9	0	0
Zr (g kg <sup>-1</sup> )	63.0	<b>0.00</b>	63	0.2	0.1	0.2	0.1	0.1	0.0	0	0

Note: Bold values indicate significant differences between the sediment sources at \*p<0.10, and -, not significant.

#### 4.3.2.2 Discriminant function analysis

In the eucalyptus catchment, the final set of elements selected by DFA result in a final value of the  $\Lambda^*$  parameter of 0.65 with 76 % of source type samples classified correctly and 0.75 with 75 % in the grassland catchment (Table 10). As the value of  $\Lambda^*$  is the proportion of the total variance due to the error of the source discrimination, the selected variables provided an error of 65 and 75%, respectively, for EC and GC. It means the set of selected variables explains approximately 35 and 25%.

Table 10 – General discriminant analysis test for coarse sediment in the catchment with eucalyptus and grassland.

Step	Property select	Discrim. Analysis		Cumulative % of source type samples classified correctly
		Wilks' Lambda	p-level	
Eucalyptus catchment				
1	Co	0.90	0.05	66
2	Ba	0.73	0.00	66
3	Sn	0.73	0.00	74
4	Ga	0.65	< 0.0001	76
Grassland catchment				
1	As	0.76	0.02	71
2	Ba	0.76	0.02	75
3	Ni	0.67	0.00	75
4	V	0.75	0.01	75

#### 4.3.2.3 Source apportionment

The relative coarse sediment contribution of each source did not have good RME ( $\% > 15$ ) for most of the sediment source in both catchments (Table 11), probably the geochemical analysis was not enough.

Table 11 – Relative contribution of coarse sediment source in the catchment with eucalyptus and grassland.

Sediment	Subsurface		Surface		RME (%)	
	EC	GC	EC	GC	EC	GC
Event 14.10.30	0	-	100	-	>15	-
Event 15.10.07	0	31	100	69	>15	6
Event 16.10.18	0	0	100	100	>15	>15
Lag deposit 14.07.05	34	0	66	100	>15	>15
Lag deposit 14.08.20	0	0	100	100	>15	>15
Lag deposit 14.09.20	43	0	57	100	>15	>15
Lag deposit 14.12.20	0	0	100	100	14	>15
Lag deposit 15.03.12	0	0	100	100	>15	>15
Lag deposit 15.06.18	20	0	80	100	>15	>15
Lag deposit 15.09.15	0	0	100	100	>15	>15
Lag deposit 15.11.24	77	0	23	100	>15	>15
Lag deposit 16.05.11	33	-	67	-	>15	-
Lag deposit 16.06.23	0	-	100	-	>15	-
Lag deposit 16.11.15	0	0	100	100	>15	>15
Trap 15.07.17	0	0	100	100	>15	>15

## 4.4 Discussion

### 4.4.1 General discussion about the dominant erosion processes

As the results for the coarse fraction (0.063 - 2 mm) were not representative, the discussion will be done only for the fine fraction. Most of the fine sediment (<0.063 mm) collected at the outlet of the catchments originated from the subsurface source, with relative mean error (RME) <15% by different combinations parameters groups in the discrimination analysis for each catchment. A relative error of less than 15% indicates that the model algorithm is able to provide an acceptable prediction of the fingerprinting property concentration associated with the deposited sediment samples (WALLING, COLLINS, 2000).

Sandier soils have higher water infiltration (OLIVEIRA, 2011), but they are also more susceptible to erosive processes. Some visual evidence of erosion process in the bank in GC was observed during high rainfall events (Appendix A). Elevated areas with lag deposits in the channel were observed after events in upstream sites, having as probable sediment source the areas of oats and pasture on low-cohesion soils. Livestock farming has cattle as a bioerosive agent that contributes to erosion in the channel banks, because of trampling and revolving soil on site while drinking water, because they have free access to these areas, as also observed in another study in the Pampa biome (CRUZ et al., 2016; VALENTE et al., 2015).

Furthermore, in the eucalyptus catchment, lag deposits were frequently observed in the channel vicinity in the upper catchment area. The natural instability of the channel results from continuous erosion, landslide and collapse, where forces of running water and surcharge from tree-weight accelerate erosion processes (RAUCH et al., 2014; SIMON, COLLISON, 2002). Contribution of banks may be provided by gravity associated with effects from variations in wetness, especially during rainfall events, which may result in undermining and collapse due to slope instability (RODRIGUES, 2015). Additionally, the riparian forest did not provide bank stabilization, because taller trees provided an overhead in the vertical axes, shifting its center of gravity to a less-stable position. Trees also transmit wind power to the slope, probably amplifying the dynamics of landslides, initially triggered by stream flow (DURLO, SUTILI, 2012; MORGAN, RICKSON, 2005).

Previous study in the present catchments identified landslides on channel banks (PELÁEZ, 2014); thus, materials can be eroded and subsequently deposited before they finally reach the river (COOPER et al., 2014; VALE et al., 2016). Accumulated bed sediment in the main drain is directly available for transport during larger events and is resuspended and



transported by mobile water (MARTILLA, KLØVE, 2010). The distance these sediments will be transported depends on particle sizes and streamflow energy for sediment transport.

Thus, the difference in the dominant erosion process contribution along the stream network occurs due to the contribution of each source and due to the energy required for transport of different sediment particle size, which may hinder sediment-source apportionment. In sediment fingerprinting, only the primary sediment source is identified, without providing information about sediment transport rates and the complexity of the pathways as locations and duration of intermediate sediment storage in the catchment and in the river (VERCRUYSSSE et al., 2017).

#### 4.5 Conclusions

The dominant erosion process for fine sediment (<0.063 mm), in the both catchments, was the subsurface source, being important the use of a large number of variables for the discrimination of this fraction.

The discrimination for the coarse fraction (0.063 - 2 mm) based only on the geochemical variables was not possible for the study areas.

These results indicate that management actions should be focused on the channel or in the riparian areas in both catchments.

#### 4.6 References

- BLAKE, W.H., et al. Tracing crop specific sediment sources in agricultural catchments. **Geomorphology**. 140, 322 e 329. 2012.
- CAITCHEON, G.G., et al. The dominant erosion processes supplying fine sediment to three major rivers in tropical Australia, the Daly (NT), Mitchell (Qld) and Flinders (Qld) Rivers. **Geomorphology** 151-152, 188–195. 2012.
- CARTER, J., et al. Fingerprinting suspended sediment sources in a large urban river system. **Science of the Total Environment**. 314–316, 513–534. 2003.
- COLLINS, A.L., WALLING, D.E., Selecting fingerprinting properties for discriminating potential suspended sediment sources in river basins. **Journal of Hydrology** 261, 218–244. 2002.
- COOPER, R.J., et al. Sensitivity of fluvial sediment source apportionment to mixing model assumptions: a Bayesian model comparison. **Water Resources Research**. 50, 9031–9047. 2014.
- CRUZ, J. C. et al. Qualitative characteristics of water resulting from the introduction of eucalyptus silviculture in Pampa Biome, RS. **Revista Brasileira de Recursos Hídricos**, v. 21, n. 3, 2016.

- DÉTRICHÉ, S. et al. Caesium-137 in sandy sediments of the River Loire (France): Assessment of an alluvial island evolving over the last 50 years. **Geomorphology**, v. 115, n. 1–2, p. 11–22, 2010.
- D'HAEN, K.; VERSTRAETEN, G.; DEGRYSE, P. Fingerprinting historical fluvial sediment fluxes. **Progress in Physical Geography**, v. 36, n. 2, p. 154–186, 3 fev. 2012.
- DURLO, M; SUTILI, F. **Bioengenharia: Manejo Biotécnico de Cursos de Água**. Santa Maria; Edição do Autor, 189p, 2012.
- ERSKINE, W. D. Soil color as a tracer of sediment dispersion from erosion of forest roads in Chichester State Forest, NSW, Australia. **Hydrological Processes**, v. 27, n. 6, p. 933–942, 2013.
- EVARD, O. et al. Tracing sediment sources in a tropical highland catchment of central Mexico by using conventional and alternative fingerprinting methods. **Hydrological Processes**, v. 27, n. 6, p. 911–922, 2013.
- FOSTER, I.D.L., LEES, J.A. Tracers in geomorphology: Theory and Applications in Tracing Fine Particulate Sediments. **In Tracers in Geomorphology**. Foster IDL (ed). Wiley: Chichester; 3–20. 2000.
- FOUCHER, A., et al. Quantifying the dominant sources of sediment in a drained lowland agricultural catchment: the application of a thorium-based particle size correction in sediment fingerprinting. **Geomorphology** 250, 271–281. 2015.
- FRANZ, C. et al. Geochemical signature and properties of sediment sources and alluvial sediments within the Lago Paranoá catchment, Brasília DF: A study on anthropogenic introduced chemical elements in an urban river basin. **Science of the Total Environment**, v. 452–453, p. 411–420, 2013.
- FRANZ, C. et al. Sediments in urban river basins: identification of sediment sources within the Lago Paranoá catchment, Brasília DF, Brazil - using the fingerprinting approach. **The Science of the total environment**, v. 466-467, p. 513–23, 1 jan. 2014.
- HOROWITZ, A.J., Determining annual suspended sediment and sediment-associated trace element and nutrient fluxes. **Science of the Total Environment**. 400 (1–3), 315–343. 2008.
- GRIEBELER, N. P., et al. Equipamento para determinação da erodibilidade e tensão crítica de cisalhamento do solo em canais de estradas. **Revista Brasileira de Engenharia Agrícola e Ambiental**, Campina Grande, PB, DEAg/UFCG. v.9, n.2, p.166-170, 2005.
- GIBBS, M. Identifying source soils in contemporary estuarine sediments: a new compound-specific isotope method. **Estuaries and Coasts**. 31, 344 e 359. 2008.
- KRAUSE, A. K., et al. Multi-parameter fingerprinting of sediment deposition in a small gullied catchment in SE Australia. **Catena** 53, 327–348. 2003.
- LACEBY, J. P. et al. Do forests represent a long-term source of contaminated particulate matter in the Fukushima Prefecture? **Journal of Environmental Management**, v. 183, p. 742–753, 2016.
- LACEBY, J. P. et al. The challenges and opportunities of addressing particle size effects in sediment source fingerprinting ing: A review. **Earth-Science Reviews**, v. 169, n. April, p. 85–103, 2017.
- LACEBY, J. P. **The Provenance of Sediment in Three Rural Catchments in South East Queensland, Australia**. July, 2012. 187f. Thesis.(Doctor of Philosophy. Griffith University. Australia. 2012.
- LE GALL, M. et al. Quantifying sediment sources in a lowland agricultural catchment pond using <sup>137</sup>Cs activities and radiogenic <sup>87</sup>Sr / <sup>86</sup>Sr ratios. **Science of the Total Environment** v. 567, p. 968–980, 2016.
- LE GALL, M. et al. Tracing Sediment Sources in a Subtropical Agricultural Catchment of Southern Brazil Cultivated With Conventional and Conservation Farming Practices. **Land Degradation and Development**, v. 28, n. 4, p. 1426–1436, 2017.

- LIÉBAULT, F. et al. Bedload tracing in a high-sediment-load mountain stream. **Earth Surface Processes and Landforms** v. 37. I. 4. p. 385–399, 2012.
- MABIT, L., BENMANSOUR, M., WALLING, D.E. Comparative advantages and limitations of the fallout radionuclides  $^{137}\text{Cs}$ ,  $^{210}\text{Pb}_{\text{ex}}$  and  $^7\text{Be}$  for assessing soil erosion and sedimentation. **Journal of Environmental Radioactivity** 99: 1799–1807. 2008.
- MARTTILA, H.; KLØVE, B. Dynamics of erosion and suspended sediment transport from drained peatland forestry. **Journal of Hydrology**, v. 388, n. 3–4, p. 414–425, 2010.
- MATISOFF, G., BONNIWELL, E.C., WHITING, P.J., Radionuclides as indicators of sediment transport in agricultural watersheds that drain to Lake Erie. **Journal of Environmental Quality**. 31, 62e72. 2002.
- MIGUEL, P. et al. Variáveis mineralógicas preditoras de fontes de produção de sedimentos, em uma bacia hidrográfica Do Rio Grande Do Sul. **Revista Brasileira de Ciência do Solo**, v. 38, n. 3, p. 783–796, 2014.
- MINELLA, J. P. G. **Utilização de técnicas hidrossedimentométricas combinadas com a identificação de fontes de sedimentos para avaliar o efeito do uso e do manejo do solo nos recursos hídricos de uma bacia hidrográfica**. 2007. 172 f. Tese (Doutorado em Recursos Hídricos e Saneamento) – Universidade Federal do Rio Grande do Sul, Porto Alegre, 2007.
- MINISTÉRIO DO MEIO AMBIENTE. M.M.A. Disponível em: <<http://www.mma.gov.br/biomas/pampa>>. Acesso em: 22 de abr. de 2018.
- MORGAN, R. P. C; RICKSON, R.J. **Slope Stabilization and Erosion Control: A Bioengineering Approach**: Published by E and fn Spon, an imprint of Chapman and Hall, 2-6 Boundary Row, London. 2005.
- MOTHA, J. A. Tracer properties of eroded sediment and source material. **Hydrological Processes**, v. 16, n. 10, p. 1983–2000. 2002.
- NAGLE, G.N., RITCHIE, J. Wheat field erosion rates and channel bottom sediment sources in an intensively cropped northeastern Oregon drainage basin. **Land Degradation and Development**. 14, 1 e 12. 2004.
- OLLEY, J., et al. The application of fallout radionuclides to determine the dominant erosion process in water supply catchments of subtropical South-east Queensland, Australia. **Hydrological Processes**. 27, 885–895, doi:10.1002/hyp.9422. 2013.
- OLIVEIRA, A. H. **Erosão hídrica e seus componentes na sub-bacia hidrográfica do horto florestal Terra Dura**. 2011. 179 f. Tese (Doutorado em Ciência do Solo) – Universidade Federal de Lavras. Minas Gerais. 2011.
- OWENS P.N., et al. Determining the effects of wildfire on sediment sources using  $^{137}\text{Cs}$  and unsupported  $^{210}\text{Pb}$ : the role of natural landscape disturbance and driving forces. **Journal of Soils and Sediments** 12: 982–994. 2012.
- PELÁEZ, J.J.Z. **Hidrologia comparativa em bacias hidrográficas com eucalipto e campo**. 156p. Tese (Doutorado em Engenharia Florestal) - Universidade Federal de Santa Maria, Santa Maria, 2014.
- POLETO, C.; MERTEN, G. H.; MINELLA, J. P. The identification of sediment sources in a small urban watershed in southern Brazil: an application of sediment fingerprinting. **Environmental technology**, v. 30, n. 11, p. 1145–53, out. 2009.
- POULENARD, J. et al., Infrared spectroscopy tracing of sediment sources in a small rural watershed (French Alps). **Sci. Total Environ**. 407, 2808–2819. 2009.
- RAUCH, H.P., SUTILI, F.J., HÖRBINGER, S. Installation of a riparian forest by means of soil bio engineering techniques - monitoring results from a river restoration work in Southern Brazil. **Open Journal of Forestry**. v. 4: p. 161-169. 2014.
- REICHERT, J. M. et al. Agricultural and Forest Meteorology Water balance in paired watersheds with eucalyptus and degraded grassland in Pampa biome. **Agricultural and Forest Meteorology**, v. 237–238, p. 282–295, 2017.

- REMUSAT, L., et al. NanoSIMS study of organic matter associated with soil aggregates: advantages, limitations, and combination with STXM. **Environ. Sci. Technol.** v.46, p. 3943-3949. 2012.
- RIBOLZI, E. et al. From shifting cultivation to teak plantation: effect on overland flow and sediment yield in a montane tropical catchment. **Nature- Scientific Reports** | 7: 3987. 2017.
- RODRIGUES, M. F. et al., Hydrosedimentology of nested subtropical watersheds with native and eucalyptus forests. **Journal of Soils and Sediments**, v. 14, n. 7, p. 1311–1324, 2014.
- RODRIGUES, M. F. **Dinâmica hidrossedimentológica de pequenas bacias hidrográficas florestais**. 2015. 126f. Tese (Doutorado em Engenharia Florestal) – Universidade Federal de Santa Maria, Santa Maria, 2015.
- RODRIGUES, M.F. et al. Coarse and fine sediment sources in nested watersheds with eucalyptus forest. **Land Degradation and Development**. <https://doi.org/10.1002/ldr.2977>. 2018.
- SIMON, A., COLLISON, J.C.A. Quantifying the mechanical and hydrological effects of riparian vegetation on stream banks stability. **Earth Surface Process Landforms** 27, 527-546. 2002.
- SCHULLER, P. et al. Using  $^{137}\text{Cs}$  and  $^{210}\text{Pb}_{\text{ex}}$  and other sediment source fingerprints to document suspended sediment sources in small forested catchments in south-central Chile. **Journal of Environmental Radioactivity**, v. 124, p. 147–159, 2013.
- SLIMANE, A. B. et al. Fingerprinting sediment sources in the outlet reservoir of a hilly cultivated catchment in Tunisia. **Journal of Soils and Sediments**. v.13, I. 4, p 801–815, 2013.
- SMITH, H.G., et al. Changes in sediment sources following wildfire in a forested upland catchment, south-eastern Australia. **Hydrological Process** 25:2878–2889. 2011.
- SMITH, H.G., et al.. Quantifying sources of fine sediment supplied to post-fire debris flows using fallout radionuclide tracers. **Geomorphology** 139–140, 403–415. 2012.
- SMITH, H.G., BLAKE, W.H., Sediment fingerprinting in agricultural catchments: a critical re-examination of source discrimination and data corrections. **Geomorphology** 204, 177–191. <http://dx.doi.org/10.1016/j.geomorph.2013.08.003>. 2014.
- TIECHER, T., et al.. The contribution of sediment sources in a rural catchment under no-tillage. **Revista Brasileira em Ciência do Solo** 38, 639–649 (in Portuguese with English abstract). 2014.
- TIECHER, T. et al. Combining visible-based-color parameters and geochemical tracers to improve sediment source discrimination and apportionment. **Science of the Total Environment**, v. 527–528, p. 135–149, 2015.
- TIECHER, T. et al. Tracing sediment sources in a subtropical rural catchment of southern Brazil by using geochemical tracers and near-infrared spectroscopy. **Soil and Tillage Research**, v. 155, p. 478–491, 2016.
- TIECHER, T. et al. Quantifying land use contributions to suspended sediment in a large cultivated catchment of Southern Brazil (Guaporé River, Rio Grande do Sul). **Agriculture, Ecosystems and Environment**, v. 237, p. 95–108, 2017.
- VALE, S.S., et al. Characterization and quantification of suspended sediment sources to the Manawatu River, New Zealand. **Science of the Total Environment**. 543, 171–186. 2016.
- VALENTE, M. L . et al. Influential factors in surface water quality in catchments within the pampa biome with different land use. **Revista Árvore**, v. 39, n. 6, p. 1135–1145, 2015.
- VERCRUYSSSE, K.; GRABOWSKI, R. C.; RICKSON, R. J. Suspended sediment transport dynamics in rivers: Multi-scale drivers of temporal variation. **Earth-Science Reviews**, v. 166, p. 38–52, 2017.
- WALLBRINK, P.J., MARTIN, C.E., WILSON, C.J. Quantifying the contributions of sediment, sediment–P and fertiliser–P from forested, cultivated and pasture areas at the landuse and catchment scale using fallout radionuclides and geochemistry. **Soil and Tillage Research** 69:53–68. 2003.

WALLING, D.E., COLLINS, A.L. **Integrated assessment of catchment sediment budgets: A technical manual**. Exeter, University of Exeter. 168p. 2000.

WALLING, D.E. Using environmental radionuclides as tracers in sediment budget investigations. In: **Erosion and sediment transport measurement in rivers: technological and methodological advances**, Bogen J, Fergus T, Walling DE (eds). IAHS Publ. No. 283, IAHS Press: Wallingford; 57–78. 2003.

WALLING D.E. Tracing suspended sediment sources in catchments and river systems. **Science of the Total Environment** 344:159–184. 2005.

WALLING, D.E., COLLINS, A.L., STROUD, R.W. Tracing suspended sediment and particulate phosphorus sources in catchments. **Journal of Hydrology** 350: 274–289. 2008.

WILKINSON, S.N., et al. Fallout radionuclide tracers identify a switch in sediment sources and transport-limited sediment yield following wildfire in a eucalypt forest. **Geomorphology** 110: 140–151. 2009.

YU, L.; OLDFIELD, F. A multivariate mixing model for identifying sediment source from magnetic measurements. **Quaternary Research**, v. 32, n. 2, p. 168–181, set. 1989.

## 5 DISCUSSION

The monitored hydro-sedimentological, on scale event, was effective to evaluate distinct sediment transfer patterns in each study area. In general, higher sediment yield was associated to lower water storage capacity of catchment, as observed by higher surface runoff, in the grassland catchment, for example. Lower runoff and sediment yield were observed in the eucalyptus catchment, with lower responses in discharge peak and suspended sediment concentration. This condition can be associated with the rainfall interception by canopy which reduces the amount of water that reaches the outlet, and water infiltration into the soil as favored by deeper rooting system.

The results of monitoring hydro-sedimentological indicate the importance of peak discharge on sediment suspension transport processes, controlling discharge was the key to effective water management and protection in erosion-sensitive areas. The dynamics of suspension sediment transport during rainfall events was described by hysteresis loops, where the hysteresis pattern revealed closer sediment sources in the grassland catchment and further distances in the eucalyptus catchment (Chapter 1).

Bank collapses were observed in both areas during the study period, being more frequent in GC near of outlet, which confirmed the findings of hysteresis analysis and indicates the importance of bank stability on suspended sediment sources. In addition, cattle, when looking for shade and water, invade legal protection areas and drainage channels, which they use as drinking fountains, forming trails, trampling or feeding on regenerating vegetation (see Appendix A). Benett et al. (2002) observed that the rivers and natural reservoirs that have animal watering have their banks unprotected due to the frequent traffic of animals, which also causes silting of rivers, degradation of riparian forests and their capacity for renewal.

Also, in the EC, large amounts of lag deposit were verified in the stream channel (see Appendix A). For forested sites, Durlo and Sutili (2012) commented that these landslides are caused by wind action on the trees, the addition of weight of the trees to the slopes during rain, the pressure caused by roots of plants, and gravity force. Furthermore, Martilla and Kløve (2010) asserted that the effects of weathering, groundwater seepage, and geotechnical instability and erosion conditions on local bank collapse are not well understood in forestry sites, and this topic requires further research. As well as being a significant source of transported sediment, bank erosion can cause structural damage because particles eroded from the bank

cannot be replaced. In larger stream systems bank sediment can account for over 50% of the total input (KNIGHTON, 1998).

The discrimination of different sediment sources and erosion process for fine fraction (<0.063 mm) were verified by the multiple parameters from two approaches: conventional approach (where included fallout radionuclides (R), stable isotopes (S) and geochemical elements (G)) and alternative approach (VIS-based-color parameters (V)), applied by different combinations. For coarse-sediment (0.063-2 mm), only the geochemical elements were examined, but the results did not have good precision due to high mean relative errors (see Chapter 3).

The dynamics of dominant erosion process was confirmed by fingerprinting approaches. The dominant erosion process for the sediment fine (<0.063 mm) was the subsurface source for both catchments, where the fine sediment in the stream channel probably comes from long distances in the EC and short distance in the GC, as suggest the results of hysteresis standards mentioned in the Chapter 1.

In the catchment with eucalyptus, the different combinations of fingerprinting parameters (GSRV, GSV, GS and GSR) were more efficient for most sediment samples and showed similar results for fine sediment source, as mentioned in the Chapter 2, and for the discrimination of erosion process (Chapter 3). The respective relative contribution sediment source was stream channel > eucalyptus > unpaved road, and the subsurface was the dominant erosion process. Greater concentration of bank collapse and sediments deposit in the channel was verified mainly from the central portion of the stream channel until the headwater portion (see Appendix A). This result agrees with the verified during the rainfall events (Chapter 1), where the suspended sediment concentration was observed later than verified in the GC, that is, anti-clockwise hysteresis observed in EC means that sediment comes from more distant sources.

However, in the catchment with grassland, the opposite was observed. The best discrimination results were observed by the VIS-based-color parameters for fine sediment source (Chapter 2) and for the discrimination of erosion process (Chapter 3). The alternative approach based only in the spectrophotometry correctly classified 70% of the samples, and shows the following order in sediment source contribution: oats > stream channel  $\geq$  pasture, with relative mean error (RME) <15%. Also, the subsurface source had a dominant contribution in this catchment and 61% of source samples were classified correctly. These results allow to verify that, although the land use soil with oats is the main source of fine sediments, the

operative erosion process is characterized by the subsurface source, in this case the stream channel. Possibly, the cattle act as a bioerosive agent that contributes to erosion in the channel banks (Appendix A), trampling and revolving soil on site while drinking water, because they have free access to these areas and the sediment becomes more susceptible to transport by flow, as evidenced by the hysteresis in Chapter 1.

Thus, the results agree with the hypotheses of the present study, since the commercial plantations with eucalyptus catchment in the Campanha region contributes to the improvement of soil physical structure, by increasing water infiltration in the soil, reducing surface runoff and the peak flow and, consequently, decreasing sediment yield. The stream channel bank as the main sediment source and subsurface erosion process due to gravity associated with effects from variations in wetness, especially when rainfall events occur, which may result in undermining and collapse due to slope instability (RODRIGUES, 2015). Additionally, the riparian forest did not provide bank stabilization, because taller trees provided an overhead in the vertical axes, shifting its center of gravity to a less-stable position. Trees also transmit wind power to the slope, probably amplifying the dynamics of landslides, initially triggered by stream flow (DURLO, SUTILI, 2012; MORGAN, RICKSON, 2005).

On the identification of sediment source and the fingerprinting approach, it was possible to confirm that the traditional sediment fingerprinting method, based only on geochemical variables, is insufficient to identify the erosive processes in the study areas, for fine and coarse sediments.



## 6 CONCLUSIONS

The hydro-sedimentary monitoring, on a scale of event, clearly demonstrated different patterns for each catchment. In general, higher surface runoff and sediment production were verified in the catchment with grassland. The mean total annual of sediment yield was 22.4 and 67.9 Mg km<sup>-2</sup>, respectively for eucalyptus (EC) and grassland catchments (GC). Also, bed load sediment was higher in the GC (0.053 Mg km<sup>-2</sup>) compared to EC (0.006 Mg km<sup>-2</sup>). These data show that commercial plantations with eucalyptus in the Brazilian Pampa biome, with good management and maintaining of permanent preservation area and legal reserve, when compared to livestock without protection, contributes to the reduction of surface runoff, peak flow, and sediment yield. Further, the dynamics of suspended-sediment transport during rainfall events were described by hysteresis loops, where the hysteresis pattern revealed sediment sources closer to the outlet in the catchment with grassland and further distances in the eucalyptus catchment.

The use of multiple parameters by conventional and alternative fingerprinting approach, as the fallout radionuclides, stable isotopes, geochemical elements and VIS-based-color parameters has been shown to be more efficient in the discrimination of fine sediment (<0.063 mm) sources and for dominant erosion processes. However, for the coarse sediment (0.063-2 mm), the discrimination was not satisfactory only with the use of geochemical elements for both catchments. Although the soils of the areas present similar classification, variable selection for fine sediment was different for each area of study. This condition evidences the complexity of erosive processes in which the hydro-sedimentological dynamics are singular to each catchment.

### 6.1 Recommendations and perspectives for further investigations

Some recommendations for future studies are:

- 1) On hydro-sedimentological dynamics: the proper functioning of turbidity and water level sensors and higher number of water-sediment samples is required during rainfall events for proper estimation of coarse sediment fraction as function of flow in order to quantify the contribution of this fraction to total sediment yield.

- 2) As analysis for coarse sediment based only on geochemical parameters was not efficient considering the low precision based on the relative error values, the analysis of others

parameters should complement the method as well the different sampling and samples preparation procedures.

3) Collect samples in areas of permanent preservation and legal reserve, even when there is no evidence of erosion process, since these areas also integrate the hydro-sedimentological dynamics.

4) Identify sediment source areas according to soil type to verify how much the soil type contributes to the erosive process compared to land use.

## REFERENCES

- ASSOCIAÇÃO GAÚCHA DE EMPRESAS FLORESTAIS. AGEFLOR. Disponível em <<http://www.ageflor.com.br/>>. Acesso em: 12 abr. 2017.
- BAUMHARDT, E. **Balanco hídrico de microbacia com eucalipto e pastagem nativa na região da campanha do RS**. 2010. 139 f. Dissertação (Mestrado em Engenharia Civil) – Universidade Federal de Santa Maria, Santa Maria, 2010.
- BAUMHARDT, E. **Hidrologia de bacia de cabeceira com eucaliptocultura e campo nativo na região da campanha gaúcha**. 2014. 166 f. Tese (Doutorado em Engenharia Florestal) – Universidade Federal de Santa Maria, Santa Maria, 2014.
- BLAKE, W.H., et al. Tracing crop specific sediment sources in agricultural catchments. **Geomorphology**. 140, 322 e 329. 2012.
- BENETT, C.; ALMEIDA, M.; CASTILHO, M. W. V. Gestão de recursos naturais: Sítio São Brás, município de Carlinda, MT”. **Revista de Biologia e Ciências da Terra**. Universidade Federal da Paraíba, Campina Grande, v. 2, n. 1, 2002.
- BIRKINSHAW, S.J., BATHURST, J.C., ROBINSON, M. 45 years of non-stationary hydrology over a forest plantation growth cycle, Coalburn catchment, Northern England. **Journal of Hydrology** 519: 559-573. 2014.
- BOLDRINI, I. I.; **Bioma Pampa: diversidade florística e fisionômica**. Porto Alegre, editora Pallotti, 2010. 64 p.
- BROSINSKY, A. et al. Spectral fingerprinting: sediment source discrimination and contribution modelling of artificial mixtures based on VNIR-SWIR spectral properties. **Journal of Soils and Sediments**. v. 14, p. 1949-1964. 2014.
- CARVALHO, N. de O. **Hidrossedimentologia prática**. 2ª ed., rev., atual e ampliada. Rio de Janeiro: Interciência, 599p. 2008.
- COLLINS, A. L.; WALLING, D. Selecting fingerprint properties for discriminating potential suspended sediment sources in river basins. **Journal of Hydrology**, v. 261, n. 1-4, p. 218–244, abr. 2002.
- DURLO, M; SUTILL, F. **Bioengenharia: Manejo Biotécnico de Cursos de Água**. Santa Maria; Edição do Autor, 189p, 2012.
- ERSKINE, W. D. Soil color as a tracer of sediment dispersion from erosion of forest roads in Chichester State Forest, NSW, Australia. **Hydrological Processes**, v. 27, n. 6, p. 933–942, 2013.
- EVRARD, O., et al. Combining suspended sediment monitoring and fingerprinting to determine the spatial origin of fine sediment in a mountainous river catchment. **Earth Surface Processes and Landforms**, Vol. 36, No. 8, pp. 1072–1089. 2011.

FRANZ, C. et al. Geochemical signature and properties of sediment sources and alluvial sediments within the Lago Paranoá catchment, Brasilia DF: A study on anthropogenic introduced chemical elements in an urban river basin. **Science of the Total Environment**, v. 452–453, p. 411–420, 2013.

FRANZ, C. et al. Sediments in urban river basins: identification of sediment sources within the Lago Paranoá catchment, Brasilia DF, Brazil - using the fingerprinting approach. **The Science of the total environment**, v. 466-467, p. 513–23, 1 jan. 2014.

KNIGHTON, D. **Fluvial Forms and Processes: A New Perspective**. Arnold, London, United Kingdom. 1998.

KOITER, A. J. et al. The behavioural characteristics of sediment properties and their implications for sediment fingerprinting as an approach for identifying sediment sources in river basins. **Earth-Science Reviews**, v. 125, p. 24–42, 2013.

LACEBY, J. P. et al. The challenges and opportunities of addressing particle size effects in sediment source fingerprinting: A review. **Earth-Science Reviews**, v. 169, n. April, p. 85–103, 2017.

LANZA, R. **Hidrologia comparativa e perda de solo e água em bacias hidrográficas cultivadas com eucalipto e campo nativo com pastagem manejada**. 151 f. 2015. Dissertação (Mestre em Ciência do Solo). Universidade Federal de Santa Maria. Santa Maria. 2015.

LE GALL, M. et al. Science of the Total Environment Quantifying sediment sources in a lowland agricultural catchment pond using  $^{137}\text{Cs}$  activities and radiogenic  $^{87}\text{Sr} / ^{86}\text{Sr}$  ratios. **Science Total Environment**. v. 567, p. 968–980, 2016.

MATEUS, R. J. G.; PADILHA, D. G. Avaliação multicritério da fragilidade do território no Brasil. A silvicultura no Estado do Rio Grande do Sul. **Finisterra**, v. 52, n. 104, p. 73–104, 2017.

MARTTILA, H.; KLØVE, B. Dynamics of erosion and suspended sediment transport from drained peatland forestry. **Journal of Hydrology**, v. 388, n. 3–4, p. 414–425, 2010.

MIGUEL, P. et al. Variáveis mineralógicas preditoras de fontes de produção de sedimentos, em uma bacia hidrográfica Do Rio Grande Do Sul. **Revista Brasileira de Ciência do Solo**, v. 38, n. 3, p. 783–796, 2014a.

MIGUEL, P. et al. Identificação de fontes de produção de sedimentos em uma bacia hidrográfica de encosta. **Revista Brasileira de Ciencia do Solo**, v. 38, n. 2, p. 585–598, 2014b.

MINELLA, J. P. G.; MERTEN, G. H.; CLARKE, R. T. Método “fingerprinting ing” para identificação de fontes de sedimentos em bacia hidrográfica rural. **Revista Brasileira de Engenharia Agrícola e Ambiental**, v. 13, n. 5, p. 633–638, 2009.

MINELLA, J. P. G. **Utilização de técnicas hidrossedimentométricas combinadas com a identificação de fontes de sedimentos para avaliar o efeito do uso e do manejo do solo nos**

**recursos hídricos de uma bacia hidrográfica.** 2007. 172 f. Tese (Doutorado em Recursos Hídricos e Saneamento) – Universidade Federal do Rio Grande do Sul, Porto Alegre, 2007.

MINELLA, J.P.G., WALLING, D.E., MERTEN, G.H., Combining sediment source tracing techniques with traditional monitoring to assess the impact of improved land management on catchment sediment yields. **Journal of Hydrology.** 348, 546–563. 2008.

MINELLA, J. P. G.; MERTEN, G. H.; CLARKE, R. T. Método “fingerprinting” para identificação de fontes de sedimentos em bacia hidrográfica rural. **Revista Brasileira de Engenharia Agrícola e Ambiental**, v. 13, n. 5, p. 633–638, 2009.

MINELLA, J.P.G., WALLING, D.E., MERTEN, G.H., Establishing a sediment budget for a small agricultural catchment in southern Brazil, to support the development of effective sediment management strategies. **Journal of Hydrology.** 519, 2189–2201. 2014.

MINISTÉRIO DO MEIO AMBIENTE. MMA. Disponível em: <<http://www.mma.gov.br/biomas/pampa>>. Acesso em: 22 de jan. de 2018.

MIZUGAKI S., et al. Estimation of suspended sediment sources using  $^{137}\text{Cs}$  and  $^{210}\text{Pb}$  in unmanaged Japanese cypress plantation watersheds in southern Japan. **Hydrological Processes**, v. 22, n. 23, pp. 4519–4531. 2008.

MORGAN, R. P. C; RICKSON, R.J. **Slope Stabilization and Erosion Control: A Bioengineering Approach.** Published by E e fn Spon, an imprint of Chapman e Hall, 2-6 Boundary Row, London. 2005.

NABINGER C., MORAES, A.; MARASCHIN G.E. Campos in Southern Brazil. In: Grassland ecophysiology and grazing ecology (eds. Lemaire G.; Hodgson, J.G.; Moraes, A.; Maraschin, G.E). **CABI Publishing Wallingford**, p. 355-376, 2000.

NAVRATIL O., et al. Temporal variability of suspended sediment sources in an alpine catchment combining river/rainfall monitoring and sediment fingerprinting. **Earth Surface Processes and Landforms**, Vol. 37, No. 8, pp. 828–846. 2012.

OWENS, P.N. et al. Determining the effects of wildfire on sediment sources using  $^{137}\text{Cs}$  and unsupported  $^{210}\text{Pb}$ : the role of natural landscape disturbance and driving forces. **Journal of Soils and Sediments** 12: 982–994. 2012.

PELÁEZ, J.J.Z. **Hidrologia comparativa em bacias hidrográficas com eucalipto e campo.** 156p. Tese (Doutorado em Engenharia Florestal) - Universidade Federal de Santa Maria, Santa Maria, 2014.

PILLAR, V.D.; et al. **Campos Sulinos conservação e uso sustentável da biodiversidade.** Brasília: MMA, 403 p. 2009.

SARI, V.; POLETO, C.; CASTRO, N. M. dos R. Caracterização dos processos hidrossedimentológicos em bacias rurais e urbanas. **Enciclopédia Biosfera**, p. 596–624, 2013.

SEAR, D.A., MALCOLM, D.N., THORNE, C.R., 2003. **Guidebook for Applied Fluvial Geomorphol-**ogy, R&D Technical Report FD1914. London.

SILVEIRA, L. et al. Effects of afforestation on groundwater recharge and water budgets in the western region of Uruguay. **Hydrological Processes**, v. 30, n. 20, p. 3596–3608, 2016.

SCHULLER, P. et al. Using <sup>137</sup>Cs and <sup>210</sup>Pbex and other sediment source fingerprints to document suspended sediment sources in small forested catchments in south-central Chile. **Journal of Environmental Radioactivity**, v. 124, p. 147–159, 2013.

SMITH, H.G. et al. Changes to sediment sources following wildfire in a forested upland catchment, southeastern Australia. **Hydrological Processes**. 25: 2878–2889. 2011.

SMITH, H.G. et al. Quantifying sources of fine sediment supplied to post–fire debris flows using fallout radionuclide tracers. **Geomorphology**. 139–140: 403–415. 2012.

SOCIEDADE BRASILEIRA DE SILVICULTURA SBS Disponível em: <<http://www.sbs.org.br/>> Acesso em: 15 mai. 2012.

REICHERT, J. M. et al. Agricultural and Forest Meteorology Water balance in paired watersheds with eucalyptus and degraded grassland in Pampa biome. **Agricultural and Forest Meteorology**, v. 237–238, p. 282–295, 2017.

RIO GRANDE DO SUL. Resolução CONSEMA nº 187, de 11 de abril de 2008. Aprova o zoneamento ambiental para a atividade de silvicultura no estado do Rio Grande do Sul. **Diário Oficial do Estado do Rio Grande do Sul**. Porto Alegre, RS, abr., 2008.

RODRIGUES, M. F. **Dinâmica hidrossedimentológica de pequenas bacias hidrográficas florestais**. 2015. 126f. Tese (Doutorado em Engenharia Florestal) – Universidade Federal de Santa Maria, Santa Maria, 2015.

RODRIGUES, M.F. et al. Coarse and fine sediment sources in nested watersheds with eucalyptus forest. **Land Degradation e Development**. <https://doi.org/10.1002/ldr.2977>. 2018.

TIECHER, T. et al. Alternative method to trace sediment sources in a subtropical rural catchment of southern Brazil by using near-infrared spectroscopy. **Soil and Tillage Research**. v. 16, p. 2014, 2014.

TIECHER, T. et al. Combining visible-based-color parameters and geochemical tracers to improve sediment source discrimination and apportionment. **Science of The Total Environment**, v. 527–528, p. 135–149, 2015.

TIECHER, T. et al. Tracing sediment sources in a subtropical rural catchment of southern Brazil by using geochemical tracers and near-infrared spectroscopy. **Soil and Tillage Research**, v. 155, p. 478–491, 2016.

TIECHER, T. et al. Quantifying land use contributions to suspended sediment in a large cultivated catchment of Southern Brazil (Guaporé River, Rio Grande do Sul). **Agriculture, Ecosystems and Environment**, v. 237, p. 95–108, 2017.a

TIECHER, T. et al. Tracing sediment sources in two paired agricultural catchments with different riparian forest and wetland proportion in southern Brazil. **Geoderma** (Amsterdam), v. 285, p. 225-239, 2017.b

TIECHER, T. et al. Fingerprinting sediment sources in a large agricultural catchment under no-tillage in southern Brazil (conceição river). **Land degradation e development**, v. 1, p. 1, 2018.

WILKINSON, S.N., et al. Fallout radionuclide tracers identify a switch in sediment sources and transport limited sediment yield following wildfire in a eucalypt forest. **Geomorphology** 110: 140–151. 2009.

YANG, S., LI, C.; YOKOYAMA, K., Elemental compositions and monazite age patterns of core sediments in the Changjiang Delta: implications for sediment provenance and development history of the Changjiang River. **Earth and Planetary Science Letters** 245, 762–776. 2006.

YU, L.; OLDFIELD, F. A multivariate mixing model for identifying sediment source from magnetic measurements. **Quaternary Research**, v. 32, n. 2, p. 168–181, set. 1989.



## APPENDIX A - CHARACTERIZATION OF STUDY AREAS



(a)



(b)



(c)



(d)



(e)



(f)

Harvester operation in the catchment with eucalyptus (EC) (a); livestock, pasture and oats field in the catchment with grassland (GC) (b); stream channel with lag deposit and collapse of bank in EC (c); wind episode in EC (d); lag deposit on stream channel in GC (e) and cattle trampling near of stream channel in the GC (f).



## APPENDIX B – MONITORING SECTIONS

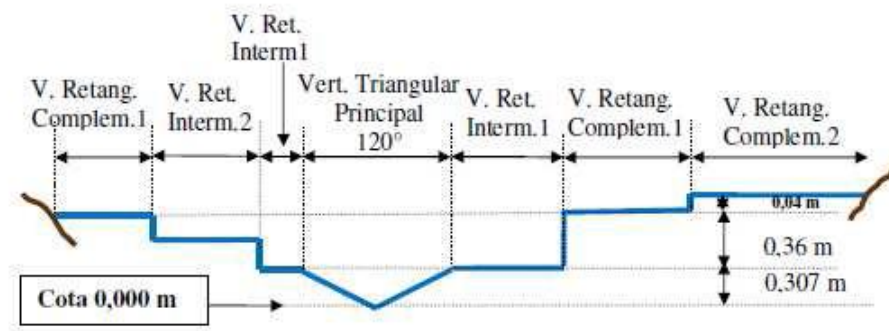


(a)

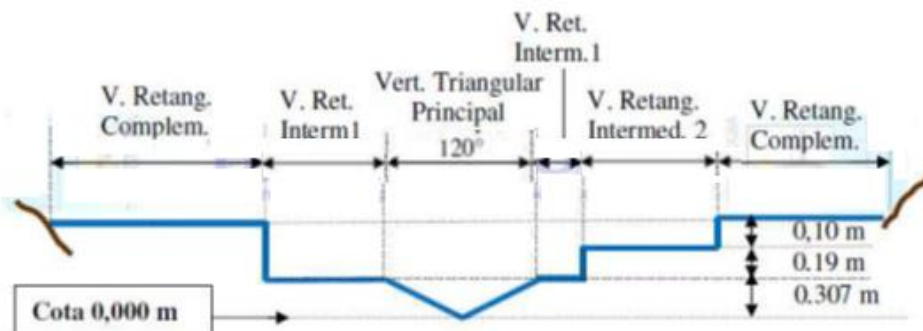


(b)

Automated hydro-sedimentometric monitoring sections in the catchment with eucalyptus (a) and with grassland (b) in São Gabriel-RS.



(a)



(b)

Lay-out of spillways installed in the hydro-sedimentological sections in the catchment with eucalyptus (a) and with grassland (b), São Gabriel-RS (Source: Adapted from Hydrotopo).

Equations used to calculate the flow in the catchments, in São Gabriel, RS.

**General equation of the composite spillway flow**      **Equations of triangular and rectangular spillways**

**Eucalyptus catchment**

$$Q = Q_{TP} + Q_{RI-1} + Q_{RI-2} + Q_{RC-1} + Q_{RC-2}$$

$$Q_{TP} = 2,40[h^{2,50} - (h - 0,307)^{2,50}]$$

$$Q_{RI-1} = 2,21(h - 0,307)^{1,50}$$

$$Q_{RI-2} = 1,87(h - 0,507)^{1,50}$$

$$Q_{RC-1} = 12,77(h - 0,667)^{1,50}$$

$$Q_{RC-2} = 2,32(h - 0,707)^{1,50}$$

**Grassland catchment**

$$Q = Q_{TP} + Q_{RI-1} + Q_{RI-2} + Q_{RC}$$

$$Q_{TP} = 2,40[h^{2,50} - (h - 0,307)^{2,50}]$$

$$Q_{RI-1} = 3,16(h - 0,307)^{1,50}$$

$$Q_{RI-2} = 5,50(h - 0,497)^{1,50}$$

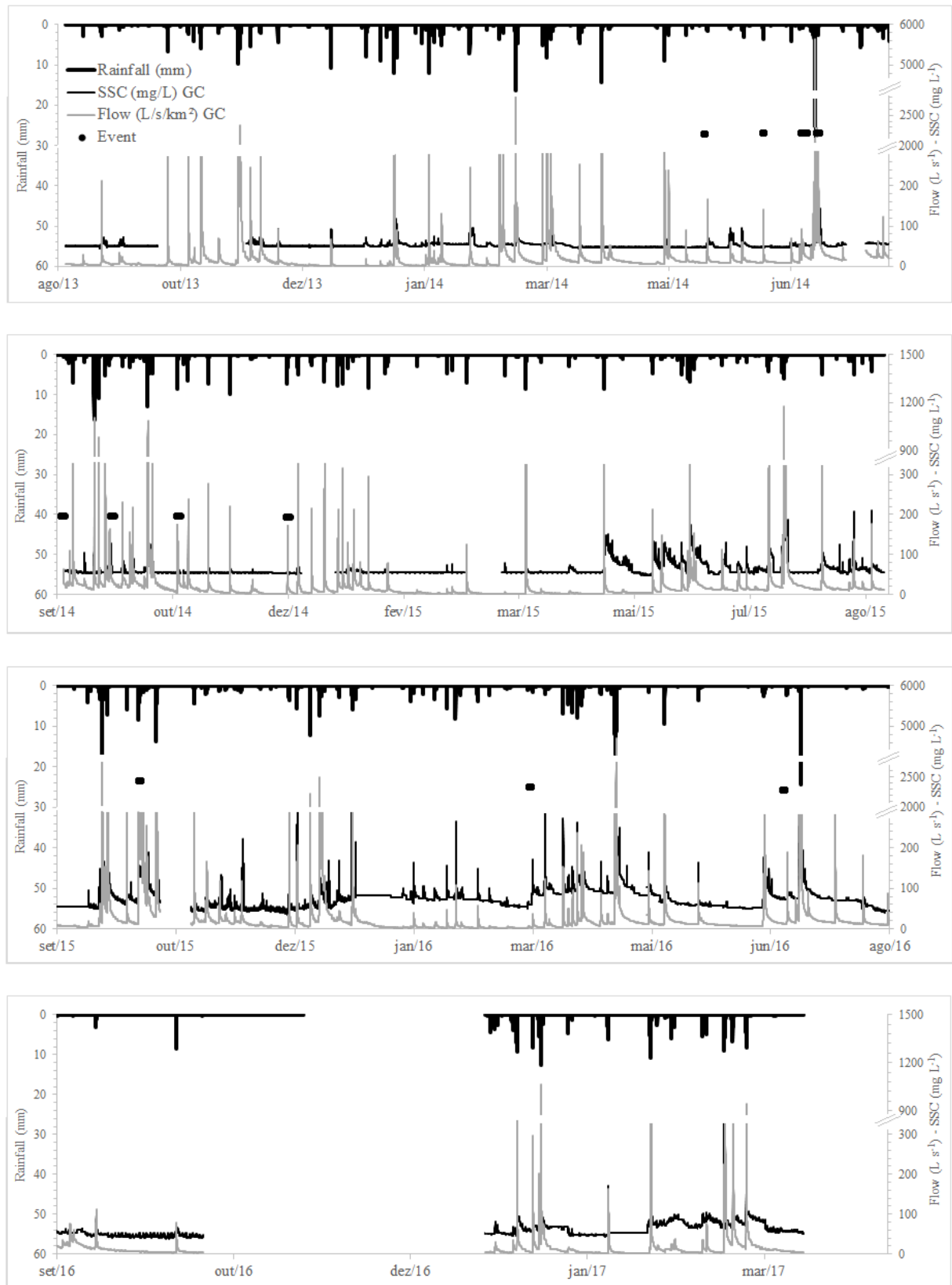
$$Q_{RC} = 12,68(h - 0,597)^{1,50}$$

Where: QTP: Principal Triangular Spillway; Q RI-1: Intermediate Rectangular Spillway 1; QRI-2: Intermediate Rectangular Spillway 2; QRC: Complementary Rectangular Spillway; QRC-1: Complementary Rectangular Spillway 1; QRC-2: Complementary Rectangular Spillway 2; where Q is given in  $m^3 s^{-1}$  and h: in m (water level).

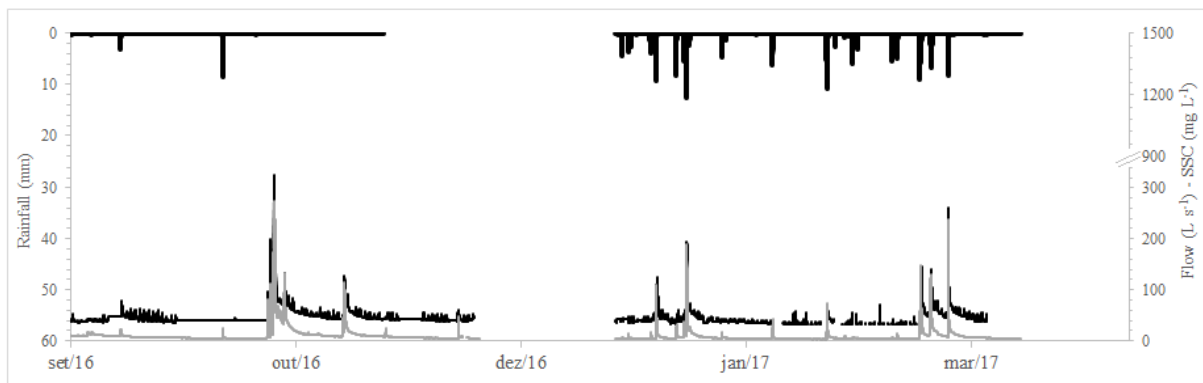
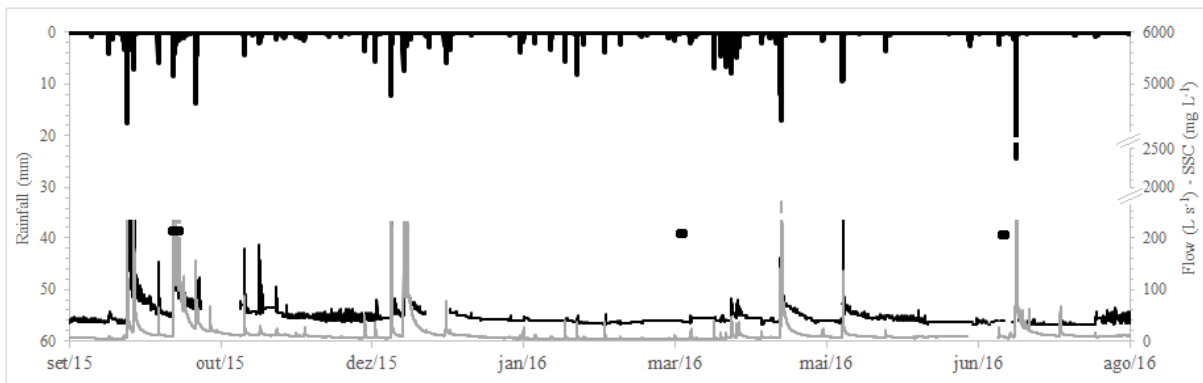
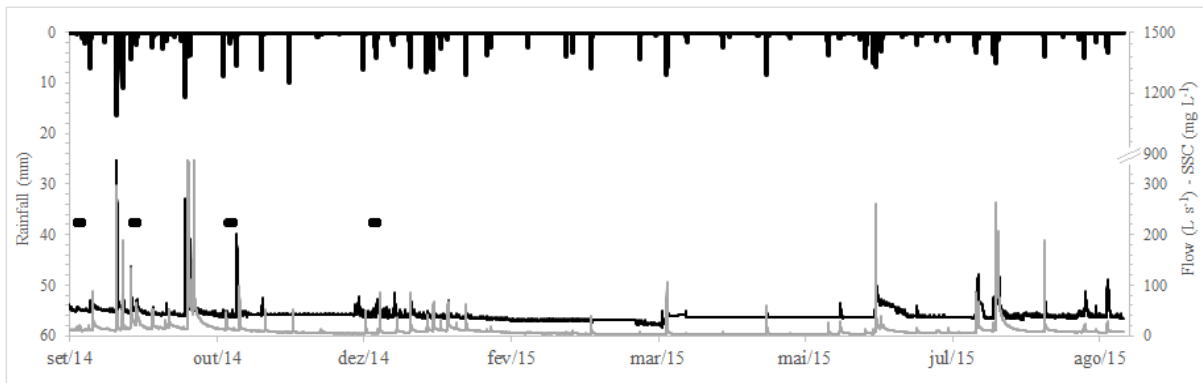
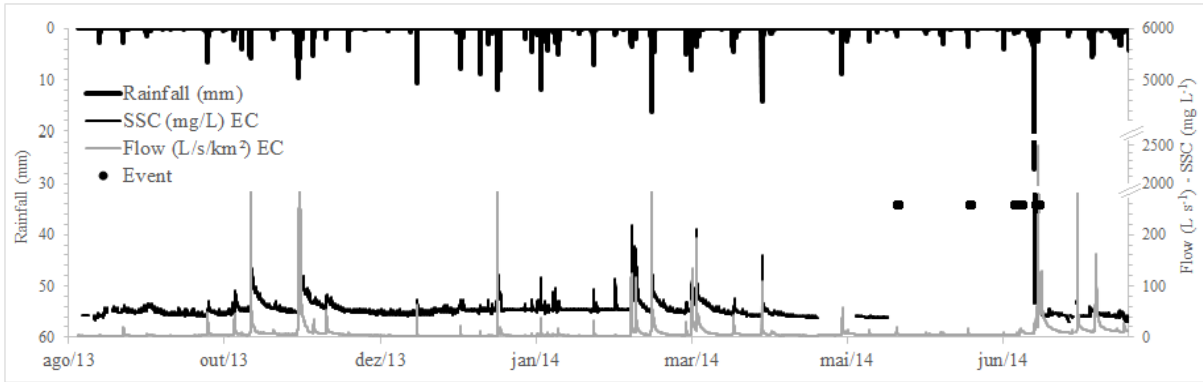


US-DH-48 type sampler used for the sampling of suspended sediments (a), time-integrating suspended sediment samplers (b) and US-BLH-84 sampler for the collection of transported sediments in drag (c) (Photos: Author).

## APPENDIX C – DATA SERIES DURING STUDY PERIOD



Measured rainfall, flow, suspended sediment concentration and events monitored in the grassland catchment.



Measured rainfall, flow, suspended sediment concentration and events monitored in the eucalyptus catchment.



Continued...

Date (m/d/y)	GC = EC		GC	EC	GC	EC	GC	EC	GC	EC	GC	EC	GC	EC	GC	GC	EC	EC
	P (mm)	IM 1h (mm h <sup>-1</sup> )	Q max. (L s <sup>-1</sup> )	Q max. (L s <sup>-1</sup> )	R (mm)	R (mm)	C (%)	C (%)	SSC max. (mg L <sup>-1</sup> )	SSC max. (mg L <sup>-1</sup> )	SSY (t km <sup>-2</sup> )	SSY (t km <sup>-2</sup> )	BL (t km <sup>-2</sup> )	BL (t km <sup>-2</sup> )	HI	Rotation		
3/3/2014	72.9	41.2	4117.0	757.9	19.3	0.3	26.4	0.4	-	365.1	-	0.95	-	-	-	-	1.21	C
3/14/2014	33.5	16.8	326.2	31.6	3.0	0.5	8.9	7.1	-	-	-	-	-	-	-	-	-	-
3/16/2014	56.1	18.8	436.5	126.6	6.5	1.5	11.6	2.6	-	127.3	-	0.38	-	-	-	-	-1	AC
3/18/2014	33.0	14.5	598.4	184.4	5.9	1.2	17.7	3.6	-	210.6	-	0.4	-	-	-	-	-0.97	AC
3/30/2014	40.5	10.8	277.7	44.8	2.0	0.2	5.0	0.4	-	66.7	-	0.07	-	-	-	-	-0.13	AC
4/8/2014	35.8	26.9	855.8	90.3	6.4	0.4	18.0	1.2	-	160.6	-	0.12	-	-	-	-	-0.91	AC
4/11/2014	11.9	3.3	56.4	9.1	0.4	0.0	3.1	0.1	-	-	-	-	-	-	-	-	-	-
5/3/2014	51.8	17.3	334.6	48.5	4.0	0.2	7.8	0.3	-	-	-	-	-	-	-	-	-	-
5/12/2014	8.6	8.4	97.8	11.6	1.0	0.1	11.2	1.7	64.7	-	0.1	-	-	-	-0.93	C	-	-
5/21/2014*	20.3	7.4	184.3	17.0	1.9	0.2	9.4	1.0	104.4	10.13*	0.2	-	-	-	-2.5	C	-	-
5/30/2014	12.7	4.3	66.3	7.6	0.7	0.1	5.9	0.7	-	-	-	-	-	-	-	-	-	-
6/13/2014*	16.5	7.9	155.6	13.5	1.3	0.1	8.1	0.9	34.48*	24.57*	-	-	-	-	-	-	-	-
6/24/2014	8.6	7.6	78.0	9.0	0.9	0.1	10.0	1.5	63.1	-	0.1	-	-	-	0.04	C	-	-
6/28/2014*	15.5	3.6	58.3	9.0	1.0	0.1	6.6	0.4	17.3	11.6*	0.02	-	-	-	-	-	-	-
6/29/2014	17.0	3.0	103.2	13.3	2.2	0.3	12.9	1.7	23.6	20.2	0.07	-	-	-	-	-	-	-
7/3/2014	22.9	6.9	145.3	23.4	1.1	0.1	4.6	0.5	-	-	-	-	-	-	-	-	-	-
7/4/2014*	77.7	53.1	6206.0	1282.0	35.4	9.0	45.5	11.3	2290.2*	1046.8	24.86	11.83	0.053	0.006	1.86	C	-0.76	AC
7/5/2014	22.4	7.1	387.1	106.8	4.3	1.3	19.0	5.6	-	-	-	-	-	-	-	-	-	-
8/7/2014	23.8	8.7	176.2	17.0	1.8	0.2	7.4	1.0	-	-	-	-	-	-	-	-	-	-
8/30/2014	27.7	13.7	360.4	45.7	2.6	0.3	9.4	1.0	84.5	86.4	0.29	0.06	-	-	-0.16	AC	-0.32	AC
9/10/2014	26.1	7.1	128.9	17.3	0.2	0.2	0.7	0.8	25.6*	34.7	0.03	-	-	-	-	-	-	-
9/13/2014	15.8	7.1	121.3	121.3	1.3	1.3	8.0	8.0	-	-	-	-	-	-	-	-	-	-
9/14/2014	37.6	14.4	399.2	399.2	3.0	3.0	8.0	8.0	-	-	-	-	-	-	-	-	-	-
9/23/2014	36.7	32.5	1212.7	245.1	5.5	0.9	15.0	2.4	-	357.5	-	0.42	-	-	-	-	-0.87	AC
9/25/2014	31.2	22.5	1083.8	149.8	5.5	0.8	17.6	2.4	-	171.2	-	0.20	-	-	-	-	-0.51	AC

Continued...

Date (m/d/y)	GC = EC P (mm)	GC IM 1h (mm h <sup>-1</sup> )	GC Q max. (L s <sup>-1</sup> )	EC Q max. (L s <sup>-1</sup> )	GC R (mm)	EC R (mm)	GC C (%)	EC C (%)	GC SSC max. (mg L <sup>-1</sup> )	EC SSC max. (mg L <sup>-1</sup> )	GC SSY (t km <sup>-2</sup> )	EC SSY (t km <sup>-2</sup> )	GC BL (t km <sup>-2</sup> )	EC BL (t km <sup>-2</sup> )	GC GC HI	EC EC Rotation	
9/28/2014	50.2	15.1	645.7	112.7	6.2	1.2	12.4	2.4	-	137.9	-	0.27	-	-	-	-0.55	AC
9/30/2014*	41.5	6.9	180.2	53.3	4.0	0.8	9.7	2.0	118.8	58.7	0.53	0.17	-	-	-	-0.24	AC
10/5/2014	37.8	10.3	254.8	43.6	2.9	0.8	7.7	2.0	-	-	-	-	-	-	-	-	-
10/9/2014	19.9	9.4	172.3	26.1	1.5	0.3	7.4	1.3	103.4	-	0.3	-	-	-	-0.08	AC	-
10/10/2014	29.1	7.6	240.2	40.1	2.8	0.4	9.6	1.5	-	-	-	-	-	-	-	-	-
10/17/2014	95.1	30.3	1191.8	296.8	22.0	7.2	23.1	7.6	-	-	-	-	-	-	-	-	-
10/18/2014	30.0	17.2	645.7	382.5	5.6	2.7	18.5	9.1	-	-	-	-	-	-	-	-	-
10/30/2014*	37.1	13.7	225.9	40.1	5.1	1.0	13.7	2.6	60.8	30.4	0.15	0.05	0.003	0.001	-	-	-
11/3/2014	17.5	13.2	262.3	89.1	2.2	0.8	12.7	4.4	-	201.5	-	0.17	-	-	-	-0.28	AC
11/12/2014	21.6	14.7	304.2	43.6	2.5	0.5	11.4	2.3	111.5	74.2	0.3	0.06	-	-	0.34	C	-0.13
11/21/2014	22.6	21.8	242.6	42.4	1.7	0.3	7.7	1.2	104.8	-	0.2	-	-	-	0.05	C	-
12/16/2014	31.5	21.8	210.0	36.4	1.6	0.3	5.1	0.7	-	-	-	-	-	-	-	-	-
12/21/2014*	55.7	16.7	471.8	63.2	3.4	0.5	6.0	1.3	46.31*	58.7	0.23	0.04	0.002	0.000	1.86	C	-0.64
1/1/2015	39.4	20.3	396.2	71.3	1.8	0.6	4.6	1.5	-	77.3	-	0.1	-	-	-	-0.82	AC
1/7/2015	25.4	14.2	235.4	33.9	2.4	0.2	9.3	0.9	-	48.5	-	0.05	-	-	-	-0.21	AC
1/9/2015	19.6	19.6	348.8	55.1	2.8	0.6	14.4	2.9	-	56.1	-	0.1	-	-	-	-0.97	AC
1/11/2015	7.9	7.6	143.7	25.4	1.5	0.4	18.7	5.1	-	-	-	-	-	-	-	-	-
1/14/2015	7.1	6.6	235.4	55.7	2.0	0.3	27.4	3.9	-	69.7	-	0.1	-	-	-	-0.81	AC
1/20/2015	27.7	24.8	323.4	52.6	2.5	0.5	8.9	1.8	-	-	-	-	-	-	-	-	-
2/25/2015	13.3	11.2	20.6	9.0	0.3	0.1	1.9	1.0	-	-	-	-	-	-	-	-	-
3/4/2015	33.9	20.4	138.9	33.0	1.4	0.2	4.3	0.6	-	-	-	-	-	-	-	-	-
3/20/2015	10.5	9.2	8.0	7.2	0.1	0.1	0.9	0.9	-	-	-	-	-	-	-	-	-
3/29/2015	91.2	35.8	703.1	89.2	7.4	0.9	8.1	1.0	427.6	60.6	1.2	0.1	-	-	2.7	C	-0.49
4/5/2015	12.8	5.3	14.3	5.4	0.3	0.1	2.1	0.4	-	-	-	-	-	-	-	-	-
4/17/2015	11.7	7.6	10.5	6.3	0.1	0.1	1.3	0.6	72.3	-	0.02	-	-	-	0.02	C	-

Continued...

Date (m/d/y)	GC = EC P (mm)	GC IM 1h (mm h <sup>-1</sup> )	GC Q max. (L s <sup>-1</sup> )	EC Q max. (L s <sup>-1</sup> )	GC R (mm)	EC R (mm)	GC C (%)	EC C (%)	GC SSC max. (mg L <sup>-1</sup> )	EC SSC max. (mg L <sup>-1</sup> )	GC SSY (t km <sup>-2</sup> )	EC SSY (t km <sup>-2</sup> )	GC BL (t km <sup>-2</sup> )	EC BL (t km <sup>-2</sup> )	GC HI	GC Rotation
5/2/2015	65.3	20.9	399.2	50.3	2.3	0.2	3.5	0.3	183.8	54.3	0.6	0.04	-	-	1.12	C -0.73 AC
5/10/2015	8.3	3.0	13.5	3.8	0.2	0.0	1.9	0.1	83.0	-	0.04	-	-	-	1.77	C - -
5/23/2015	46.8	14.9	235.4	20.9	2.0	0.2	4.2	0.4	143.6	-	0.3	-	-	-	4.27	C - -
5/27/2015	51.8	6.6	162.8	23.4	1.7	0.0	3.3	0.0	107.0	-	0.4	-	-	-	-1.4	AC - -
6/5/2015	23.8	10.8	85.9	10.5	1.2	0.1	4.9	0.5	130.4	-	0.2	-	-	-	-0.75	AC - -
6/7/2015	16.3	11.2	119.3	12.0	1.4	0.2	8.3	1.2	105.9	58.7	0.2	0.04	-	-	-0.97	AC - -
6/8/2015	58.4	24.5	811.1	216.0	6.4	1.5	10.9	2.6	186.9	236.3	1.5	0.5	-	-	0.15	C -0.64 AC
6/10/2015	18.6	8.5	168.5	32.5	1.9	0.5	10.0	2.8	-	72.7	-	0.1	-	-	-	- -0.2 AC
6/11/2015	12.8	4.4	90.9	18.6	1.1	0.3	8.2	2.3	104.4	66.4	0.31	0.07	-	-	-0.05	AC -0.2 AC
6/22/2015	17.0	9.4	122.3	13.5	1.3	0.1	7.4	0.6	95.2	-	0.2	-	-	-	-0.14	AC - -
6/29/2015	11.9	5.3	74.3	9.9	1.2	0.2	10.4	1.4	82.5	-	0.2	-	-	-	-0.14	AC - -
7/3/2015	6.1	3.8	69.9	12.7	0.9	0.2	15.3	3.5	121.2	-	0.1	-	-	-	0.05	C - -
7/12/2015	30.0	14.5	488.2	70.6	3.5	0.5	11.6	1.7	214.9	113.6	0.9	0.1	-	-	0.21	C -0.54 AC
7/18/2015	10.7	6.1	162.8	20.9	1.6	0.3	14.6	3.2	148.2	-	0.3	-	-	-	0.29	C - -
7/19/2015	46.1	21.8	1292.5	218.0	15.0	2.9	32.5	6.5	288.1	253.0	4.6	0.9	-	-	-0.38	AC -0.28 AC
7/19/2015	46.1	21.8	1292.5	218.0	15.0	2.9	32.5	6.5	288.1	253.0	4.62	0.9	-	-	-0.38	AC -0.75 AC
8/4/2015	36.8	16.5	649.7	156.0	2.5	0.4	6.7	1.2	185.4	107.6	0.9	0.1	-	-	0.17	C -0.28 AC
8/18/2015	21.1	8.9	152.0	19.5	1.3	0.4	6.4	3.1	207.8	55.8	0.4	0.04	-	-	0.49	C -0.16 AC
8/22/2015	4.6	4.6	36.8	10.5	0.7	0.2	14.5	4.8	91.7	59.1	0.1	0.02	-	-	2.37	C 0.02 C
8/26/2015	20.6	9.4	194.7	23.8	1.7	0.3	8.5	1.5	210.8	111.4	0.4	0.1	-	-	2.13	C -0.18 AC
8/30/2015	27.7	13.7	360.4	42.4	2.6	0.3	9.4	1.0	84.5	86.3	0.29	0.05	-	-	-0.16	AC -0.32 AC
9/20/2015	19.3	5.3	38.3	7.8	0.4	0.3	1.9	1.8	149.8	-	0.2	-	-	-	0.66	C - -
9/22/2015	105.2	54.1	3021.9	381.4	18.2	2.9	17.3	2.8	515.2	595.0	6.1	2.36	-	-	2.37	C 0.02 C
9/24/2015	39.4	11.2	1770.8	432.5	14.3	2.1	36.3	5.3	-	407.5	-	1.5	-	-	-	- -0.61 AC
10/2/2015	19.1	16.8	366.3	53.9	2.6	0.6	13.6	3.0	173.1	153.0	0.5	0.1	-	-	0.84	C -0.79 AC



Continued...

Date (m/d/y)	GC = EC P (mm)	GC IM 1h (mm h <sup>-1</sup> )	GC Q max. (L s <sup>-1</sup> )	EC Q max. (L s <sup>-1</sup> )	GC R (mm)	EC R (mm)	GC C (%)	EC C (%)	GC SSC max. (mg L <sup>-1</sup> )	EC SSC max. (mg L <sup>-1</sup> )	GC SSY (t km <sup>-2</sup> )	EC SSY (t km <sup>-2</sup> )	GC BL (t km <sup>-2</sup> )	EC BL (t km <sup>-2</sup> )	GC HI	EC Rotation		
10/7/2015	154.5	34.4	2105.9	651.9	30.9	6.8	20.0	4.4	-	465.1	-	3.59	0.002	0.001	-	-	-0.89	AC
10/8/2015	69.7	11.0	1493.8	521.1	15.9	4.7	22.9	6.7	-	209.1	-	2.71	0.008	0.030	-	-	-0.89	AC
10/9/2015	23.9	5.8	800.2	296.9	7.4	3.0	30.9	12.4	-	142.4	-	1.1	-	-	-	-	-0.24	AC
10/10/2015	17.3	4.6	280.3	104.1	3.0	1.4	17.2	7.9	-	100.0	-	0.4	-	-	-	-	-0.6	AC
10/14/2015	19.3	19.1	850.1	130.0	4.5	0.6	23.5	3.1	283.0	145.4	1.6	0.3	-	-	1.06	C	-0.6	AC
10/15/2015	10.4	6.6	264.9	65.6	2.8	1.0	27.3	9.4	-	118.2	-	0.2	-	-	-	-	-0.6	AC
10/30/2015	30.7	15.0	616.4	72.8	2.7	0.4	8.7	1.3	162.9	180.3	0.7	0.2	-	-	0.63	C	-0.58	AC
11/4/2015	24.9	6.4	182.3	25.0	0.8	0.2	3.0	0.9	-	-	-	-	-	-	-	-	-	-
11/10/2015	17.8	4.1	128.9	19.9	1.3	0.2	7.5	1.2	-	-	-	-	-	-	-	-	-	-
11/16/2015	6.9	3.3	50.3	13.0	0.4	0.2	5.3	3.3	83.5	53.0	0.1	0.03	-	-	0.16	C	-0.83	AC
11/19/2015	13.5	4.8	128.9	22.3	0.9	0.2	6.6	1.1	150.7	63.6	0.3	0.05	-	-	0.49	C	-0.05	AC
12/9/2015	31.8	13.5	393.1	41.3	1.6	0.2	4.9	0.5	319.9	62.1	0.7	0.04	-	-	2.1	C	0	AC
12/12/2015	23.6	16.3	228.3	31.6	1.0	0.2	4.3	0.6	327.9	-	0.4	-	-	-	1.11	C	-	-
12/18/2015	54.9	40.6	2444.7	230.3	8.5	1.0	15.5	1.8	592.4	309.0	3.6	0.3	-	-	0.07	C	-0.82	AC
12/22/2015	83.1	31.0	2748.5	670.0	27.1	9.7	32.7	11.7	-	375.7	-	3.3	-	-	-	-	-0.99	AC
12/23/2015	40.6	7.6	1157.5	391.9	11.4	2.8	28.2	6.9	-	200.0	-	1.4	-	-	-	-	-0.84	AC
1/4/2016	41.1	12.7	384.1	64.3	0.5	0.1	1.3	0.3	566.8	-	1.6	-	-	-	2.56	C	-	-
1/30/2016	14.7	6.9	43.5	21.6	0.4	0.1	2.6	0.8	183.0	-	0.2	-	-	-	-2.01	AC	-	-
2/13/2016	17.3	15.0	52.0	33.0	0.5	0.2	2.9	1.2	175.9	-	0.2	-	-	-	0.46	C	-	-
2/17/2016	17.5	15.5	120.3	31.2	0.8	0.2	4.5	1.2	284.9	50.4	0.3	0.03	-	-	0.02	C	0.49	C
2/26/2016	15.0	10.4	64.3	29.9	0.3	0.1	1.9	0.8	168.8	-	0.1	-	-	-	5.73	C	-	-
3/20/2016	11.9	5.1	40.3	9.4	0.2	0.0	1.8	0.2	192.0	-	0.2	-	-	-	-0.98	AC	-	-
3/25/2016	17.8	8.4	134.4	19.9	1.0	0.1	5.4	0.7	223.4	-	0.4	-	-	-	9.16	C	-	-
4/2/2016	18.8	14.5	170.4	32.5	1.1	0.2	6.0	1.0	293.4	-	0.4	-	-	-	-0.93	AC	-	-
4/4/2016	10.7	6.9	55.7	13.8	0.4	0.1	3.8	1.2	154.0	-	0.2	-	-	-	1.74	C	-	-
4/6/2016	14.7	10.2	105.0	14.1	0.8	0.1	5.6	0.8	172.6	42.3	0.3	0.03	-	-	-0.86	AC	-0.26	AC

Continued...

Date (m/d/y)	GC = EC P (mm)	GC IM 1h (mm h <sup>-1</sup> )	GC Q max. (L s <sup>-1</sup> )	EC Q max. (L s <sup>-1</sup> )	GC R (mm)	EC R (mm)	GC C (%)	EC C (%)	GC SSC max. (mg L <sup>-1</sup> )	EC SSC max. (mg L <sup>-1</sup> )	GC SSY (t km <sup>-2</sup> )	EC SSY (t km <sup>-2</sup> )	GC BL (t km <sup>-2</sup> )	EC BL (t km <sup>-2</sup> )	GC HI	GC Rotation
4/8/2016	32.5	16.3	259.8	39.8	2.0	0.4	6.0	1.3	283.7	82.9	0.9	0.09	-	-	1.95	C 0.59 C
4/10/2016	19.1	11.9	228.3	29.0	1.4	0.3	7.3	1.5	191.3	68.3	0.6	0.06	-	-	0.14	C -0.29 AC
4/11/2016	16.0	7.6	207.8	30.3	1.2	0.2	7.3	1.0	161.7	68.3	0.6	0.1	-	-	0.06	C -0.27 AC
4/18/2016	21.8	6.9	96.9	15.5	0.5	0.1	2.1	0.4	187.4	-	0.3	-	-	-	3.98	C - -
4/24/2016	45.7	33.8	722.5	117.3	1.9	0.7	4.1	1.4	699.1	161.0	2.2	0.2	-	-	1.29	C -0.3 AC
4/25/2016	121.4	34.8	5169.0	1513.6	26.7	6.5	22.0	5.4	829.6	692.6	26.7	6.2	-	-	-0.01	C -0.2 AC
5/8/2016	20.6	6.9	159.1	19.5	1.2	0.2	5.6	0.8	208.7	-	0.4	-	-	-	-0.96	AC - -
5/15/2016	56.1	18.8	580.6	112.5	5.3	0.8	9.4	1.4	389.8	362.6	1.9	0.3	-	-	1.07	C -0.78 AC
5/29/2016	20.1	9.7	124.3	17.9	1.0	0.2	4.8	0.8	184.9	50.4	0.3	0.04	-	-	0.11	C -0.1 AC
7/5/2016	21.8	6.9	207.8	21.6	1.7	0.2	7.8	0.8	190.0	-	0.5	-	-	-	0.18	C - -
7/10/2016	82.0	6.1	722.5	410.7	12.0	4.8	14.6	5.8	513.2	-	11.3	-	-	-	0.63	C - -
10/5/2016	19.6	15.0	87.6	20.6	0.9	0.2	4.5	0.8	93.8	-	0.1	-	-	-	-0.23	AC - -
1/3/2017	13.2	8.9	33.0	11.7	0.3	0.1	2.1	0.7	82.1	-	0.1	-	-	-	0.23	C - -
1/8/2017	10.2	9.1	37.8	13.5	0.4	0.1	4.3	1.2	69.3	-	0.1	-	-	-	-0.25	AC - -
1/10/2017	37.1	32.0	800.2	90.9	4.0	0.6	10.7	1.6	364.6	125.2	1.1	0.13	-	-	-0.46	AC -0.53 AC
1/14/2017	30.7	13.2	326.2	26.1	2.0	0.2	6.6	0.6	206.7	52.0	0.4	0.04	-	-	0.86	C -0.24 AC
1/16/2017	20.3	13.0	223.6	30.3	1.8	0.3	8.7	1.3	119.4	56.9	0.3	0.05	-	-	0.37	C -0.29 AC
1/17/2017	28.7	27.7	1171.2	157.7	5.7	1.0	20.0	3.5	234.3	193.5	1.2	0.28	-	-	0.52	C -0.75 AC
2/4/2017	27.2	21.8	180.2	36.3	1.3	0.2	4.8	0.8	168.3	-	0.2	-	-	-	-0.05	AC - -
2/16/2017	40.6	23.4	580.6	62.2	3.2	0.4	7.9	1.1	241.5	71.5	0.7	0.1	-	-	1.51	C -0.3 AC
3/9/2017	73.9	25.9	511.6	122.3	4.9	0.7	6.7	1.0	344.8	144.7	1.7	0.2	-	-	2.02	C -0.72 AC
3/15/2017	31.8	25.9	1038.3	196.5	4.8	1.1	15.2	3.5	173.4	260.1	1.2	0.4	-	-	0.4	C -1.29 AC
<b>Max</b>	154.5	54.1	6206.0	1513.6	35.4	9.7	45.5	12.4	829.6	1046.8	26.7	11.8	0.05	0.03	9.2	- 1.2 -
<b>Mean</b>	31.2	14.5	520.0	113.5	4.1	0.9	10.5	2.3	197.6	168.4	1.4	0.7	0.01	0.01	0.6	- -0.5 -
<b>Min</b>	4.6	1.8	5.5	3.7	0.1	0.0	0.6	0.0	17.3	20.2	0.0	0.0	0.00	0.00	-2.5	- -1.4 -
<b>SD</b>	23.9	10.0	875.1	214.3	6.1	1.6	8.2	2.5	150.5	173.0	4.1	1.7	0.02	0.01	1.6	- 0.4 -

Note: -: sensor failures for some of the monitored events).

## APPENDIX E - MONTHLY HYDRO-SEDIMENTOLOGICAL VALUES

Monthly values of precipitation (mm), flow (Q), suspended sediments concentration (SSC), sediment discharge (Qss) and sediment production (SY) occurred in the time monitored (Sep/2013-Mar/2017) in the catchment with grassland, São Gabriel, RS.

Month /Year	P (mm)	Q (L s <sup>-1</sup> )			SSC (mg L <sup>-1</sup> )			Qss (mg s <sup>-1</sup> )	SY (t)
		Mean	Min	Max	Mean	Min	Max		
<b>Catchment with Grassland</b>									
Sep-13	63.4	8.2	2.4	233.0	51.5	45.0	73.0	19635.5	1.2
*Out/13	158.0	21.2	1.8	1866.5	50.0	49.0	50.9	2018.0	0.1
*Nov/13	222.5	45.1	4.2	2558.5	55.6	49.0	91.9	38395.6	2.3
Dec-13	35.6	2.6	0.2	72.8	50.2	46.8	93.7	6117.3	0.4
<b>**General</b>	<b>479.5</b>	<b>19.3</b>	<b>0.2</b>	<b>2558.5</b>	<b>51.8</b>	<b>45.0</b>	<b>93.7</b>	<b>66166.4</b>	<b>4.0</b>
Jan-14	237.8	12.8	0.2	1384.1	55.9	48.4	174.6	41686.1	2.5
Feb-14	197.4	20.7	1.9	1025.4	56.7	48.4	111.5	53161.6	3.2
Mar-14	249.1	47.6	6.2	4117.0	56.6	45.3	103.9	138776.0	8.3
Apr-14	50.8	17.1	6.2	855.8	48.1	46.8	94.2	37548.1	2.3
May-14	110.0	18.7	6.7	334.6	50.7	46.2	103.9	45627.5	2.7
Jun-14	81.5	16.3	9.0	155.6	51.0	46.4	95.1	37213.3	2.2
*Jul/14	235.7	1299.9	16.1	8646.3	285.1	47.9	2290.2	418732.0	29.1
*Ago/14	113.9	24.4	8.4	360.4	54.1	47.9	84.5	42741.9	2.6
*Set/14	231.2	47.7	12.7	1212.7	58.1	52.0	111.5	84568.2	5.1
*Out/14	275.7	44.8	5.2	1191.8	61.1	51.6	128.4	139076.6	8.3
*Nov/14	78.0	14.0	2.4	304.2	55.2	52.8	111.5	34352.7	2.1
*Dez/14	139.4	10.6	0.8	471.8	54.3	51.1	72.8	17986.4	1.1
<b>**General</b>	<b>2000.4</b>	<b>131.2</b>	<b>0.2</b>	<b>8646.3</b>	<b>73.9</b>	<b>45.3</b>	<b>2290.2</b>	<b>1091470.5</b>	<b>69.5</b>
*Jan/15	197.1	25.0	5.5	396.2	56.1	52.9	70.7	53521.1	3.2
Feb-15	37.1	4.3	1.6	20.6	54.7	53.6	76.4	9492.4	0.6
*Mar/15	144.4	8.2	1.0	703.1	57.0	54.1	427.6	26222.7	1.6
Apr-15	36.2	3.7	1.8	14.3	55.5	53.9	72.3	8831.7	0.5
May-15	192.3	13.0	2.0	399.2	76.7	46.8	183.8	54668.4	3.3
Jun-15	183.2	25.6	9.2	811.1	75.3	49.8	186.9	104873.0	6.3
Jul-15	140.2	41.9	10.8	1292.5	67.4	51.6	288.1	217013.7	13.0
*Ago/15	93.5	21.9	10.8	649.7	65.1	51.4	210.8	77090.0	4.6
Sep-15	153.2	38.1	4.5	3021.9	69.4	49.9	515.2	241538.1	14.5
Oct-15	300.2	86.8	11.5	2105.9	62.0	20.4	283.0	428546.5	25.7
Nov-15	81.5	21.7	5.5	182.3	24.9	21.4	61.1	24390.0	1.5
Dec-15	262.1	62.2	3.3	2748.5	26.4	20.3	139.5	102765.3	6.2
<b>**General</b>	<b>1820.9</b>	<b>29.4</b>	<b>1.0</b>	<b>3021.9</b>	<b>57.6</b>	<b>20.3</b>	<b>515.2</b>	<b>112412.7</b>	<b>80.9</b>
Jan-16	76.2	14.2	2.4	384.1	120.2	71.2	566.8	91616.9	5.5
Feb-16	80.8	7.1	2.2	120.3	103.1	85.3	284.9	33349.2	2.0
Mar-16	80.8	6.1	0.6	134.4	97.0	69.3	330.7	32314.4	1.9
Apr-16	321.8	53.4	3.8	3359.7	132.7	106.5	829.6	631761.5	37.9

Continued...

Month/Year	P (mm)	Q (L s <sup>-1</sup> )			SSC (mg L <sup>-1</sup> )			Qss (mg s <sup>-1</sup> )	SY (t)
		Mean	Min	Max	Mean	Min	Max		
<b>Grassland catchment</b>									
May-16	104.1	23.2	11.2	580.6	97.4	75.8	389.8	119954.5	7.2
Jun-16	64.5	16.8	6.9	348.8	85.8	58.5	220.9	83436.2	5.0
Jul-16	120.1	43.1	12.2	1839.0	111.5	89.8	513.2	349280.4	21.0
Aug-16	72.1	18.3	6.3	199.0	74.5	58.4	121.4	66066.6	4.0
Sep-16	92.4	16.8	3.9	124.3	70.2	59.1	122.7	54542.6	3.3
Oct-16	20.8	2.4	0.0	87.6	27.8	2.3	177.9	7616.7	0.5
*Nov-16									
*Dec-16									
<b>**General</b>	<b>728.2</b>	<b>20.1</b>	<b>0.6</b>	<b>3359.7</b>	<b>106.0</b>	<b>58.5</b>	<b>829.6</b>	<b>992432.5</b>	<b>59.5</b>
Jan-17	175.3	20.5	3.1	1171.2	60.4	44.9	364.6	83940.1	5.0
Feb-17	119.1	11.1	1.3	580.6	66.5	42.3	241.5	37572.9	2.3
Mar-17	177.0	27.0	3.1	1038.3	84.0	22.5	344.8	128203.2	7.7
<b>**General</b>	<b>471.4</b>	<b>19.5</b>	<b>1.3</b>	<b>1171.2</b>	<b>70.3</b>	<b>22.5</b>	<b>364.6</b>	<b>83238.7</b>	<b>15.0</b>

\* Sensor failure during the month.

Monthly values of precipitation (mm), flow (Q), suspended sediments concentration (SSC), sediment discharge (Qss) and sediment production (SY) occurred in the time monitored (Sep/2013-Mar/2017) in the catchment with eucalyptus, São Gabriel, RS.

Month/Year	P (mm)	Q (L s <sup>-1</sup> )			SSC (mg L <sup>-1</sup> )			Qss (mg s <sup>-1</sup> )	SY (t)
		Mean	Min	Max	Mean	Min	Max		
<b>Eucalyptus catchment</b>									
*Set/13	61.7	2.6	1.9	17.3	47.0	2.3	71.2	4493.9	0.3
Oct-13	153.4	6.4	1.7	363.5	56.3	19.7	257.5	27410.2	1.6
Nov-13	220.0	11.7	2.8	407.8	62.3	43.9	349.9	46343.9	2.8
Dec-13	37.6	2.3	0.8	53.3	49.3	30.3	407.5	5023.0	0.3
<b>**General</b>	<b>472.7</b>	<b>5.8</b>	<b>0.8</b>	<b>407.8</b>	<b>53.7</b>	<b>2.3</b>	<b>407.5</b>	<b>83271.1</b>	<b>5.0</b>
Jan-14	230.3	7.9	3.5	823.8	57.5	45.4	563.5	38891.7	2.3
Feb-14	214.8	7.9	3.3	120.6	59.9	47.0	218.1	24384.9	1.5
Mar-14	270.2	12.6	3.3	757.9	60.2	43.9	443.9	50099.2	3.0
*Abr/14	57.6	4.2	1.3	90.3	44.4	36.4	160.6	7792.7	0.5
*Mai/14	124.4	4.2	2.6	48.5	39.2	36.4	43.9	2314.6	0.1
*Jun/14	80.5	4.0	2.7	13.5	-	-	-	-	-
*Jul/14	235.7	24.2	5.2	1282.0	50.3	27.3	1046.8	158018.5	9.5
Aug-14	113.9	7.8	4.9	45.7	39.5	28.8	86.3	14057.0	0.8
Sep-14	328.9	13.8	4.9	245.1	54.0	39.4	357.5	38616.4	2.3
Oct-14	276.1	22.3	10.5	382.5	48.2	37.9	271.2	66374.7	4.0
*Nov/14	112.8	8.4	3.0	89.1	43.6	37.9	201.5	16583.6	1.0
Dec-14	207.6	4.8	2.1	63.2	42.2	34.8	86.3	9289.9	0.6
<b>**General</b>	<b>2252.9</b>	<b>10.2</b>	<b>1.3</b>	<b>1282.0</b>	<b>49.0</b>	<b>27.3</b>	<b>1046.8</b>	<b>426423.2</b>	<b>25.6</b>
Jan-15	275.7	10.5	5.5	71.3	37.9	31.8	77.3	18512.9	1.1
Feb-15	41.7	4.6	2.8	9.0	30.6	28.8	36.4	5651.9	0.3
Mar-15	149.9	3.5	1.9	89.2	25.3	9.1	60.6	4488.3	0.3
*Abr/15	32.5	2.7	1.6	6.3	24.6	12.1	60.6	2925.3	0.2
May-15	192.3	3.6	2.4	50.3	25.7	18.2	100.0	4672.1	0.3
*Jun/15	197.6	7.7	3.1	216.0	43.8	22.7	236.3	20722.6	1.2
Jul-15	216.9	14.2	4.6	218.0	43.2	31.8	253.0	40119.7	2.4
Aug-15	150.8	7.8	5.1	156.0	40.8	34.8	111.4	15276.6	0.9
Sep-15	233.9	12.4	3.9	432.5	64.1	34.8	925.6	83053.9	5.0
Oct-15	465.7	34.2	7.4	651.9	72.2	47.0	465.1	169352.5	10.2
Nov-15	154.2	8.9	5.4	25.0	54.5	37.9	183.3	21731.5	1.3
Dec-15	99.9	22.7	4.3	670.0	54.8	9.1	375.7	110846.8	6.7
<b>**General</b>	<b>2211.3</b>	<b>11.1</b>	<b>1.6</b>	<b>670.0</b>	<b>43.1</b>	<b>9.1</b>	<b>925.6</b>	<b>41446.2</b>	<b>29.8</b>
Jan-16	76.2	8.1	2.1	64.3	36.4	1.4	63.4	11898.3	0.7
Feb-16	80.8	4.5	3.3	33.0	36.4	1.4	52.0	6731.6	0.4
Mar-16	80.8	3.8	2.8	19.9	37.3	1.4	76.4	6273.5	0.4
Apr-16	321.8	17.2	3.2	1513.6	51.3	1.4	692.6	112920.8	6.8
May-16	123.2	8.5	5.2	112.5	47.3	1.4	362.6	20698.5	1.2
Jun-16	99.2	7.0	4.2	8.6	36.5	1.4	60.2	9739.9	0.6

Continued...

Month/Year	P (mm)	Q (L s <sup>-1</sup> )			SSC (mg L <sup>-1</sup> )			Qss (mg s <sup>-1</sup> )	SY (t)
		Mean	Min	Max	Mean	Min	Max		
<b>Eucalyptus catchment</b>									
Jul-16	111.0	16.6	4.5	410.7	17.9	1.4	48.8	9747.6	0.6
Aug-16	119.6	8.2	4.5	31.2	11.8	1.4	50.4	3936.2	0.2
Sep-16	92.4	7.0	4.1	18.6	43.5	1.4	79.7	13176.1	0.8
Oct-16	323.2	13.5	3.2	228.3	52.0	35.8	325.2	48549.0	2.9
Nov-16	176.9	7.5	0.0	96.0	47.4	39.0	128.4	17853.4	1.1
Dec-16	0.0	0.0	0.0	0.0	0.0	0.0	0.0	0.0	0.0
<b>**General</b>	<b>1605.2</b>	<b>8.5</b>	<b>0.0</b>	<b>1513.6</b>	<b>34.8</b>	<b>0.0</b>	<b>692.6</b>	<b>21793.7</b>	<b>15.7</b>
Jan-17	175.3	6.3	2.9	157.7	43.7	32.5	193.5	15414.9	0.9
Feb-17	119.1	4.1	2.5	62.2	20.7	1.4	71.5	3737.1	0.2
Mar-17	177.0	8.3	2.7	196.5	32.8	1.4	260.1	20662.1	1.2
<b>**General</b>	<b>471.4</b>	<b>5.8</b>	<b>2.5</b>	<b>196.5</b>	<b>25.3</b>	<b>1.4</b>	<b>260.1</b>	<b>10475.0</b>	<b>2.5</b>

\* Sensor failure during the month.